

Optimal placement of green, blue and yellow roofs under uncertainty

Maximizing the societal benefits for a
municipality

by

Lisa Marie Talia

to obtain the degree of Master of Science in Applied Mathematics
at the Delft University of Technology,
to be defended publicly on October 8, 2021

Student number: 5142032
Project duration: January 1, 2021 – October 1, 2021
Thesis committee: Dr. Krzysztof Postek, TU Delft, supervisor
Dr. Ir. Jos H. Weber, TU Delft,
Dr. Ir. Karel Mulder, TU Delft,
Stefan Talboom, Sweco.

An electronic version of this thesis is available at <http://repository.tudelft.nl/>.

Preface

I had the incredible opportunity to perform this research in collaboration with Sweco Netherlands, department of Environmental consultancy. Thanks to this, today I am glad to recognize that my two main passions have been merged in this master thesis: mathematics and sustainability. Throughout this nine-months journey, I had the chance to learn a lot about climate change, mitigation/adaptation strategies, and mathematical techniques for optimization and uncertainty analysis. I am more than happy to have concluded my academic career with an in-depth study of the latter topics.

First and foremost, I would like to express my sincere gratitude to my mentors, Krzysztof Postek and Stefan Talboom. Your guidance, knowledge and patience turned this project from a simple idea to a working tool. Moreover, I am more than grateful to the whole Geodata consultancy team at Sweco. You have been the most welcoming, innovative and enthusiastic environment.

In these pandemic times, the virtual and physical the support of many made this project possible but also special. I would like to thank Anastasia, for the amazing work days spent together and the support in the thesis design choices. Thank you Andrea: even from a distance our discussions have been so fruitful and helpful for this study. Thank you Aline and Sushanth, for sharing with me all the student's phases of this masters, and being always there to discuss details of this work. Most of all, thank you all for being part, directly or from a distance, of my life in this period. Moreover, I would like to thank Matteo, for encouraging me even in the hardest periods, and for supporting me throughout the process of growth that this thesis is part of. Lastly, I can not express how grateful I am to my parents and brother, who have always been supporting my life and study choices indiscriminately. Without you, nothing similar could have ever been possible.

Lisa Marie Talia
Delft, October 2021

Contents

1	Introduction	1
1.1	Research motivation	1
1.1.1	Green, blue and yellow roofs	2
1.1.2	Optimal placement of roofing options	2
1.1.3	Problem uncertainty	3
1.2	Research objective	3
1.2.1	Research question	4
1.2.2	Research scope	4
1.3	Relevance	4
1.3.1	Scientific relevance	4
1.3.2	Practical relevance	4
1.4	Report outline	5
2	Background	7
2.1	Climate data	7
2.1.1	Climate change	7
2.1.2	Climate scenarios and projections	8
2.2	Working of green, blue and yellow roofs	9
2.3	Quantification of costs and benefits	11
2.3.1	Costs	12
2.3.2	Benefits	12
2.4	Modeling green, blue and yellow roofs' societal benefits	13
2.4.1	Single building analysis	13
2.4.2	Multiple buildings analysis	14
2.5	GIS	15
2.6	Uncertainty in Optimization	15
3	Deterministic model	17
3.1	Real life problem description	17
3.2	General characteristics	17
3.3	Model construction process	19
3.4	Deterministic model	20
3.4.1	Sets and indices	20
3.4.2	Parameters	21
3.4.3	Decision Variables	21
3.4.4	Constraints	22
3.4.5	Objective function	24
3.4.6	Deterministic problem overview	24

4	Uncertainty in the problem	25
4.1	Uncertain aspects of the problem	25
4.2	Climate change uncertainty	26
4.3	Tackling climate uncertainty in optimization	27
4.3.1	Robust optimization	27
4.3.2	Stochastic optimization	28
4.4	Parameters uncertainty.	29
4.5	Tackling parameters' uncertainty in optimization.	29
4.5.1	Sampling method	29
4.5.2	Format of the input for uncertainty analysis	30
4.5.3	Similarity matrix	31
4.5.4	Clustering technique	32
4.5.5	Choosing the number of clusters.	33
4.5.6	Subspace partitioning	33
4.6	Modeling uncertainties: overview	34
5	Case study	35
5.1	Input Climate data	35
5.1.1	Choice of climate data	35
5.1.2	Climate data analysis.	36
5.2	Set of suitable roofs	37
5.3	Spatial Parameters.	38
5.3.1	Flooding risk	38
5.3.2	Urban Heat Island	39
5.3.3	Solar Radiation Potential	40
5.3.4	Technical parameters	40
5.4	Stochastic model with fixed parameters: results.	41
5.4.1	Results	41
5.4.2	Insights about Budget variation	44
5.5	Stochastic model: uncertainty analysis	46
5.5.1	Results	47
5.5.2	Clustering of results	48
5.5.3	Parametric trade-offs.	50
5.6	Multi-time step model: results	54
5.6.1	Results RCP 4.5 CNRM	54
5.6.2	Results RCP 8.5 ICHEC.	56
5.7	Multi-time step model and uncertainty	57
5.7.1	Climate scenarios uncertainty	57
5.7.2	Climate and parametric uncertainty.	58
6	Conclusion	61
6.1	Limitations	61
6.1.1	Data limitations.	61
6.1.2	Modeling limitations	62
6.1.3	Analysis limitations.	63
6.2	Conclusions	64
6.3	Recommendations	65

Bibliography	67
A Appendix	73
A.1 GIS parameters	73
A.2 Computational insights	80
A.3 Linear version of the model	85
A.4 Codes	86
A.5 Acknowledgement data	86

1

Introduction

In this introduction, we expound on the motivation behind this thesis research by introducing the need for climate adaptation and mitigation strategies like green, blue and yellow roofs within the Netherlands. We also explain why optimal placement of these roofing options is needed. After that, we explain why uncertainty plays an essential role in the formulation of this problem. Hence, we introduce the research questions and objectives and highlight both the scientific and practical relevance of this study. Lastly, we present the outline this report.

1.1. Research motivation

Being aware of climate change and its consequences, the Netherlands has implemented National and Regional climate adaptation and mitigation strategies, which municipalities and provinces are translating into plans of action [35]. Within those plans, green, blue and yellow roofs are often cited as potential solutions to adapt to climate change and mitigate its effects [8, 10]. Green roofs are systems which allow for the growth of different types of vegetation on top of buildings. Blue roofs are layers for water collection, which can be installed beneath the green roofs or autonomously to provide temporary storage and slow release of rainwater[6]. Yellow roofs is another name to indicate roofs with photovoltaic (PV) panels.

Cities are densely paved. Thus, there is often no room for cheap and easy implementation of green or blue spaces like parks and new canals or solar fields. On the contrary, roofs are empty spaces that are often also flat [6], thus suitable for PV panels and green and blue roofs. Many municipalities subsidize the installation of green, blue and yellow roofs. However, it is impossible to implement every roofing option on every building, as there is a limited budget to fund such projects. Moreover, it has been noted both by researchers and civil servants in the Netherlands that green, blue and yellow roofs placement is currently not always occurring where they can provide the more added value [47, 51]. As stressed in [47], there is a demand for a tool that determines which roofs type are needed in which parts of the city that can be used both by municipalities and stakeholders to enhance decision making. We thus believe it is important to investigate the optimal placement of these roofing options through the means offered by optimization.

1.1.1. Green, blue and yellow roofs

By replacing the existing impervious black covers of roofs with a multi-functional roof, many benefits can be yielded, both to the private owners of the buildings and the society living in the area [16, 37]. From a private perspective, as an example, green and blue roofs are believed to increase the property value of the construction and to increase the lifespan of the roof [16, 37]. From the societal perspective, green roofs are believed to be beneficial, e.g., in terms of urban heat island mitigation [11, 14, 38], while blue roofs are helpful in rainfall water management [38, 43]. Both green and blue options are most suitable on flat roofs [7] and are considered as adaptation strategies, as they can help to temper the effects of extreme climate events such as heatwaves and heavy rainfall. Yellow roofs, instead, offer great opportunities for municipalities to contribute to climate mitigation. The production of clean energy is indeed beneficial to society as a whole, as fewer greenhouse gases are produced compared to commonly used energy sources.

1.1.2. Optimal placement of roofing options

The effectiveness of green, blue and yellow roofs installation are highly dependent on the municipality' structure [47, 51]. There may be areas more subjected to flooding due to a lack of efficient urban drainage systems or areas where heat stress is predominant [4]. Besides, some roofs may be better exposed to solar radiation, and some spaces may have too little greenery. From the perspective of a municipality, optimally placing these infrastructures can convey long-lasting benefits, mitigating the economic and social impact of climate change [18]. Therefore, understanding which projects to prioritize with the limited budget available may be the key to the success of municipalities and other stakeholders in reaching their climate adaptation and mitigation goals.

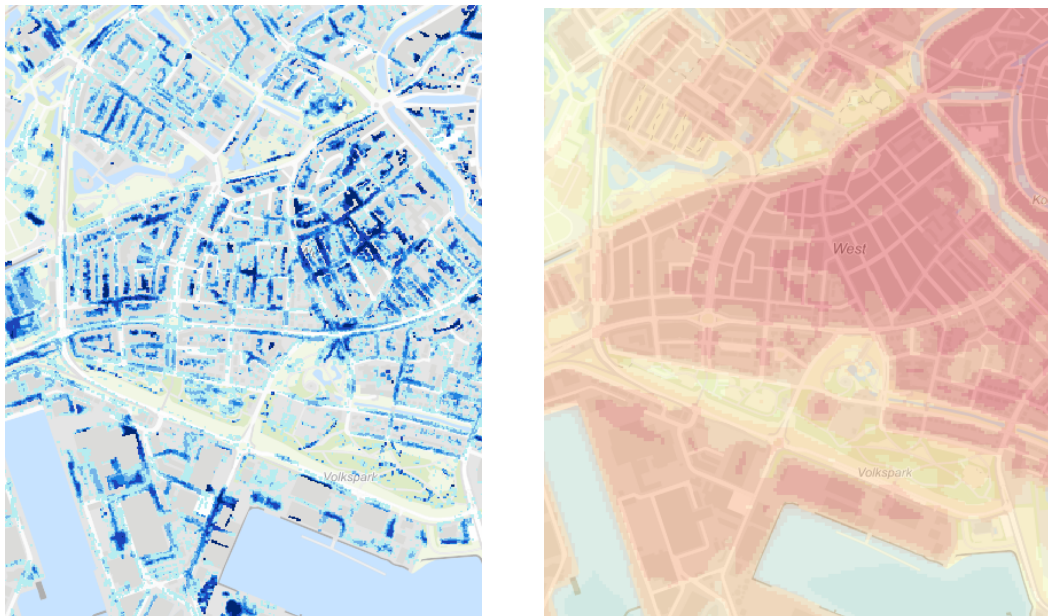


Figure 1.1: Water level during heavy rainfall, and urban heat island. Source: [4]

1.1.3. Problem uncertainty

Uncertainty characterizes this optimal placement problem for two main reasons: climate change and uncertainty around the working of the roofs. Firstly, the added value of these roofing options is contingent on climate variables, such as the amount of warm days and rainfall. For the Dutch climate, the more the climate is going to change, the more green and blue roofs will be needed, as heatwaves and rainfalls are predicted to appear more often and be heavier. Moreover, sunshine presence and thus solar radiation is the key for the performance of PV panels, and that also changes over the years and is hard to predict [32]. Secondly, parameters that reflect the actual working of these roofing types are not agreed upon in the literature. For example, an open discussion is how much heat green and blue roofs can capture during a heatwave. Furthermore, many authors use economic equivalents to weigh the positive and negative aspects of green, blue and yellow roofs, but they are always just estimations. Making use of such values adds another level of uncertainty to the problem.

1.2. Research objective

Within this study, we aim to capture, in a simple yet insightful formulation, the interaction between climate, multi-functional roofs and the urban environment, and to output the societal benefits derived by the optimal placement of different roofing options (Fig 1.2). Optimization under uncertainty techniques will be used and compared to incorporate climate change predictions within the formulation. Moreover, given the deep uncertainty underlying the used parameters, a sensitivity analysis will be performed to outline the main parametric trade-offs.

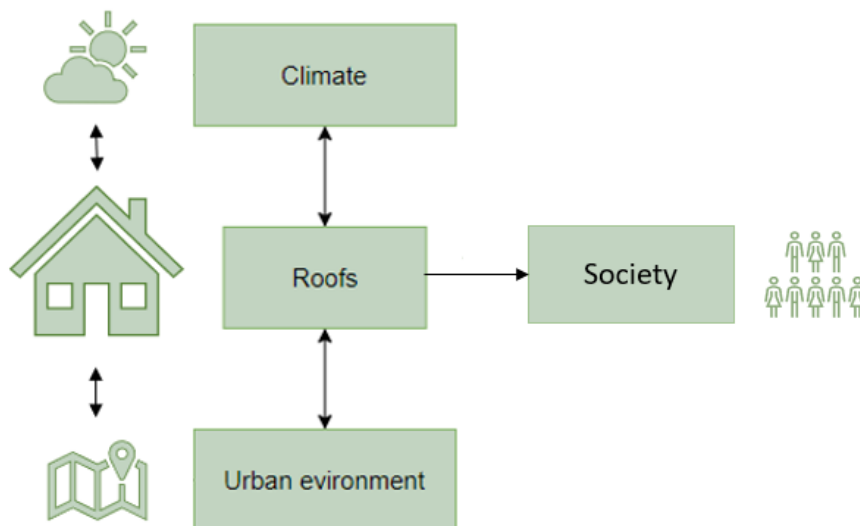


Figure 1.2: The system modeled in this study.

1.2.1. Research question

The following will be our main research question:

How to identify specific buildings where the placement of green, blue and/or yellow roofs will maximize the municipalities' climate adaptation and mitigation goals?

The following sub-questions will be answered during the investigation.

- What is the best way to model the functionality of green, blue and yellow roofs from a municipality perspective, so that the effect on a societal level can be captured?
- How can different climate scenarios be incorporated into the problem?
- How do the uncertainties in the problem's parameters affect the optimal solution?
- How robust is the model' solution?

1.2.2. Research scope

The optimal placement model for green, blue and yellow roofs can be formulated in different ways. Even though specific aspects of the functioning of these roofing options can be very complex, we limit this research to the most simplified yet correct modelling choice possible. We will make specific design choices for this study, specially tailored to the practical use requirements. In addition, a big focus will be the uncertainty behind the problem, for reasons that will become clear in the following chapters. A case study will be presented for a specific municipality, but our method can be extended to any other location in the Netherlands.

1.3. Relevance

1.3.1. Scientific relevance

To the best of our knowledge, there is no example in literature where the optimal placement of green, blue and yellow roofs has been studied as a combination and with the means offered by mathematical optimization. Some authors have indeed studied the optimal placement of green, and blue options using other techniques [47, 51]. Others have used optimization methods to find the optimal placement of yellow and green roofing options, but only for energy production goals [38]. Uncertainty has instead mainly be studied in relation with single green roofs performance [16, 30, 38]. Therefore, we wish to fill this research gap by constructing an optimization model that uses building-specific parameters to output a list of optimal locations for each roofing option. We also aim to analyze the interaction between uncertain parameters and the optimal solution.

1.3.2. Practical relevance

This thesis is developed in collaboration with Sweco, a European engineering consultancy company, active in the fields of consulting engineering, environmental technology and architecture. The outcomes and tool resulting from this study will be deployed by Sweco colleagues in the team of Geodata Consultancy, active in the Netherlands.

The overall goal of this study is to create a tool that helps decision-makers understand where to place green, blue and yellow roofs to maximize their contribution to climate adaptation and mitigation. This tool should be available and ready to use for colleagues at Sweco. Investigating the societal benefits generated by the different roofing options, we will provide the stakeholders with a method to quantify their added values in terms of location-specific characteristics. Overall, we will offer a quick scan tailored to the city's climate-related issues, visible from the *klimaateffectatlas* [4]. The *klimaateffectatlas* is an organized viewer that comprises multiple themes (drought, heat, flooding and waterlogging) and shows how climate change will impact different areas of the Netherlands. It is often used at Sweco as a base for climate stress tests. Moreover, we will be able to underline the unpredictability of some factors that influence the solutions of our model, increasing the awareness of the decision-makers regarding climate variables and technical aspects of the different roofing options.

1.4. Report outline

In the first part of this report, we will introduce the concept of climate uncertainty, as well as the fundamentals of roofing options design. Relevant previous work will be presented in Chapter 2. Then, we intend to answer the first sub-question, presenting the choices for the model construction in Chapter 3. In Chapter 4, we introduce details of the model and present the methodologies used to analyse the parametric uncertainty. In addition, we analyze the model's behaviour in a case study for the municipality of Schiedam in Chapter 5. With our findings, we aim to eventually answer the main question and provide ideas and suggestions for future research in Chapter 6.

2

Background

In this chapter, we provide an overview of the key aspects of the proposed problem, and we review past research on the topic. More in detail, we first explain the importance of using climate data to assess the benefits derived by sustainable roofing options. Following, we briefly review the processes that scientists follow to create climate evolution data, which will clarify the reason for its intrinsic uncertainty. Second, we introduce the technical features of the roofing options, and we discuss previous work on quantifying their benefits, costs, and effects on a societal level. Third, we introduce the concept of a Geographic information system (GIS), which will be the base for the data pre-processing in this work. In the fourth section, we review the main features that will define our problem. Lastly, we disclose the theory behind optimization under uncertainty methods and sensitivity analysis.

2.1. Climate data

Green, blue and yellow roofs are part of the so-called climate adaptation and mitigation strategies [37]. The climate conditions they are inserted in can influence their performance and usefulness [48]. For example, a blue roof will positively contribute to the water management of an area if the same area faces unusual rainfall quantities, for which the existing sewage system is not prepared. However, the climate is not easy to predict, and the uncertainties in future roof performance are directly determined by the uncertainties within the climate data used [48]. The intrinsic uncertainty present in climate data prediction lies mainly in two aspects: climate change and the complexity of the climate system.

2.1.1. Climate change

"Climate is the statistical description of the weather at a location and describes the likelihoods for a range of states and phenomena" [26]. Due to its intrinsic statistical nature, the climate has some natural variability, which consists of some variation in time of the climate system around a mean state within a time scale of months up to decades [29]. In normal conditions, this statistical nature could be analyzed and reproduced in future prediction, which would be uncertain, in a statistically measurable way. However, there is another aspect to consider, which is different from climate variability: climate change. The latter term refers to variations in the state of climate variables that are statistically significant and persistent within an extended period (more than a decade). When such a variation in climate variables is proved, then it can be concluded that some human-induced climate change is

happening [26]. Furthermore, this makes the description and prediction of future events even harder since the statistical average states of the past cannot be deployed for drawing the future state of the climate.

Numerical models are constructed to describe the complex interaction between the earth system's components and simulate future climate variables values. These numerical models are called General Circulation Models (GCM) when they are deployed for a global perspective. A GCM has on average a spatial resolution of 100x100 km, which can exclude the representation of smaller-scale phenomena. GCM can be downscaled and be representative a smaller area with a higher resolution (up to 11km). In that case, they are called Regional Climate Models (RCMs). A RCM can has a finer grid for its computations, and it is "guided" at the boundaries of its domain by a GCM [50]. Such models also take into account climate change in order to provide the most reliable outcomes.

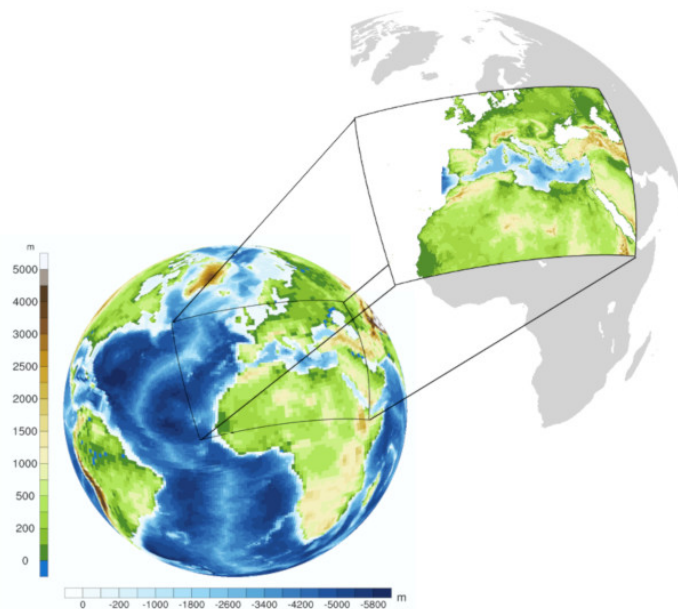


Figure 2.1: Scale of a RCM area. Source:[50]

2.1.2. Climate scenarios and projections

When making predictions about the future evolution of the climate, numerical models need to simulate the complexity of the climate system. However, they also need to explore and handle information about human interactions with such a system, which determine climate change. They are called anthropogenic factors, and they involve socio-economic, technological and demographic development. The evolution of such factors is not known in advance. Nonetheless, its effects can be represented by different scenarios, where a single scenario can result from a range of human development possibilities [26].

Those different scenarios can be represented by the emission pathways symbolizing the possible increase in greenhouse gases concentration. The most common used emis-

sion pathway method is the RCP (Representative Concentration Pathway). RCP is based on the concept of radiative forcing: the difference between solar irradiance absorbed by the Earth and the energy reflected, predicted in the year 2100 and expressed in W/m^2 . Radiative forcing is the key figure for explaining the greenhouse effect and can thus well represent the anthropogenic factors that influence climate models outputs. Common RCP values are 2.6, 4.5 and 8.5. Each of these values of radiative force would lead to different greenhouse gases concentrations and thus different global temperature increases. RCP 2.6 is likely to represent the situation in which the global temperature rises below 2 degrees Celsius by 2100. RCP 4.5 is considered as an intermediate scenario determining an increase of 2-3 degrees Celsius. In comparison, RCP 8.5 is considered the worst-case scenario with an increase in global temperatures of up to 3.7 degrees Celsius [26]. Each RCP combined with a GCM and its RCM downscaling leads to a precise climate projection.

Climate variables values are dependent on a specific climate projection, thus on a system model bounded by specific future anthropogenic forcing, constructed on a precise GCM and downscaled to an RCM. Therefore, those climate variables values over time and space do not have to be considered as forecasts derived by some initial condition, but more like projections based on specific scenarios [29].

In this study, we will extrapolate climate variables from multiple projections from the EURO-CORDEX platform. The latter is a portal where scientific communities worldwide publish their data about the predicted future evolution of the climate. The user of the platform can choose, e.g., the GCM, RCM, type of RCP and variables. In this study, we will make use of climate projections for the values of precipitation, maximum temperature, downwelling shortwave radiation, and sunshine duration. We will thus be able to extract both extreme weather events (heavy rainfall and heatwaves) and also the amount of sun-peak hours per year, which are determinants for the production of energy given by PV panels [28]. Scientists suggest that the best way to address uncertainties and make good use of climate projections outputs is to employ ensemble simulations [29]. Therefore, we will consider multiple climate projections for each considered variable to capture and properly handle the uncertainty present within the climate data.

2.2. Working of green, blue and yellow roofs

Roof surfaces constitute up to 50% of the urban area and thus have a great potential to mitigate climate change in the urban environment [37]. Roofs can host different combinations of green, blue and yellow roofs. An example is reported in Fig.2.2, where photovoltaic (PV) panels are placed in combination with green roofs. In this section, we will present the main characteristics of the roofing options considered in this study.

Green roof systems consist in a vegetation layer lying on some growing medium, called substrate layer. There is a thin drainage layer underneath that, which collects the rainwater in excess in small quantities. Depending on the type of vegetation, the soil type, and the layers' depth, many different green roofs exist. The most common are called *extensive roofs*. They include a substrate layer between 5 and 20 cm depth, and they are suitable for sedum, grasses and mosses, and other drought-resistant vegetation types. Thanks to the thin substrate, extensive green roofs can be installed on buildings that can not bear a high



Figure 2.2: A Green-yellow roof.

load due to their construction characteristics.

On the contrary, *intensive roofs* have a thick tier of soil (>1m), which makes them appropriate for the growing of bigger shrubs and trees. Although the aesthetic and biodiversity value of such a choice might be higher than the extensive equivalent, the thicker substrate layer also results in higher loads and construction costs. Hence, extensive roofs are more often selected, especially for implementation on existing buildings that were not conceived to carry high loads [48].

Blue roofs are roof layers designed to retain water, thus delaying the amount of runoff to the sewer system. The amount of storage depends on the layer's thickness and consequently is highly related to the load-bearing capacity of the construction. A control system can be installed to regulate the drainage, making the blue roof what is called an *active blue roof*. In these systems, a mechanical valve is present to control the amount of water stored on the roof and automatically choose the timing of drainage. On the contrary, *passive blue roofs* have no control of the water flow: when the water level reaches the outlet drain, the water is released either into the sewage system or onto the streets. In such passive systems, rain-water is stored on the roof until it evaporates [48].

A combination of green and blue functions is possible, and it is called **Green-Blue system**. When blue roofs are not installed as stand-alone, they can be placed beneath a green roof layer, enhancing the water retention capacity of the system (Fig. 2.3).

In this work, when not differently specified, we will consider only one type of green roof, the *extensive green roofs*. Moreover, blue roofs will not be analyzed as stand-alone but always coupled with green roofs as water retention layers beneath the vegetation. This choice is made because studies have shown that the combination of the two functions has a much greater impact [48]. Furthermore, since the performance of the roofs is maximized, and real values are provided in literature for specific parameters, *active blue roofs parameters* will be considered.

Yellow roofs, also called PV panels systems, can be implemented on roofs to supply the building or the grid with clean electricity. When the sunlight hits the solar panels, it is

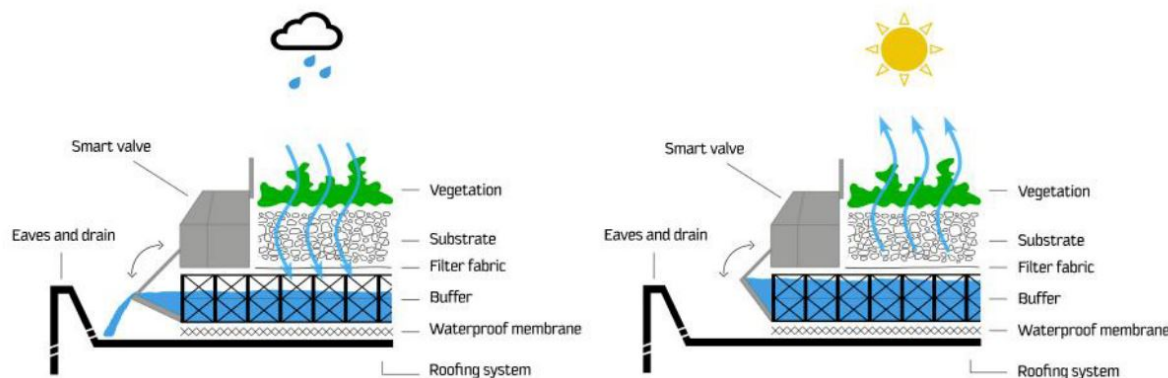


Figure 2.3: A Green-blue roof.

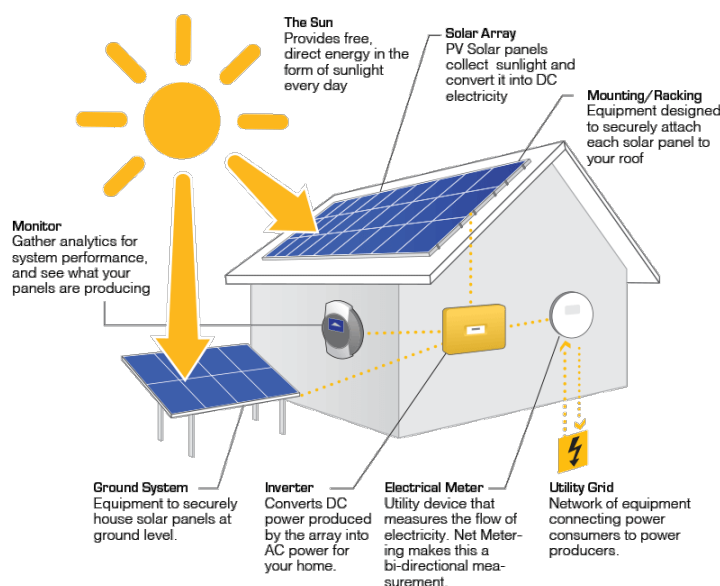


Figure 2.4: Yellow roofs: the photovoltaic system absorbs the energy from the sun and translates in into power.

converted into electricity (Fig 2.4). The efficiency of such translation depends on multiple factors: the system losses, the amount of sunlight received, the shadowing, the inclination and the direction of the roof. In this study, we will make use of a software called *ArcGIS Pro*, which computes the amount of solar radiation received by each building. Furthermore, it has been shown that putting green roofs beneath the PV panels can foster energy production. Indeed the operating temperature of PV panels is one of the main parameters on which the efficiency of the system depends, and green roofs can decrease the temperature in the surrounding [38].

2.3. Quantification of costs and benefits

This section will analyze costs and benefits linked to the placement of green, blue and yellow roofs. Costs must be considered taking into account the user of this model. As for benefits, a distinction can be made between effects that occur mainly to owners/users of the roofs (private) and the social effects (public) [37].

2.3.1. Costs

For the aim of this study, it is important to define the cost item in relation to the user of the tool. On the one hand, private entities such as residents and companies which own the buildings will be responsible for the investment costs. Such costs can be reduced thanks to the introduction of subsidies [49], which offset the costs to be more competitive with standard roof types [47]. Actors involved in the creation and sponsoring of such grants in the Netherlands could be municipalities, but also in the future regional water authorities [49]. Indeed, the latter parties may also be interested in the analysis proposed in this study. In this case, the item cost will be represented by the allocation of funds for subsidies, which usually cover a percentage of the total investment.

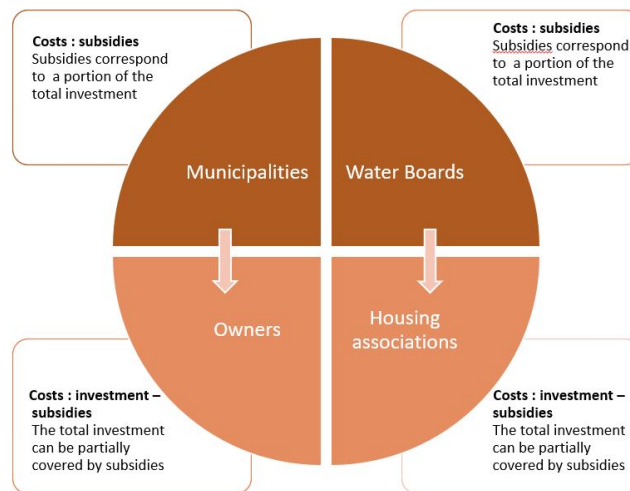


Figure 2.5: Definition of cost for this study, based on the user of the model. Source: [49]

2.3.2. Benefits

In literature, benefits derived by green, blue and yellow roofs are often differentiated into private and social benefits [15, 31, 37]. Private benefits include the ones reported in the following table (Tab 2.1):

Private benefit	Roof type	Details
Electricity yield	yellow	Less electricity from the grid has to be purchased.
Energy savings	green,blue	Better isolation is achieved, resulting in less need of heating and cooling systems.
Property value	all	Multi functional roofs increase the value of the building.
Lifespan increase	green,blue	Covering the roofs from damaging light and climate events increases their lifespan.

Table 2.1: Private benefits derived by different roofing options.

These private advantages derived by the different roofing options are disclosed for completeness of discussion. However, they will not be taken into account further since the

focus of this thesis will be on the societal benefits. Indeed, those benefits are the most recognized in literature, and they are the reasons why such multi-functional roofs are subsidized and installed in the first place: mitigate and adapt to climate change. The societal advantages will be incorporated into the model, linked to the spatial characteristics of the city whenever possible, and translated into economic benefits, as will be explained in the next section. Below (Tab 2.2), we present a list of the most commonly cited societal advantages derived by green, blue and yellow roofs [18, 37, 38].

Societal benefit	Roof type	Details
Clean energy production	yellow	Less greenhouse gases emissions.
Urban heat island reduction	green	Green roof can cool down the air.
Storm water runoff reduction	green,blue	Water buffering is made possible on top of roofs.
Increase of biodiversity	green	Different plant species increases biodiversity.
Pollution absorption	green	Plants covering the roof can absorb pollution.
Noise reduction	green	Noise is buffered by the plant and soil layers.

Table 2.2: Societal benefits derived by different roofing options.

2.4. Modeling green, blue and yellow roofs' societal benefits

Different techniques have been adopted to quantify costs and societal benefits derived from different roofing options.

2.4.1. Single building analysis

Costs and benefits of the different roofing options have been evaluated from the perspective of a single roof or a quantity of 1 m^2 of roof. Multiple approaches have been used for quantifying such aspects.

Cost-benefit analysis. Costs and benefits are the main aspects that decision-makers consider when evaluating the placement of green, blue and yellow roofs. The economic feasibility of such roofing systems has thus interested the scientific community, and many examples of cost-benefit analysis for green and blue roofs can be found in literature [18, 33]. The latter most often concern the evaluation of monetary equivalents of the mentioned societal benefits. As an example, PV panels' benefits are usually quantified in terms of avoided emissions compared to non-renewable sources and investment and maintenance costs [37].

MCA. Multi-Criteria Analysis (MCA) is used in several studies to compare different roofing solutions to be applied to one specific building. In [41] the authors review the main factors for the selection of a green roof vs a traditional roof through the use of expert-based weights and Analytic Hierarchy Process. The choice between extensive, semi-intensive and intensive green roofs is instead considered in [46]. Here expert judgment is used again as a tool to create the weights for the MCA.

Optimization problems. Optimization methods are used to tackle the problem of roofing option selection too. A first approach is provided in [36]. Here, different types of green and

yellow roofs are evaluated to maximize the return of investment based on constructed sustainability factors. Energy simulations are deployed to derive the main parameters for the optimization formulation. The objective is to maximize energy saving costs while minimizing the total expenses for installation of different types of green, white and yellow roofs on one building.

2.4.2. Multiple buildings analysis

Zooming out from the single roof perspective, introducing multiple potential locations for the different roofing options becomes a question of great interest in literature. Therefore, many studies analyze location-specific benefits and costs to determine the most suitable locations for the different roofing options.

MCA Multi-functional roofs are evaluated through economic criteria within the study conducted by Arcadis, on behalf of the municipality of Rotterdam [37]. In this research, the authors compare different roofing options on a common ground (the monetary equivalents of benefits and costs), including green, blue and yellow roofs. An Excel tool is constructed, which can receive as input the dimensions of a roof, the type of roofing applied, and the subsidy rate to compute the economic advantages of the chosen option. On the one hand, the approach is insightful in terms of evaluations of the pros and cons of every roofing system and offers the possibility of comparing multiple buildings' areas. On the other hand, the tool cannot indicate which is the most viable or favourable option for buildings choice among a set of suitable buildings, nor provides location-specific insights.

Spatial MCA An evolution of the analysis made in [37] is made by Versluis et al. in [49], where a spatial analysis is performed based on the economic equivalents provided in the original study. Here, the opportunities for roofing options on a municipality scale are obtained per type of neighbourhood, deploying the adjusted monetary equivalents of benefits. However, these costs are generalized and are not building-specific.

A finer grid is used for the analysis made in [51]. Here, green roofs' potential is mapped for the municipality of Rotterdam. Layers with opportunities and risks are created as a grid over the city of Rotterdam. This allows for a visualization, e.g., of high heat stress or flooding risk areas. This information is stored in fixed-dimension grid parts. Moreover, the best areas for green roofs are identified, in terms of grid position, not in building-specific terms.

Optimization Multiple roofs' focus and spatial analysis is instead merged through the means of optimization in [38]. Here the authors construct an optimization model, which aims at defining the best joint placement of PV panels and green roofs in order to maximize the energy production of each building. The authors also choose to deal mathematically with climate change uncertainty and parametric uncertainty. However, the considerations about green roofs are partial since the only computed benefits are linked to the energy efficiency of the building. The authors recommend researching the other positive aspects of green roofs to refine the outcomes of such optimization problems.

2.5. GIS

A geographic information system (GIS) is a framework that captures and analyses spatial and geographic data. GIS applications are tools and software that allow the user to handle and analyze spatial information data for visualization and mapping [17]. During this research, GIS software used are ArcGIS Pro, FME and QGIS. ArcGIS Pro is used to compute solar radiation potential for each building. FME, instead, is deployed to process the data extrapolated from the Klimaateffectatlas [4] and construct building-specific parameters for climate adaptation insights. Final results are mapped into the software QGIS.

2.6. Uncertainty in Optimization

In order to treat the uncertainty present in this problem, we adopt the framework and nomenclature proposed in [19]. According to [19], data uncertainty in optimization can be integrated into modelling problems through two main approaches: uncertainty/sensitivity analysis and optimization under uncertainty. The first approach does not provide specific unique solutions to the modelling of the problem, but it can explain alternative outputs in light of different parameters' choices. On the contrary, optimization under uncertainty is implemented when a specific solution is needed. It can be divided into two main categories, namely robust and stochastic optimization. Robust optimization assumes that the uncertain data lies within an uncertainty set and that it is not possible to infer anything about its probability of occurrence [22]. Stochastic optimization assumes that the probability distribution of uncertain data is known or can be estimated. In the following sections, both approaches (sensitivity analysis and optimization under uncertainty) will be used: the first will be deployed to understand which variation in the parameters leads to certain trends in the decision variables. In contrast, the second will enable integrating different climate projection data within one single model, producing a unique solution.

3

Deterministic model

In this chapter, we will present the reasoning behind the construction of the model, which looks for the optimal placement of green, blue and yellow roofs among a set of suitable buildings. After providing the real-life problem description, we will explain the general characteristics of the formulation in the second section. Such guidelines will be proposed following the aim of filling some research gaps and of satisfying usability requirements. Following this part, a comprehensive methodology will be constructed, which will guide the reader towards the deterministic version of the model. Lastly, insights about the uncertainty of the parameters will be provided to lead the reader to the optimization under uncertainty model, which will be developed in the following chapters.

3.1. Real life problem description

A municipality or another interested stakeholder has a budget B to apply three roofing systems on the city's buildings. The aim is to reduce the negative impact of climate change on the city and reduce greenhouse gas emissions. Therefore, the roofing options among which to choose are green, blue and yellow roofs. By allocating some budget now for green and blue roofs, the costs derived by extreme events such as heatwaves and heavy rainfall would be avoided in the future, thus achieving climate adaptation targets. Moreover, yellow roofs (PV panels) can determine a positive impact in terms of climate mitigation, allowing for a reduction in total greenhouse gases emissions, leading to some economic benefit for the municipality [37]. Therefore, the objective of the problem is to maximize adaptation and mitigation goals of the municipality analyzed in monetary terms by placing the three types of roofs in the optimal locations, considering the difference in buildings' suitability, potential, and added value to the neighbourhood.

3.2. General characteristics

A deterministic formulation of the problem is provided in this section. The variability of climate change scenarios is not yet considered, nor is the uncertainty behind certain parameters. The time frame where the effects of green, blue and yellow roofs are analysed is 25 years; thus, the time frame will be 2021-2045. This choice is determined by looking at the average lifespan of green, blue and yellow roofs. The roofing option with the shortest lifespan is yellow roofs: they last on average 25 years [18, 37, 38]. This choice forces the

analysis to focus on 25 years in the future, as including more time would not allow a comparison between all roofing options on the same ground.

To properly formulate the problem in terms of optimization, we outline some modeling requirements and assumptions. The following are the major aspects that have been considered for the problem formulation.

1. **Computational complexity:**

As explained in section 2.6, the problem is subject to two major types of uncertainty to be tackled: the first deriving from climate variables which are uncertain by nature, and the second linked to a lack of consensus in the literature regarding the parameters used in the formulation. Therefore, one aim of this study is to identify the robustness of the optimal solution under all these uncertainties. Performing optimization under uncertainty methods and sensitivity analysis can be costly in terms of computational complexity. Consequently, it is important to reduce to the minimum the complexity of the formulation, allow for a feasible running time, and identify sensitivity analysis results.

2. **A location-specific solution:**

It is important to stress that the goal of this model is to identify which buildings, among the set of suitable ones, are most befitted to host green, blue and yellow roofs. Therefore, specific characteristics of each roof should be used to define the constraints. They should include, e.g. the risk of flooding in the area close to the building and the irradiation potential of each roof.

3. **The societal perspective:**

Many benefits are mentioned for the three types of roofs, and literature divides those into societal and individuals' benefits [18][30][16]. In formulating the problem, a scope limitation choice has been made to only account for the societal perspective. Firstly, because such benefits have a strong link with location-specific characteristics, thus they respect criterion 2. Secondly, because of Sweco's interest in the project.

As a consequence, the following choices were made:

1. **Simplify roofs functioning modeling:**

Green, blue and yellow roofs have specific characteristics which make their performances vary in different contexts. For example, green roofs can cool the air under specific characteristics of the building and the climate condition. In contrast, blue roofs can collect more or less water depending on the amount of rain already present in the water storage layer. This study does not aim to precisely evaluate the quantities of heat absorbed or water drained but to offer an overview. Thus, the choice has been made to simplify as much as possible the treatment of such complexities. Therefore, to describe the operations of the roofs in terms of mathematical constraints, a literature study has been performed to find parameters and functions that would allow for such a correct but straightforward mathematical formulation of complex physical phenomena.

2. **Include parameters which reflect the municipality's structure:**

It is important to consider the shape of the city where the roofs are placed to achieve a

result that reflects and incorporates the unique characteristics of each building. Such characteristics need to be summarized into building-specific parameters, which express the impact on the municipality-scale of potentially placing one roofing option on top of some specific building. For example, it is straightforward to think that blue roofs may be beneficial for areas with high flooding risk. Thus a flooding risk utility indicator needs to be constructed for each roof, referring to its location.

3. Include climate variables:

Climate variables can deeply influence the performance of green, blue and yellow roofs [28, 48]. Therefore average values for climate variables would not be sufficient for the time frame considered. Moreover, the climate is believed to see sharp changes in the next decades. Thus current averages would not be able to represent the future utility of the installations. Therefore, it is crucial to include climate variables as much as possible in the formulation of the problem to underline within the solution the functionality of the installations concerning the climate they operate in.

3.3. Model construction process

As outlined in Section 2.4, many possible societal benefits can be outlined for the placement of green, blue and yellow roofs, while even more perspectives could be considered when integrating them into a mathematical model. Therefore, it is important to make modelling choices that allow the societal benefits of each roofing type to be comparable, reliable, and consistent. We have thus chosen to take one source as the base for the modelling choices. The funnel chart below indicates which steps are further taken to develop from that a location-specific optimal placement model for different roofing options.

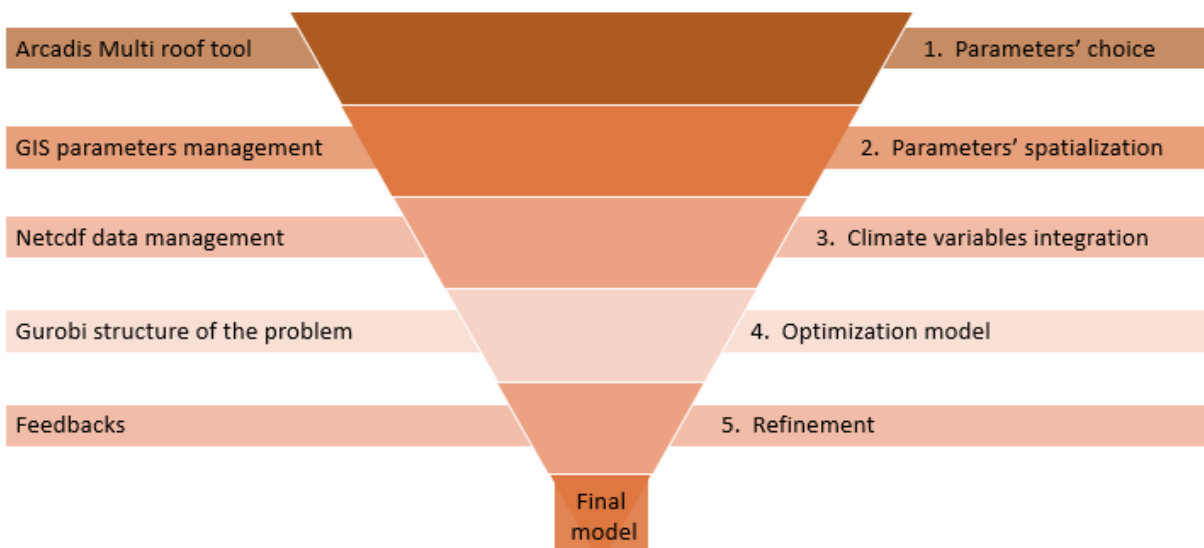


Figure 3.1: Modeling choices' funnel.

For the study chosen as starting point of the model, named *LIFE@Urban Roofs* [37], the municipality of Rotterdam and its partners received a subsidy from the European Commission's LIFE program for environmental and climate action. The aim of *LIFE@Urban Roofs* is to provide insights into the advantages of multi-functional roofs. Therefore, it is developed as a complete overview of costs and societal benefits, gathered together for all roof types considered, using Dutch sources. The reference to the Dutch context is one of the main reasons the study was considered well suited to be further deployed in this study. Many other pieces of research [12, 47, 51] have tried to gather data and parameters for identifying the best locations for implementing climate adaptation strategies. However, the different approaches and sources used do not allow merging these multiple perspectives: the merging would result in non-consistent modelling choices. As an example, the damages caused by stormwater flooding has been considered in [51] as the damage to buildings and streets. In contrast, in [37] they have been considered in terms of shadow costs, thus the avoided costs for renewing the sewage system in the area. If all those aspects were considered together, the benefits for different roofing options would be less comparable.

As stated in 2.4 the overview made in [37] is not location-specific. Parameters have a fixed value or range of values, but there is no link between them and the location of the considered roof. Therefore, the first step which we will go through is the *Parameters' spatialization*. Indeed, through FME software and open data sources, the impact of climate change can be modelled and consequently used to modify the parameters into a location-specific form. In this study, we include the impact of flooding, heat and solar radiation. Instead, we exclude benefits derived by biodiversity increase and pollution mitigation of green roofs, as those are far more complex to model in a location-specific way, and not of great interest for the applicability aims required by Sweco.

Moreover, it is mentioned in the literature that climate variables can deeply influence the results of the model. However, in [37] the parameters are not specified in such a way that they become climate-dependent. We will, therefore, also integrate climate variables into our model, modifying the parameters accordingly. *Gurobi* solver will be used to solve the model and provide a solution.

3.4. Deterministic model

The following section provides an overview of the problem sets, decision variables, parameters, constraints, and objective function. Here, we consider only one climate projection as input, and we assume fixed values for the parameters.

3.4.1. Sets and indices

- $i \in R$ set of roofs available for the installations.
- $j \in P$ set of mm of precipitation occurring within a period of intense rainfall.
- $z \in H$ set of max temperatures during heatwaves in deg Celsius.

3.4.2. Parameters

In Table 3.1 the subscript G will indicate Green roofs, B Blue roofs and Y Yellow roofs.

Parameter	Description	Unit
B	budget available from municipality	€
s	rate of subsidy	$\in [0, 1]$
p_G, p_B, p_Y	price of the different installations	€/m ²
a_i	roof area available for installation	m ²
$m(i, z)$	people affected by heat in day z	people/day
$w(j)$	water falling during a heavy rainfall event j	mm/day
d	total sun peak hours in the considered period	hours
$r_G(i)$	utility rate for heat reduction. Areas with higher urban heat island effect are assigned higher values	$\in [0, 1]$
$r_B(i)$	utility rate of flooding reduction. Areas with higher levels of water are assigned higher values	$\in [0, 1]$
$r_Y(i)$	rate of solar radiation which is actually captured by the roof, due to shadowing and orientation	$\in [0, 1]$
h_G	thickness of water retention layer for green roofs, thus the water which can be stored into the water layer during a heavy rainfall	mm
k_G	rate of absorption of water for green roofs, during a heavy rainfall event	mm
k_B	rate of absorption of water for blue roofs, during a heavy rainfall event	mm
Q	kWh produced during one peak hour by a PV panel	kWh/m ²
θ	rate of increase in efficiency for PV panels due to GR presence	$\in [0, 1]$
c_G	avoided cost of heatwave	€/person
c_B	avoided cost of extreme rainfall	€/m ³
c_Y	economic benefit of producing clean energy, computed based on avoided green house gasses emissions	€/kWh
$b_G(i)$	benefit derived by Green roof installation: sum of the previous three factors	€
$b_B(i)$	benefit derived by Blue roof installation (adaptation)	€
$b_Y(i)$	benefit derived by Yellow roof installation (mitigation)	€

Table 3.1: Overview of the parameters and variables' names.

3.4.3. Decision Variables

$$\begin{aligned}
 x_Y(i) &\in \mathbb{R}^+ && m^2 \text{ of yellow roofs to be placed on roof } i \\
 y_G(i), y_B(i) &\in \{0, 1\} && \text{active if Green and Blue roofs are to be placed on roof } i \text{ respectively.}
 \end{aligned}$$

When green and blue roofs are placed, we assume they cover the whole available area; we later derive the m^2 of green and blue roofs to be placed on building i by simply multiplying the binary variables with $a(i)$, the area of the roof.

3.4.4. Constraints

- Budget constraint:

$$\sum_{i \in R} s \cdot (p_G \cdot y_G(i) \cdot a(i) + p_B \cdot y_B(i) \cdot a(i) + p_Y \cdot x_Y(i)) \leq B$$

Each entity which aims to apply green, blue and yellow roofs will have a specified maximum budget for it. The actual prices p_G, p_Y, p_B may partially be funded by the municipality. In the latter case the subsidy rate s would have a value different than zero.

- Space constraint:

$$x_Y(i) \leq a(i) \quad \forall i \in R \quad (3.1)$$

$$y_G(i) \geq y_B(i) \quad \forall i \in R \quad (3.2)$$

A physical constraint must be modelled: the roof area available for installing different roofing options cannot be exceeded. Green and blue roofs are considered roofing substitutes, meaning they are installed over the whole roof area. Thus the binary variables are explanatory of this when multiplied by the total area. On the contrary, the amount of PV panels to be placed is selected depending on the household's needs. In this frame, we will determine in this model the m^2 of yellow roofs to be placed per roof as a continuous variable, bounded as in Eq. 3.1.

We choose to allow blue roofs only as layers that can be placed beneath green roofs, not as stand-alone systems. This is presented in Eq. 3.2.

Flat roofs and low sloped roofs are suitable for Green and Blue roofs, while PV panels can also be placed on sloped roofs. In this frame, we will only consider as suitable the flat roofs. otherwise, the non-flat roofs N set should be available only for Yellow roofs installations, thus imposing by default $y_G(j) = 0, y_B(j) = 0 \forall j \in N$.

- Benefit: clean energy production

$$b_Y(i) = c_Y \cdot Q \cdot d \cdot x_Y(i) \cdot r_Y(i) \cdot (1 + \theta \cdot y_G(i)) \quad \forall i \in R$$

Producing and deploying clean energy, i.e. energy derived by solar panels, can help municipalities reach some important goals in terms of climate mitigation. In [37] a study from *CEDeft* is used as a reference, to assign to each kWh of clean energy produced, an equivalent in €. This economic equivalent is derived considering the avoided emissions of different pollutants, which would be emitted in case the same amount of energy would come from common dutch grey sources [37]. The latter are summarized in the value c_Y and expressed in €/kWh of energy produced.

A formula is taken from [38] in order to compute the energy yield in kWh of yellow roofs installations. This formula is indeed reflecting the major goals mentioned

in section 4.4: the inclusion of both climate variables and specific characteristics of each building. The energy yield provided by each m^2 of PV panels is given by the average amount of energy produced by 1 m^2 , Q , during a peak hour, multiplied by the total amount of peak hours d . Then this factor is scaled with $r_{Y,i}$, which captures the intensity of the average solar radiation received by each rooftop. It takes values $\in [0, 1]$.

- Benefit: avoided storm water flooding

$$b_B(i) = c_B(i) \cdot \sum_{j \in P} (k_B \cdot w(j) \cdot y_B(i) + k_G \cdot h_G \cdot y_G(i)) \cdot a(i) \cdot r_B(i) \quad \forall i \in R$$

It is possible to evaluate avoided costs determined by runoff water in terms of $\text{€}/m^3$ of water in excess on the streets, as is done as an example in [37].

Here, $b_B(i)$ represents the total avoided costs, derived from the m^3 of water which was retained by blue and green roofs for each heavy rainfall event. Such volume of water is computed taking the area of blue ($y_B(i) \cdot a(i)$) and/or Green roofs ($y_G(i) \cdot a(i)$) multiplied by the amount of water fallen during even $j \in J$, w_j . The water can be captured only if the capacity of the layer allows for that. Thus, we consider that a portion of the total water fallen k_B can be stored by a blue roof layer. Also, green roofs will store only a portion of k_G of the maximum capacity h_G .

During heavy rainfall, water gathers in the streets and may cause disruptions and damage. Due to the shape of the city, some areas are more affected than others. The difference among such areas is reflected in the usefulness of applying water retention roofs. Such usefulness is encapsulated into the parameter $r_B(i)$. This approach is similar to the one presented in [38], where the roofs with the higher solar radiation potential were provided with higher scores between 0 and 1. As done in [47, 51], it is assumed that roofs that are right on top of a high flooding-risk street have to be prioritized. Thus they have to be assigned a high utility since they allow water management in the areas where it is most needed.

- Benefit: urban heat island mitigation

$$b_G(i) = \sum_{z \in H} c_G(i) \cdot m_G(i, z) \cdot y_G(i) \cdot r_G(i) \quad \forall i \in R$$

Green roofs have the ability to alleviate heat stress in cities [18, 48], which, in turn, can determine a reduction in costs derived by health effects on the population [37]. Results in [37] define the reduction in temperature obtained by green roofs in the surrounding micro-climate in terms of impacted population. For every degree Celsius higher than 25 and smaller than 31, some amount of people $m_G(i, z)$ can avoid hospitalization due to heat. More information about its computations is given in Appendix A.1. Parameter $m_G(i, z)$ is roof-specific: the dimension of the roof, the amount of greenery in the area, and the population density of the area are all considered.

3.4.5. Objective function

$$\max \sum_{i \in R} (b_G(i) + b_B(i) + b_Y(i))$$

We chose to convert all the beneficial aspects of Green, Blue and Yellow roofs into economic benefits to quantify a municipality's adaptation and mitigation goals. Hence, the objective function maximizes the economic benefit derived from the avoided costs and gained benefits, as defined in the equality constraints.

3.4.6. Deterministic problem overview

$$\begin{aligned} & \max \sum_{i \in R} b_G(i) + b_B(i) + b_Y(i) \\ & \sum_{i \in R} s \cdot (p_G \cdot y_G(i) \cdot a(i) + p_B \cdot y_B(i) \cdot a(i) + p_Y \cdot x_Y(i)) \leq B \\ & x_Y(i) \leq a(i) \quad \forall i \in R \\ & y_G(i) \geq y_B(i) \quad \forall i \in R \\ & b_G(i) = \sum_{z \in H} c_G \cdot m_G(i, z) \cdot y_G(i) \cdot r_G(i) \quad \forall i \in R \\ & b_B(i) = c_B(i) \cdot r_B(i) \cdot a(i) \cdot \sum_{j \in P} (k_B \cdot w(j) \cdot y_B(i) + k_G \cdot h_G \cdot y_G(i)) \quad \forall i \in R \\ & b_Y(i) = c_Y \cdot Q \cdot d \cdot x_Y(i) \cdot r_Y(i) \cdot (1 + \theta \cdot y_G(i)) \quad \forall i \in R \end{aligned}$$

4

Uncertainty in the problem

Real-life optimization problems often contain uncertain data, which can be inherently stochastic or uncertain due to errors or lack of knowledge [22]. The task of uncertainty characterization can be complex, but exploring the nature of uncertainty for parameters' values provides more realistic outcomes than using deterministic values. Indeed, using fixed values for parameters can lead to sub-optimal model outcomes [19]. This discussion aims to characterize the different types of uncertainty that arise in the construction of the model and to expound on the methodologies used to analyze and handle them.

4.1. Uncertain aspects of the problem

Green, blue and yellow roofs are highly interesting solutions for municipalities in the Netherlands which wish to adapt to climate change and to contribute to its mitigation [14, 37]. Finding the optimal placement for these roofing types is subject to three significant forms of uncertainties: climate change, parameters and modeling uncertainty.

Climate uncertainty plays a role within the model because climate variables, such as daily temperatures and rainfall influence how green, blue and yellow roofs work. Climate predictions, however, are far from certain [25], especially when considering long-term predictions, which are also affected by climate change [26]. Nonetheless, long term predictions need to be employed within this frame since it is important to evaluate the performance of green, blue and yellow roofs over their entire lifespan [38]. These roofing systems are reported to have an average lifespan of 40-50 years (green and blue roofs) and 25 years (yellow roofs) [38]. Therefore, climate scenarios will be here considered up to the year 2045, and they will lead to another uncertainty factor within the constructed model.

Parameters' uncertainty is strongly linked to the functioning of green, blue and yellow roofs, as this is very complex in itself. As an example, it is not known precisely how much a green roof can cool the air, as this phenomenon depends on fluid interactions and often unavailable data, such as wind direction and evaporation potential [39]. Consequently, some parameters linked to the operation of the roof systems will also determine uncertainty within the model. In this discussion, this type of uncertainty will be referred to as technical uncertainty.

Another source of parametric uncertainty within the model arises from adopting economic equivalents for the benefits derived from green, blue and yellow roofs. Indeed, different roofing systems provide different benefits. For example, green roofs can mitigate urban heat island, blue roofs can reduce stormwater runoff, and yellow roofs produce clean energy. It is thus important to compare these roofing systems on common ground to avoid the complexity of multi-objective formulations. These types of sustainable development technologies need to be supported by quantitative estimates of the costs and benefits to encourage their use [16]. Some scholars have focused on determining the economic benefits that arise with each roofing option by computing the monetary equivalents for their different functions [16, 18, 31]. Moreover, during the discussions with the daily supervisor at Sweco, it has been underlined that potential users of this model would be highly interested in the economic aspects of the optimal placement of green, blue and yellow roofs.

Modelling uncertainty originates from the assumptions made in the translation of physical phenomena into mathematical formulas. Even if replicating the real functioning of these roofing systems through a mathematical model can be very complex, formulas are constructed to represent in a simplified way the working of green, blue and yellow roofs in relation to the municipalities' system. Assumption and modelling choices are thus necessary. However, since the model will be constructed with the best available knowledge and with underlined limitations, modelling uncertainty will not further be taken into account nor analyzed within this study.

4.2. Climate change uncertainty

As explained in Section 2.1, when dealing with climate adaptation and mitigation strategies like green, blue and yellow roofs, climate change represents an aspect of deep uncertainty that is not eliminated over the short, or long term [25]. Three primary sources of uncertainty are recognized in climate long term predictions: natural climate variability, uncertainties of the responses to climate forcing factors, uncertainties within those factors' nature [25, 44]. As an example, political choices which would determine future greenhouse gases emissions are unknown, and they would determine hard-to-predict values for a forcing factor like CO_2 . Due to the complexity of these uncertainties, no method exists to understand the reliability of every scenario's output.

To properly insert climate variables derived by future prediction within the model of green, blue and yellow roofs' optimal placement, it has been chosen to work on an ensemble of possible future predictions. Indeed, scientists suggest employing ensemble simulations to address uncertainties and make good use of climate projections outputs. Thus multiple outputs are derived by different models [29] and further used. Considering different possible future scenarios through multiple climate projections allows for more robust and aware decision making. Different methods exist which can integrate this suggestion within the frame of an optimization model.

4.3. Tackling climate uncertainty in optimization

On the one hand, performing uncertainty and sensitivity analysis for climate variables can lead to interesting insights regarding the influence of climate events' occurrence on the choice of installing green, blue and yellow roofs. On the other hand, it is believed that the practical aims of this model will best be met when the climate uncertainty is incorporated through the means of optimization under uncertainty. In literature, insights provided by sensitivity analysis of climate variables are mainly used to choose whether or not climate adaptation strategies need to be implemented at all [25]. For the aim of this model, it is of no importance to decide whether or not to place the roofs by evaluating the response of the roofs to certain climate events. Indeed, the model is constructed to be used by policymakers who are already willing to allocate a budget to implement this type of climate adaptation strategy. Therefore, optimization under uncertainty will be adopted for climate uncertainty. More specifically, we will integrate climate projections into the optimization model through robust and stochastic optimization techniques.

4.3.1. Robust optimization

Some authors strongly suggest the use of robust optimization techniques for integrating climate projection ensembles within decision-making models [34] [25]. Robust decision making consists of a decision framework specifically suited for decisions with long-term consequences and deep uncertainty [25]. More specifically, the goal of robust optimization is to make a decision that is feasible for every possible set of constraints and optimal with respect to some measure, an indication of robustness [21]. Several concepts can be gathered under the name of robust optimization: from the classical strict robustness, or min-max optimization, to the more recently developed light robustness and regret robustness [21].

We reformulate our deterministic problem into a strict robust optimization problem. Since the objective function is uncertain while the constraints (inequalities) are not, maximizing for the worst-case scenario corresponds to maximizing the benefits for the minimum-benefit scenario. Let $\omega \in \Omega$ denote each possible projected climate scenario, where Ω is a finite discrete set of such scenarios. In this case, climate variables d , $w(j)$ and $m(i, z)$ - respectively being the amount of sun-peak hours, the amount of rain during heavy rainfall days, the impacted people during heatwaves - become $d(\omega)$, $w(j, \omega)$, $m(i, z, \omega)$. The computed benefits also become stochastic and receive an ω as a subscript. Indeed the climate variables change for every scenario considered. Thus all variables depending on those climate variables also become uncertain.

$$\begin{aligned}
\max \quad & \min_{\omega \in \Omega} \left(\sum_i b_G(i, \omega) + b_B(i, \omega) + b_Y(i, \omega) \right) \\
\text{s.t.} \quad & \sum_i s \cdot (p_G \cdot y_G(i) \cdot a(i) + p_B \cdot y_B(i) \cdot a(i) + p_Y \cdot x_Y(i)) \leq B \\
& x_Y(i) \leq a_i \quad \forall i \in R \\
& y_G(i) \geq y_B(i) \quad \forall i \in R \\
& b_G(i, \omega) = \sum_{z \in H} c_G \cdot m_G(i, z, \omega) \cdot y_G(i) \cdot r_G(i) \quad \forall i \in R \quad \forall \omega \in \Omega \\
& b_B(i, \omega) = \sum_{j \in P} c_B(i) \cdot r_B(i) \cdot a(i) (w(j, \omega) \cdot y_B(i) + k_G \cdot y_G(i)) \quad \forall i \in R \quad \forall \omega \in \Omega \\
& b_Y(i, \omega) = c_Y \cdot Q \cdot d(\omega) \cdot x_Y(i) \cdot r_Y(i) \cdot (1 + \theta \cdot y_G(i)) \quad \forall i \in R \quad \forall \omega \in \Omega
\end{aligned}$$

4.3.2. Stochastic optimization

In the literature, there exist some examples where stochastic optimization is used to incorporate climate uncertainty within optimization models [20, 38]. In these cases, two- and multi-stage stochastic programming is used. The objective function is represented by maximizing the expected value of benefits derived by different climate scenarios. Each scenario is part of the chosen ensemble of climate projections, and equal probability is assigned to each of them.

Here a transcription of the optimal placement model for green, blue and yellow roofs is performed, using a similar approach to the one presented in [20, 38]. Let η_ω denote the realization probability of scenario $\omega \in \Omega$, where Ω is a finite discrete set of projected climate scenarios. Another change occurring within the transcription of the model into a stochastic optimization model is the fact that the benefits $b_Y(i)$, $b_B(i)$, $b_{GR}(i)$ become second stage variables with an ω subscript. Specifically, once the first stage decision is taken about where to place green, blue and yellow roofs ($y_{GR}(i)$, $y_B(i)$, $x_Y(i)$ assume some value), then the benefits are computed for each scenario ω .

$$\begin{aligned}
\max \quad & \sum_{i \in R} \sum_{\omega \in \Omega} \eta_\omega (b_G(i, \omega) + b_B(i, \omega) + b_Y(i, \omega)) \\
\text{s.t.} \quad & \sum_i s \cdot (p_G \cdot x_G(i) + p_Y \cdot x_Y(i) + p_B \cdot x_B(i)) \leq B \\
& x_Y(i) \leq a_i \quad \forall i \in R \\
& y_G(i) \geq y_B(i) \quad \forall i \in R \\
& b_G(i, \omega) = \sum_{z \in H} c_G \cdot m_G(i, z, \omega) \cdot y_G(i) \cdot r_G(i) \quad \forall i \in R \quad \forall \omega \in \Omega \\
& b_B(i, \omega) = \sum_{j \in P} c_B(i) \cdot r_B(i) \cdot a(i) (w(j, \omega) \cdot y_B(i) + k_G \cdot y_G(i)) \cdot \eta_\omega \quad \forall i \in R \quad \forall \omega \in \Omega \\
& b_Y(i, \omega) = c_Y \cdot Q \cdot d(\omega) \cdot x_Y(i) \cdot r_Y(i) \cdot (1 + \theta \cdot y_G(i)) \quad \forall i \in R \quad \forall \omega \in \Omega
\end{aligned}$$

In the frame of this project, the outcome of both robust optimization and stochastic optimization will be provided. Such outcomes will result in a unique solution for each run in terms of optimal location and objective value. Such results will be then analyzed under different combinations of parameters values, which are not linked with climate uncertainty, but with technical and monetary parameter uncertainty, as will be explained in Section 4.4.

4.4. Parameters uncertainty

In the formulation of the optimal placement model for green, blue and yellow roofs, a total of 8 parameters among the monetary equivalents and the roofing technical parameters are considered uncertain. Indeed, literature often does not agree on the degree of advantages these roofing systems can have nor provides unique fixed values for economic equivalents of their benefits. Furthermore, cost-benefit analysis for green, blue and yellow roofs found in literature often assume average monetary values are representative enough [18], or propose that model users provide those values as inputs [37]. Investigating the consequences of some choices or others can be crucial for a deeper understanding of the matter.

Therefore, the uncertainty underlying the parameters will be investigated in this study. The concept of uncertainty and sensitivity analysis will thus be applied to the economic and technical parameters, as will be explained in the next sections, with the following aims:

- Identify the combination of parameters choices that provide similar results;
- Shed light on the impact of uncertain parameters on the model output;
- Suggest how to handle these uncertainties when solving a real-life problem.

4.5. Tackling parameters' uncertainty in optimization

In this study, the method proposed in [19] is followed to analyze the parametric uncertainty behind the problem. We sample the parameters from their uncertainty ranges and solve the model for multiple combinations of such parameters. We thus obtain multiple solutions, which differ both by roof placement and total benefits gained. The approach introduced in this section offers tools to understand which parameters' values lead to which type of solutions. We analyse the similarity between solutions through a specific measure: cosine similarity. The output of this phase is later provided as input to a clustering algorithm that identifies similar solutions. Eventually, CART subspace partitioning analyses the classification made in the clustering and provides insights into the variation of the model outcomes in relation to the sampled parameters. The reasons for the choices made are elaborated in the following sections.

4.5.1. Sampling method

Different literature sources provide different values for the parameters used in this model. Initially, a collection of potential values for each parameter was made with the aim of using all of them to perform different model experiments (Table 4.1). However, the methodology expounded in Section 3.3 underlines the importance of starting from one single proposed approach for the sake of consistency. Furthermore, many parameters were expressed with different units and had thus to be contextualized and appropriately converted, which turned

out to be a very complex issue. Therefore, parameters' values are taken from the single source chosen as a starting point ([37]) but are considered as random variables instead of deterministic values. The mentioned overview of parameters (Tab 4.1) made it possible to clearly define the ranges inside which the uncertain parameters would lie. Since we consider all sources equally reliable, each uncertain parameter is associated with a uniform distribution within the provided range.

Parameter	Values	Unit	Source	Note
Water retention	300-800	€/m ³ of water	[37]	m3 water stored
	30	\$/m ² roof per year	[18]	
	0.73-2.06	\$/m ² roof per year	[30]	
	8-26	\$/m ² roof per year	[16]	infrastr. improvement
	0.00071-0.0024	\$/m ² roof per year	[16]	avoided flooding
Heat stress mit.	0.5-1.5	° Celsius	[33]	unknown GR unit
	0.0083-0.0012	\$/m ²	[16]	convert in €/°
	less patients	-	[37]	summarize
Clean energy	per pollutant	€/m ² of roof	[37]	summarize
	CO2 equivalent	kg/CO ₂ eq	[23]	convert in €/m ²
Efficiency PV+GR	1.35–3.35	%	[33]	
	3.33–8	%	[38]	

Table 4.1: Different sources provide different estimations for the economic and technical parameters.

The first step of the proposed methodology starts with randomly sampling the parameters from the specified ranges to later solve the problem with different combinations of such parameters and output different experiments-specific solutions. The most common sampling technique used in the literature concerning green roofs is the Latin hypercube sampling technique [19, 30].

Latin hypercube sampling (LHS) is a method that generates a near-random sample of parameter values from a known uncertainty range [5]. It generates a random sample of N points for each uncertain input. The sample points are distributed across all possible values within the provided ranges, contrary to other sampling methods like Monte Carlo, where sampled points can end up all clustered closely. It works as follows: first, each input distribution is partitioned into N intervals of equal probability, then one sample from each interval is taken [5]. The LHS method is considered to be appropriate for the model under analysis in this thesis. Indeed, choosing a uniform distribution associated with LHS will make it possible to consider sampled parameters distributed across the whole considered ranges.

4.5.2. Format of the input for uncertainty analysis

The vectors representative of the experiment-specific output must be formatted appropriately to perform the next steps present in this Chapter. Since the aim is to provide vectors representing the variation in locations chosen for each type of roof, we chose to output for each roof $i \in R$ the associated vector of benefits for the three roofing options. Let n be the number of roofs in set R . Then for every combination of parameters m , vector \mathbf{X} , will con-

The cosine distance is preferred over other distance metrics, such as the Euclidean distance. Indeed, cosine distance evaluates the angle spanned by the vectors in the $3 \cdot n$ dimensional space. Thus it is heavily influenced by the presence of 0 in the vector since that would correspond to a missed vector component in one dimension [40]. Since each entrance of the vector corresponds to a direction in the space, cosine similarity considers the ordering we have chosen for the input. Indeed, value $x_G(i, m)$ will contribute to the similarity if it is close to value $x_G(i, l)$ for some combination of samples m and l . On the contrary, Euclidean distance does not take this order into account, and compute the distance based on the module of the vectors.

The cosine measure is also helpful in this case as it applies well to high-dimensional and sparse vectors[40]: our output matrix indeed contains a majority of zero-values. All in all, the cosine distance can reflect similar investment patterns between the m experiment vectors, which depend on the uncertain parameters.

4.5.4. Clustering technique

The cosine distance matrix is provided as input to a clustering algorithm to cluster the outcomes and identify similar groups of results. Among all existing clustering techniques, a hierarchical clustering algorithm is chosen in this frame, as done in a similar problem handled in [19]. Hierarchical clustering is preferred over non-hierarchical clustering because it systematically evaluates all potential groupings and lets the analyst choose the number of clusters after visualizing the potential clusters on a dendrogram.

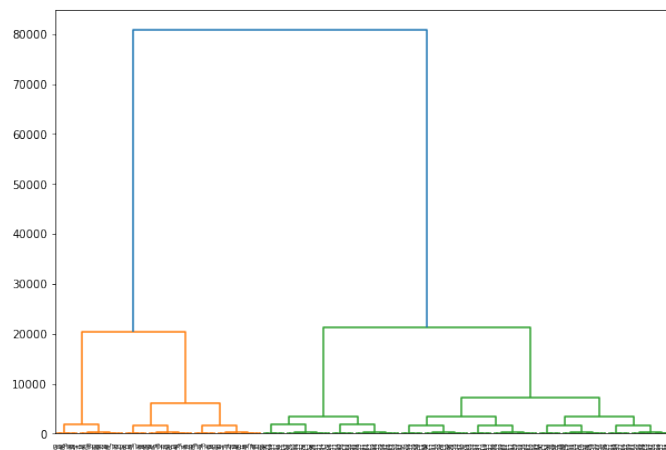


Figure 4.2: Dendrogram example for hierarchical clustering.

Between the existing agglomerative and non-agglomerative clustering options, agglomerative hierarchical clustering is preferred. It relies less on the initialization of parameters and thus on fewer external choices [1]. The algorithm receives as input the similarity matrix described in Section 4.5.3. A linkage criterion must be chosen. In the case of a predefined cosine distance, there are three possible linkage methods: single, complete and average [1]. Computing single linkage proximity between two clusters means computing the distance between their two closest objects. On the contrary, complete linkage defines the shortest link-distance as the proximity between their two furthest removed objects. Consequently,

the clusters that are combined have the smallest distance between any two cluster elements. Finally, with average linkage, the proximity between two clusters is the mean of all proximities between the objects of both clusters in comparison [1]. Therefore, all data points within each of the two clusters have equal influence on the proximity. We use the complete linkage method, as is done in [19], to ensure the creation of compact clusters with a high in-cluster design similarity.

4.5.5. Choosing the number of clusters

The choice of the number of clusters for the chosen method lies in the hands of the analyst. First of all, the practical utility of clustering needs to be taken into account. For example, clustering the high number of solutions in a high number of clusters may result in a lack of insights. Furthermore, by looking at the dendrogram, it is possible to feel the distribution of the considered experiments. However, a precise method exists which is able to quantify how well clustered the data is: the silhouette score or coefficient. Let us call a the average intra-cluster distance, namely the average distance between each point within a cluster and b the average inter-cluster distance, namely the average distance between all clusters. Then the silhouette score is defined as follows [42]:

$$\frac{(b - a)}{\max(a, b)}$$

4.5.6. Subspace partitioning

The final aim of the sensitivity analysis is to identify which uncertainties lead to high similarity of outcomes. Classification and Regression Trees (CART) is used to explore such patterns, following the example contained in [19]. After each experiment is processed by hierarchical clustering, it gets a clustering label assigned. Understanding which variable determines the most such classification is the role of CART algorithm. CART receives as an independent input of data (X^1, \dots, X^p, Y) consisting of some explanatory variable X^k and a categorical variable Y , which needs to 'be explained'. In our case, each X^k corresponds to one of the sampled uncertain parameters and Y to the cluster label. A CART tree is formed through recursive partitioning: the 'rule' defined by the underlying parameters is identified for each split in the branches. It follows the principle of minimizing some heterogeneity criterion. The criteria considered in this thesis to check on the performance of the tree are entropy and Gini index [13].

We can look at the CART tree as a mapping process, which we call map T . To each sample (X_i^1, \dots, X_i^p, Y) the map assigns a leaf t . We call $p(j|t)$ the proportion of data labels j in a leaf t . The entropy index E_t and the Gini index D_t quantify how well the splitting represents the data. They are composed as follows [13]:

$$E_t = \sum_j p(j|t) \log p(j|t)$$

$$D_t = \sum_i \sum_{j \neq i} p(i|t) p(j|t) = 1 - \sum_i p(i|t)^2$$

Both indices are equal to 0 when only one label is present in leaf t , and they are maximum when all labels are present with equal probability. CART thus splits a leaf into two

sub-leaves, identifying a threshold for a key variable. The difference between the heterogeneity of a leaf and the total resulting heterogeneity within the two sub-leaves is maximized and positive. The procedure stops when no more splitting is possible [13].

4.6. Modeling uncertainties: overview

Overall, climate uncertainty will be integrated into the model with optimization under uncertainty techniques. In contrast, parameters uncertainty will be tackled through the means offered by uncertainty analysis. Thanks to the nature of the objective functions in robust and stochastic optimization, the model will consider different climate scenarios but always output unique solutions. The run of the model will then be replicated for multiple combinations of uncertain economic and technical parameters. Thus, this phase will output a solution assigned to each combination of parameters, which will later be analyzed with the mentioned sensitivity methods. This methodology will identify the key parametric uncertainties which influence the model's solutions. The process will help both the analyst and the client understand which aspects to focus on when deciding about the placement of green, blue and yellow roofs.

5

Case study

In this chapter, we provide the results of a case study, for which the municipality of Schiedam is selected as the area of interest. Schiedam is chosen due to a nice and long collaboration between the Sweco team and the municipality. An overview is here provided of the inputs and outputs of the constructed model. First, climate data is presented and analysed. We then explain how the set of suitable roofs is constructed, given an area of interest. After that, we present how the parameters that summarize the structure of the city and the technical working of the roofs for each building are created. In the fourth section, the model settings and performance are expounded, leading to the model output analysis. The solution is further processed during the uncertainty analysis in the fifth section. The last two sections replicate the analysis of results and uncertainty for another version of the model: the multi-time step model.

5.1. Input Climate data

As pointed out in Section 2.1 the performance of the sustainable roofing options heavily depends on climate and its uncertainty [28, 48]. Thus the use of future climate projection is the key to understand how useful their application is and to quantify their benefits [38]. In this section we will explain which climate projections are used in this thesis, and how they were handled to be used by the model.

5.1.1. Choice of climate data

Since this model is going to be potentially deployed for Dutch clients, it has been suggested by Sweco experts to chose the KNMI (Koninklijk Nederlands Meteorologisch Instituut) as the scientific institute to take the data from. Since we wanted to analyse different RCP scenarios and the variables of precipitation, maximum temperature, downwelling shortwave radiation and sunshine duration, two main GCM were left in the EURO-CORDEX portal: the CNRM-CM5, developed by the french National Centre for Meteorological Research, and the ICHEC-EC-EARTH, developed by the Irish Center of High-end Computing. KNMI has downscaled those GCM using the RACMO22E RCM. Furthermore, to allow consistency in the data for different variables, it has been chosen to extrapolate the daily values for each of them, even if some of the variables has smaller time-steps available, e.g., one record every 3 hours. In the following table, an overview of the selected climate projections is provided.

Institute	Driving Model	Experiment	Ensemble	RCM model
KNMI	CNRM-CM5	RCP 2.6	r1i1p1	RACMOE22
KNMI	CNRM-CM5	RCP 4.5	r1i1p1	RACMOE22
KNMI	CNRM-CM5	RCP 8.5	r1i1p1	RACMOE22
KNMI	ICHEC-EARTH	RCP 2.6	r12i1p1	RACMOE22
KNMI	ICHEC-EARTH	RCP 4.5	r12i1p1	RACMOE22
KNMI	ICHEC-EARTH	RCP 8.5	r12i1p1	RACMOE22

5.1.2. Climate data analysis

The chosen data is first downloaded from the EUROCORDEX platform and then processed to extract the features needed for the application to the problem. We wish to extrapolate the days in which precipitation quantities and maximum temperatures are high enough to determine some positive contribution provided by the adaptation measures. Moreover, we wish to determine the amount of hours in which PV panels can produce a reasonable amount of energy

Heavy rainfall For the Dutch climate, the KNMI defines an extreme rainfall event in correspondence to a precipitation exceeding 25 mm/h or 50 mm/day [48]. However, it is noted that the ability of green and blue roofs to delay runoff, and thus mitigate the stress on the sewage system, can be appreciated already starting from a daily precipitation amount of 25mm/day [48]. The sum of the *mm* for the days in which this condition applies are reported in Fig 5.1 grouped by climate projection. In this study, we will refer to the days with a daily precipitation amount of 25mm/day as *mid-intense rainfall days*

Heat The KNMI defines heatwaves as 5 consecutive days of which at least 2 present temperatures above 30° Celsius and 3 above 25° Celsius [48]. However, following the approach presented in [48], we consider that cooling is desired independently of the duration of the warm period, and for all days with a maximum temperature above 25° Celsius. Moreover, as in [47], we assume that a green roof can cool maximum 1° at the pedestrian level. So we consider days in which the temperatures do not go over 31°. Indeed, we consider that, above that temperature, the potential mitigation achieved by a green roof would not be enough to avoid hospitalization. In Fig 5.1 we report the average degrees reached during hot days for every climate projection considered.

Sun peak hours With respect to climate mitigation, the performance of yellow roofs can be measured by taking into account what are called sun peak hours [38]. A sun peak hour refers to a moment in time in which the measured solar radiation is at least 1 kW/m² in one hour. In correspondence to this condition of solar radiation, it is possible to state how much energy a certain amount of PV panels can produce [38]. To compute such quantity we use two datasets taken from the EUROCORDEX platform: the daily downwelling short-wave radiation, expressed in *W/m²* and the sunshine hours per day, expressed in *h*. We thus multiply the two quantities to obtain a value of *Wh/m²* which represents the daily average of solar insolation. This value corresponds to the amount of sun peak hours. In Fig 5.2, the difference over specific climate projections is presented for this quantity.

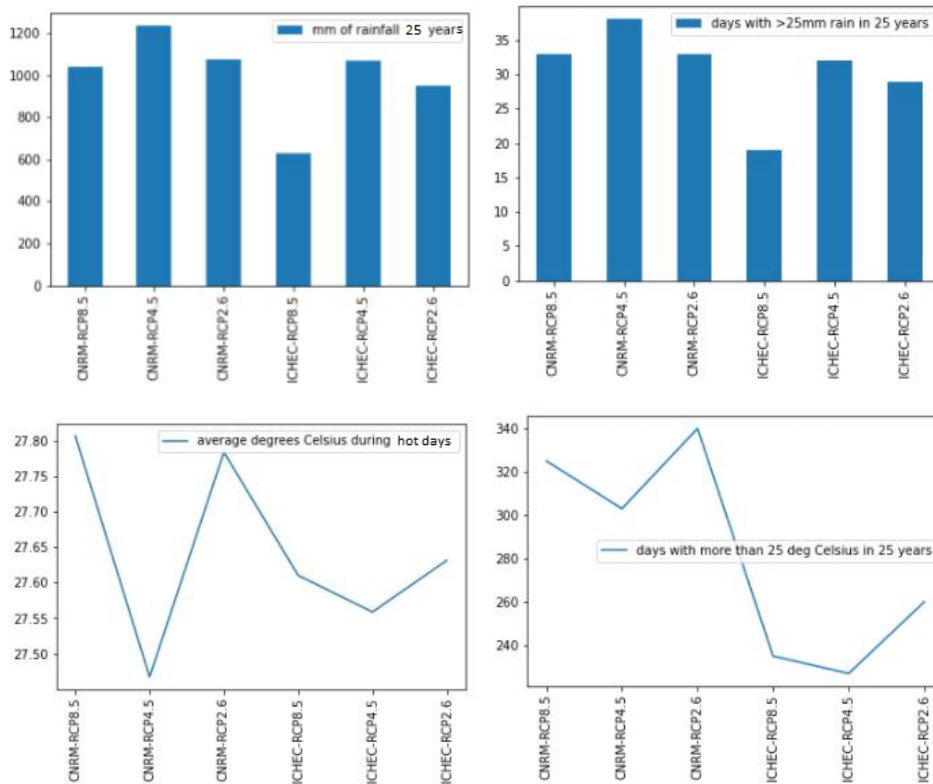


Figure 5.1: Total mm of rain during mid-heavy rainfall, and average max temperature during hot days in the period from 2021 to 2045.

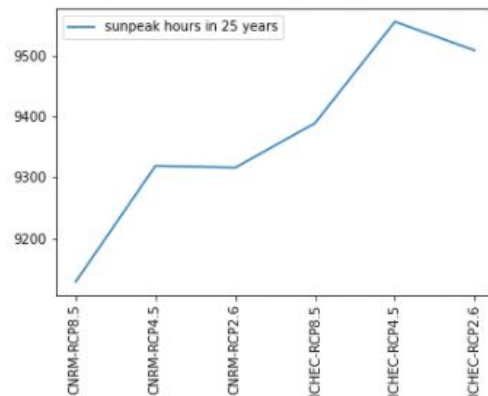


Figure 5.2: Amount of sun peak hours in 25 years (2021-2045) at the selected location.

5.2. Set of suitable roofs

Not every building is suitable for the placement of all roofing options. Therefore, once the area of interest is selected, it is crucial to identify the buildings whose roofs are adequate for hosting green, blue and/or yellow roofs.

In Appendix A.1 we expound the details and procedures which allows us to select the set of suitable roofs in the selected area. We mainly consider two factors: the roofs' slope and area. In Fig 5.3 we report an overview of the area of interest, with the suitable roofs. The latter account for a total of 1120 roofs.

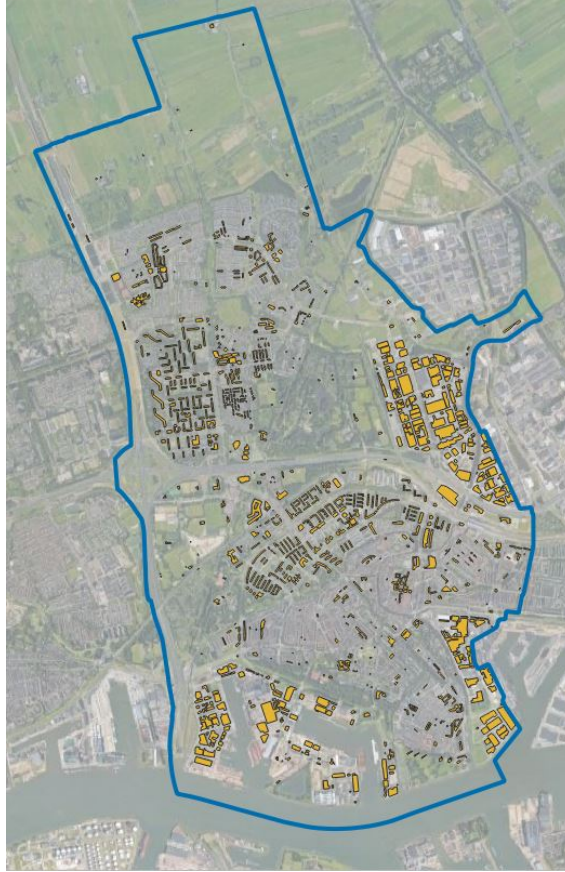


Figure 5.3: Suitable buildings in the municipality of Schiedam

5.3. Spatial Parameters

As explained in Section 3.2, the model inputs are required to be building-specific and to encapsulate the usefulness of applying green, blue or yellow roofs solutions on each roof. In the following subsection an overview is provided about how each climate-derived risk can be encapsulated into modeling parameters. More details are given in Appendix A.1

5.3.1. Flooding risk

Heavy precipitation over a short period can cause local flooding. A large part of the Dutch streets and squares can be flooded during heavy showers [4] (Fig:5.4). The factor $r_B(i)$ used in the formulation expresses the usefulness of applying water retention roofs (green and blue roofs) on top of buildings, based on their location (Fig. 5.5). The parameter $c_B(i)$ is instead assessing the costs due to flooding that are avoided thanks to the installation of some m^2 of green or blue roof. Both factor are dependent on the location of roof i .

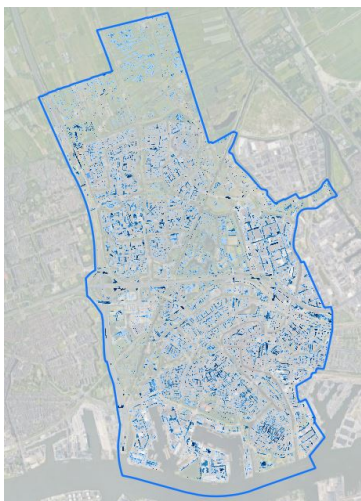


Figure 5.4: Water level during heavy rainfall event.



Figure 5.5: Water level during heavy rainfall event. The volume of water found in the building buffer is used to construct r_B .

5.3.2. Urban Heat Island

In any city in the world the Urban Heat Island (UHI) effect is a phenomenon affecting the health and well-being of its inhabitants. Compared to its surroundings, a urban area indeed experiences significant higher temperatures, which compose the ‘island’ of heat. The main sources of this problem can be found in the increased use of materials with high solar absorption and in anthropogenic heat production [45]. Since future temperatures are predicted to rise also in the Netherlands [47, 48], it is important to find smart ways for mitigating this effect. We make use the klimaateffect atlas layer for UHI [4] to compute the utility factor $r_G(i)$ for heat reduction in correspondence to each building (Figs. 5.6, 5.7). The parameter $m_G(i, z)$ instead evaluates for each building i and each hot day z how many people can avoid health issues due to heat thanks to the placement of a green roof. Details about this procedure are provided in Appendix A.1.

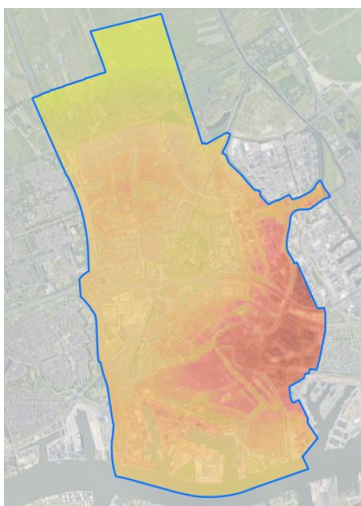


Figure 5.6: Heat stress is modeled through the use of a urban heat island layer.



Figure 5.7: Heat stress is modeled through the use of a urban heat island layer. The average increase in temperature for the buffered area is used to construct r_G .

5.3.3. Solar Radiation Potential

Following the workflow reported in [38] another input, $r_Y(i)$, is needed for the model. This parameter expresses how much solar radiation potential there is on each building, thus provides an indication about how useful and/or efficient it will be to place solar panels on a specific roof. The outlook of such quantities for our area of interest are reported in Figs. 5.8, 5.9.

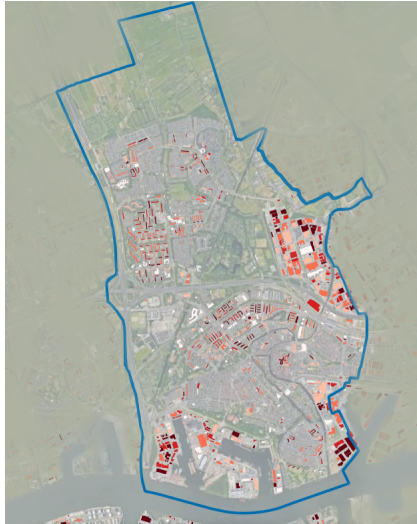


Figure 5.8: Overview: the darker the roof, the higher the value of r_Y .

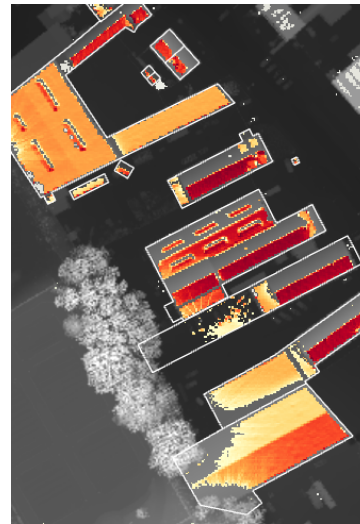


Figure 5.9: Zoom into computations of solar potential.

5.3.4. Technical parameters

The contribution to the urban climate resilience is not only mapped through the construction of spatially-derived parameters, but it is also linked to the technical functioning of the roofs, and their response to climate. We report a detailed discussion about this in Appendix A.1.

Response to heavy rainfall For the fixed-parameters model we refer to [48] and assume a depth of water layer of 10mm and 60mm respectively for green and blue roofs. Moreover we consider that for the amount of mid-heavy rainfall, the roofs have an absorption rate of the incoming water of 80%.

Performance during heatwaves As reported before, it is assumed that green roofs can help mitigating the urban heat in its surroundings by maximum 1° Celsius, as is done in [47].

Relation with solar radiation The production of energy from yellow roofs is strictly linked to the amount of solar radiation received by the roof [37, 38]. Among multiple possible methods, we will estimate how much energy is produced by each m^2 of PV panels by looking at the amount of sun peak hours, as is done in [38].

5.4. Stochastic model with fixed parameters: results

Provided with the input of the computed parameters per building and the climate data, the model will find the optimal location for the three different roofing options. In this paragraph, we will discuss the solutions obtained when running the stochastic and robust formulation of the model with fixed parameters. In this case, the uncertainty behind these parameters is not considered, and average values taken from literature are deployed, as shown in the following table.

Parameter	Value	Description	Source
B	5000000	budget available from municipality (€)	choice
s	0.2	subsidy rate covering the total investment costs ($\in [0, 1]$)	choice
p_G	80	cost for installation of green roofs ($\text{€}/\text{m}^2$)	[37]
p_B	30	cost for installation of blue roof, as a layer beneath the green roof layer ($\text{€}/\text{m}^2$)	[9]
p_Y	315	cost for installation of yellow roofs roofs ($\text{€}/\text{m}^2$)	[37]
h_G	10	thickness of water retention layer for green roofs (mm)	[48]
k_G	0.8	water absorption rate for green roofs, during a heavy rainfall event (%)	[48]
$m(i, z)$	1.079e-5*	people per hot day affected by heat *rescaled per building i and temperature z	[27]
k_B	0.8	rate of absorption of water for blue roofs, during a heavy rainfall event (%)	[48]
Q	187.5	Wh produced during one peak hour by a m^2 PV panels (Wh/m^2)	[37]
θ	0.05	rate of increase in efficiency for PV panels due to GR presence ($\in [0, 1]$)	[38]
c_G	5000	avoided heat cost healthcare per heat day ($\text{€}/\text{person}$)	[49]
c_B	500,300,200	depending on city area and then rescaled on the number of rainfall events ($\text{€}/\text{m}^3$)	[24]
c_Y	0.0700734e-3	economic benefit of producing clean energy, based on avoided green house gasses emissions ($\text{€}/\text{Wh}$)	[37]

Table 5.1: Overview of the values for each parameter used in the model.

The user of the model can choose a budget and subsidy scenario. In this case we chose to allocate 5 million € of budget and to cover the cost of installation by 20%.

5.4.1. Results

We will present in this Sections the results derived both by the stochastic model and the robust model, presented in Section 4.3. The stochastic model finds the combination of locations and roof types which maximizes the average benefits, considering that each climate scenario has the same probability of occurrence. In this case, since the available climate scenarios are 6, each benefit computed per roof and climate projection has a weight of 1/6. Conversely, the robust model finds the best locations for the three types of roofing options,

which yields the highest amount of total benefit in the case in which this is minimum. More specifically, it computes the total benefit for each climate scenario, and chooses the locations which sum up to the max benefit for the worst (least beneficial) projection. In the following Table (5.2), an overview of the solution is provided for the two models.

Model	m^2 GR	m^2 BR	m^2 YR	benefit heat	benefit flood	benefit energy	tot benefit
Stoch	19,164.9	1,651.4	74,341.1	773,028.3 €	50,449 €	8,109,866.6 €	8,933,343.9 €
Robust	19,164.9	3,136.1	74,199.1	638,216 €	63,430.1 €	6,673,950 €	7,375,596 €

Table 5.2: Solutions of stochastic and robust model, compared.

The difference between the two models -stochastic and robust- with the chosen fixed parameters is not extreme: the decision variables differ for a small amount only in the case of blue and yellow roofs. The total computed benefits decrease in the robust case, for heat mitigation and clean energy production. As can be seen in figure 5.10, the budget distribution is not extremely different in the two solutions.

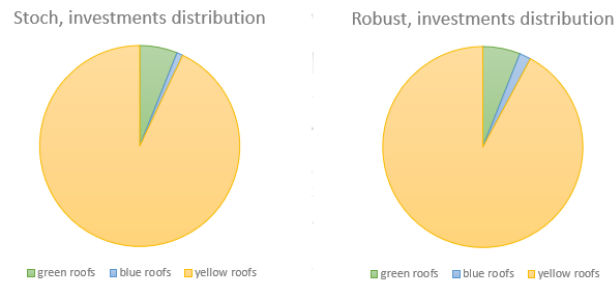


Figure 5.10: Budget distribution in the stochastic and robust models; starting budget of 5 Million € and 20% subsidy rate.

Looking deeper into the data, the variation of m^2 in yellow and blue roofs appears to be due to a modification of two roofing options in two roofs only: one building receives an addition of blue roof layer, while another will have its yellow roof removed. The small observed variation can be attributed to two causes.

On the one hand, as observed in Section 5.1, the highest variation in climate variables is present among the projection for sun peak hours. Indeed, for the scenario with RCP 8.5 and GCM CNMR, which happens to be the worst case scenario, the amount of sun peak hours is sensibly smaller than for the other scenarios. This difference persists when considering the average of all climate projection's sun peak hours. This explains why there is one yellow roof less in the robust case than in the stochastic one. On the other hand, the observed variation between the two models does not involve many changes in the decision variables, because of how the model is constructed. Indeed, the computed parameters per building are not changing, while the climate variables values are. Looking again at the model as a knapsack problem, we deduce that all benefits are scaled in a linear way depending on the climate, but that the order of the ratios benefit/costs has less occasions to face a change.

On the contrary, a big variation can be seen in the computed benefits. Indeed those directly depend on the climate. The worst case climate scenario presents more precipitation, less

hot days and less sun peak hours in total. Therefore, even if the total m^2 of green roofs do not change, the benefit derived from heat mitigation decreases. Furthermore, a small decrease in the total m^2 of yellow roofs, associated with less sun peak hours, yields to a reduction in the total benefit derived from the production of clean energy. Vice versa, a small blue roofs' increase contributes to a benefit increase for flooding protection.

Lastly, it is interesting to notice that the difference in total amount of m^2 for blue and yellow roofs is not proportional: blue roofs covering is nearly double for the robust case with respect to the stochastic one, while the yellow roofs are reduced by an amount which is only close to 1%. The cause of that can be traced back to the the difference in costs per m^2 of the two options, 315 €/m² for yellow roofs and 30 €/m² for blue roofs.



Figure 5.11: Zoom of one area of the map, showing the solution of the stochastic model.

In Fig 5.11 a portion of the solution is shown in a map constructed in *QGIS*. We observe that densely populated and less green areas are preferred for the placement of green roofs. This is completely in line with the idea that there is a high utility in placing green roofs where there is a higher chance of finding people suffering from heatwaves. Moreover, industrial areas are preferred for the placement of PV panels. This can be easily explained by the fact that industrial buildings usually have a very big flat area, that determines on average high values of solar radiation. It is also possible to deduce that the utility of reducing the effects of a flooding event or heatwave in industrial areas is not appreciable from the fact that the model does not propose the installation of green or blue roofs in such areas. At last, the blue roofs are placed on residential buildings (thus having a higher monetary benefit), with a relatively big area and located where the level of predicted water made it rank high in the value of utility r_B .

5.4.2. Insights about Budget variation

Clearly, a higher budget availability will determine a higher amount of roofing options installed (Fig.5.12). To provide insights about how the selected roofs will be chosen when a different budget is allocated, we run the model for a budget B varying from 1 million € to 90 million €, with steps of 10 million at a time. For completeness we also show the results for 5 Million budget, which is our base case. The results show a linear increase in the total benefit (objective function) in correspondence to the proposed linear increase of the budget (Fig 5.13). The last part of the graph has a change in the slope, due to the fact that green and blue roofs (in big quantity in the last trial) do not lead to linearly increasing benefits with the same impact that yellow roofs do. Indeed, they depend on rainfall and heat events which are not constant, nor force the value of benefits as much as the amount of sun-peak hours do.

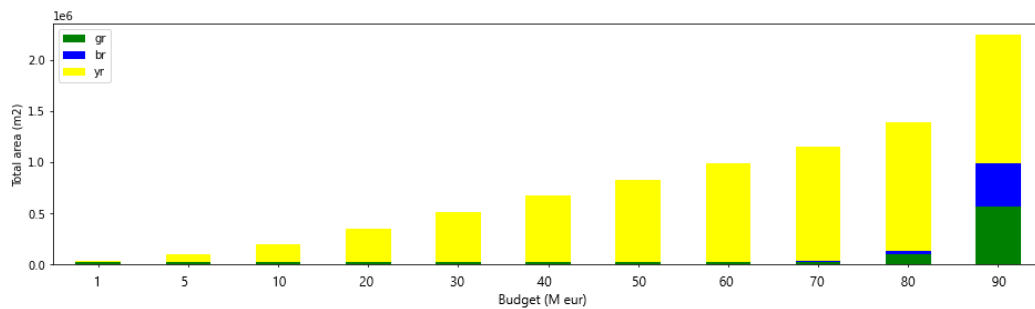


Figure 5.12: Plot showing the total m^2 of each roof type chosen, in correspondence to different budget.

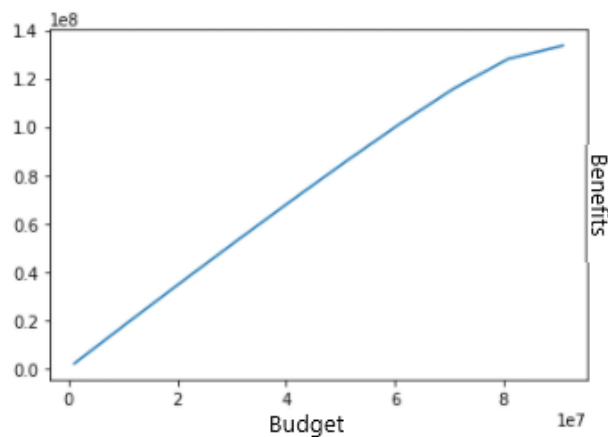
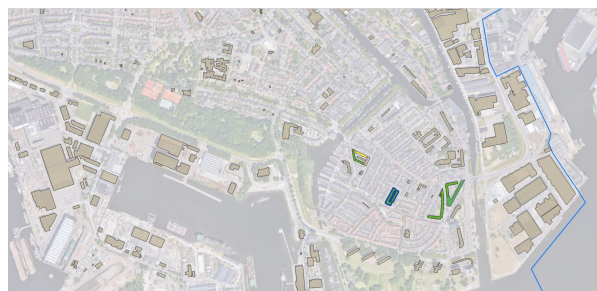


Figure 5.13: Plot of changing budget against determined total benefits.

Another interesting aspect to notice, and shown in Fig 5.12, is the prevalence of yellow roofs in correspondence to low and medium budgets, while for model runs where more budget is available green and blue roofs will be chosen in greater quantities. This aspect can be explained looking at the model as a 'knapsack problem'. Given a certain capacity of the knapsack (budget), and some items which have their value (benefit) and weight (cost), which combination of items maximises the total value of the knapsack? In our case, there are three items per building (one green, one blue and pv panels in a certain amount) that can be placed in the municipality. Each of the options has its cost and its benefits. It is

possible to notice that the highest benefit/cost ratio is achieved by some buildings with yellow roof options before that happens for the equivalent blue and green option. Given the higher cost per m^2 for the yellow roofs, this can be explained by looking at the relatively high benefits derived from yellow roof options. Indeed, the parameters used on average determine higher benefits for the yellow roofs, derived by the total energy production of the 25 years. A big variation for the m^2 quantities of green and blue roofs is present in correspondence to the step between 80 and 90 million budget. This is determined by the fact that, once all possible or useful roofs are covered with the yellow option, green and blue roofs can be placed in relatively high amounts due to their relative low price (80 and 30 € compared to 315 per m^2).

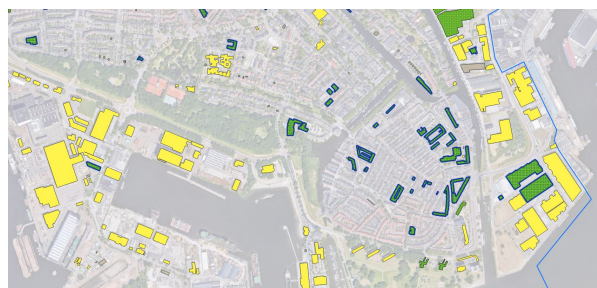
Location-wise yellow roofs are gradually added with preference to bigger and flatter buildings, which have as a consequence higher r_Y expressing relative radiation potential. In correspondence to higher budgets, green and blue roofs are placed in locations where the higher levels of water are found in the *Klimaateffect atlas*. In the following figure, some scenarios related to sampled solutions from different budgets are reported in Fig.5.14.



(a) Zoom into the solution map, budget of 1 million.



(b) Zoom into the solution map, budget of 40 million.



(c) Zoom into the solution map, budget of 90 million.

Figure 5.14: Variation in the solution for a portion of Schiedam, with a budget changing from 1 Million to 40 Million, and 90 Million €.

5.5. Stochastic model: uncertainty analysis

In the following analysis, we will explore which variations can be observed in the model's outcomes when the parameters are considered in their uncertain nature. We first randomly sample the parameters, and run the model one time for each combination of parameters. The resulting solutions are later grouped in clusters to treat the outcome in a more compact way. The final step consists in applying CART algorithms to infer the link between the sampled parameters and the solutions' characteristics.

Like in [38], we perform the uncertainty analysis for the stochastic model, among the two proposed models. The first motivation for this choice is that it is not known how probable each climate scenario is. Thus, optimizing for a worst-case scenario that may have a smaller probability of occurrence may not be beneficial. Furthermore, from the practical perspective, using a combination of climate scenarios may provide more insights into further uncertainty and sensitivity analysis steps. We report in the following table (Tab. 5.3) the uncertain parameters and their uncertainty range. Whenever possible, the ranges are taken directly from the literature; otherwise, a variation of + or - 20% is used.

Parameter	Range	Type	Source
k_G	[0, 0.8]	param (%)	[48]
$m(i, z)$	+/-20% applied each value	param (people/day)	[27]
k_B	[0.3, 0.8]	param (%)	[48]
Q	[120, 200]	param (Wh/ m^2)	[38]
θ	[0.005, 0.08]	param (%)	[38]
c_G	[3000, 11000]	econom (€/person)	[49]
$c_B(i)$	+/-20% applied to value per building	econom (€/m ³)	[24]
c_Y	[0.056058e-3, 0.084088e-3]	econom (€/Wh)	[37]

Table 5.3: Uncertain parameters: ranges.

As explained in Section 4.5, each parameter is sampled using Latin Hypercube method from a uniform distribution over the specified ranges. We sample 3 values from the distribution of each parameter. In Fig. 5.15 we provide an example of the distribution of a sampled parameter, Q .

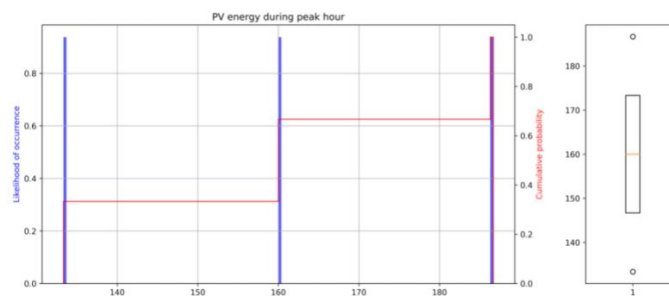


Figure 5.15: Example for sampling 3 values from the distribution of Q .

We wish to run the same model with a different combination of parameters. With eight parameters, 3^8 total runs have to be performed. However, due to computing restrictions, 3^8 experiments could not be completed. Therefore, we merge the uncertainty of $m(i, z)$ and c_B under the name ad_u , *adaptation strategies uncertainty*; thus, we run the model 3^7 times.

5.5.1. Results

The results of these runs can be seen in Fig. 5.16. Here, we plot the total amount of m^2 covered by each roofing option in correspondence to each experiment. Like in the fixed parameters model, yellow roofs have a dominant presence in most runs. Moreover, a trade-off exists between the yellow roofs number and the total number of roofs placed. Indeed, the highest peaks in the y axis are reached when yellow roofs are less present. With the same budget, more green and blue m^2 can be placed than m^2 of yellow roofs, due to their price.

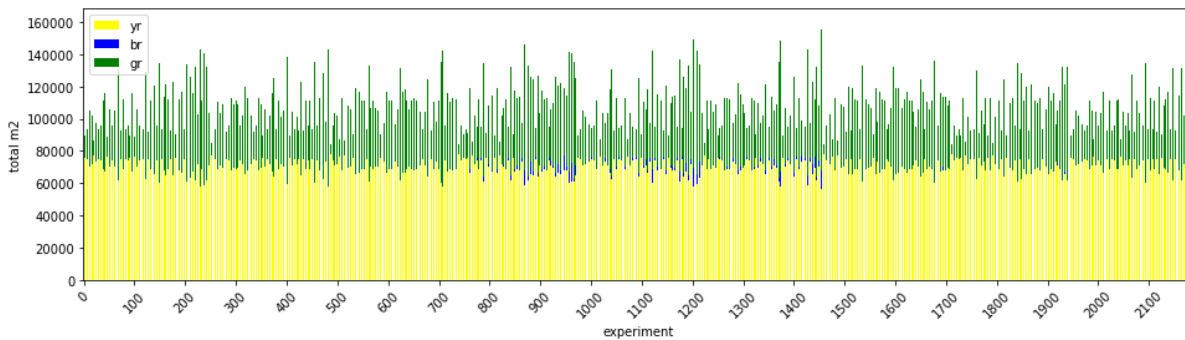


Figure 5.16: Amount of m^2 chosen for green, blue and yellow roofs in correspondence to different parameters sampling.

To better visualize the variation happening among the different experiments, we zoom into 100 random experiments and report the amount of m^2 and the total benefits derived in Fig. 5.18. Fig. 5.17 reports the same information, but in a pie-chart scatter plot, which reports total benefits on y axis, experiment number on x axis and has a dimension proportional to the total m^2 of roofs placed. Moreover, the ratios of roofing option are represented by the slices of the pie (blue proportion is increased to make it visible).

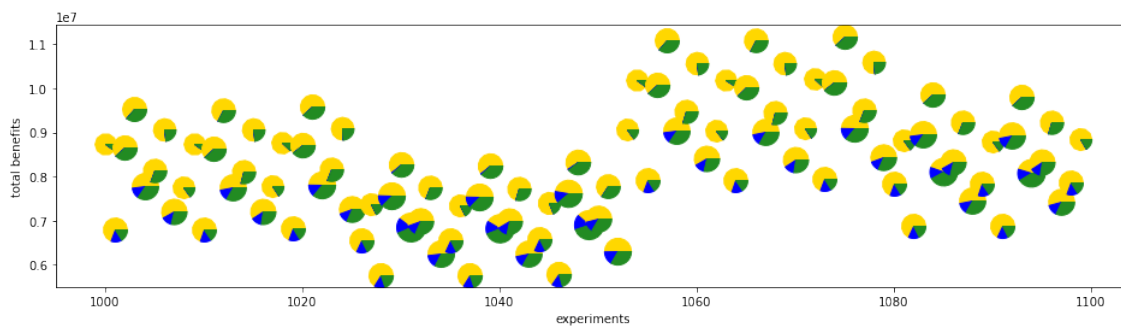
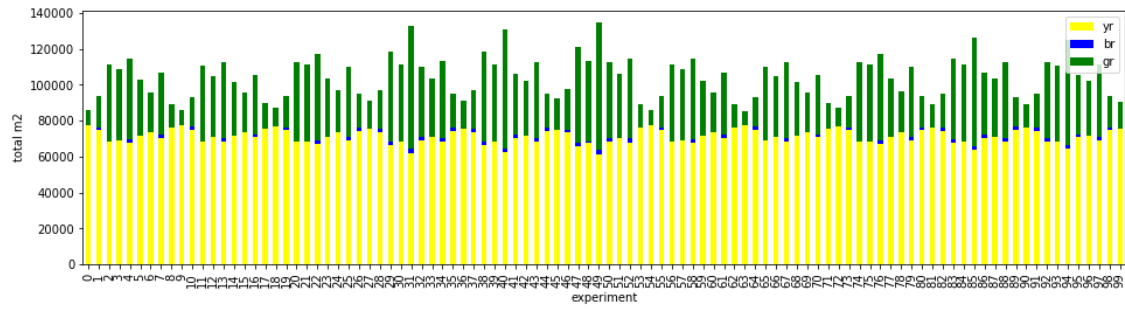
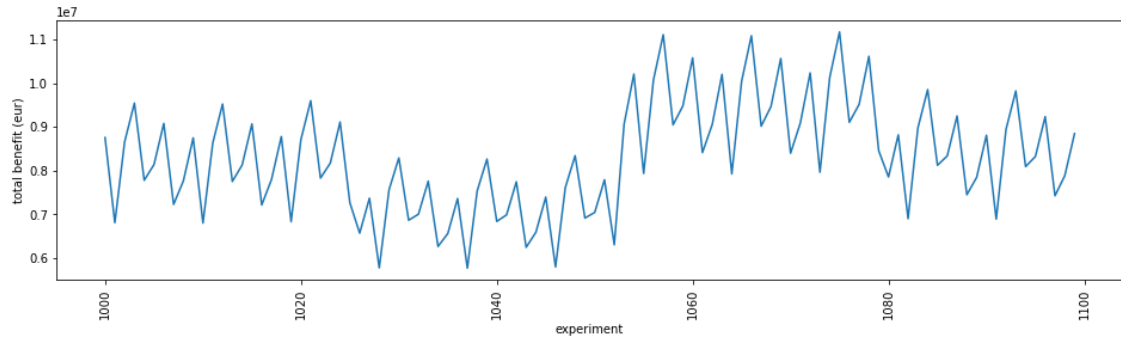


Figure 5.17: Plot of 100 experiments. y axis represents total benefits.

From Figs 5.17 and 5.18 it is possible to see that the variation in total benefit is not linearly dependent on the amount of m^2 for the different roofing options. In general, a tendency appears: results with smaller quantities of blue roofs tend to have higher total benefits, and smaller total m^2 of roofs. Different combinations of sampled parameters contribute to these variations in a non-trivial way. In the following section, we will analyze in more detail which experiments lead to the most similar solutions, and which combinations of parameters lead to which optimal placement to answer our research questions.



(a) Zoom into the solution of 100 experiments, total m^2 placed per type of roof for every experiment



(b) Zoom into the solution of 100 experiments, total benefits in €

Figure 5.18: A detail of different experiments outputs: total m^2 per roofing option and total benefit.

5.5.2. Clustering of results

As explained in Section 4.5.3, post-processing the outcomes of the previous phase is necessary due to high number of experiments. Otherwise, it would be hard to draw insights about how the parameters influence the solutions. The cosine similarity is chosen to understand how each solution relates to the others in terms of distribution of roofing types around the municipality. We first compute similarity and plot the results in the matrix presented in Fig. 5.19. The darker the colour, the higher similarity between experiments' results.

The experiments' results are obtained combining multiple values for the uncertain parameters and they tend to be very similar on average. It is thus possible to conclude that the parametric changes influence the choice of location less than the total benefits. This high average similarity across experiments could be a good sign for the robustness of the proposed model. It is worth noticing that the cosine similarity can spot the similarities as for roof placement and not for the benefit derived by each placement, as it considered the angle spanned by two vectors and not their modules.

Nonetheless, 'stripes' of clearer colour are present in Fig. 5.19. They indicate that some experiments are very different from others. Such stripes, however, do not form a repetitive grid. This characteristic makes the following analysis even more interesting: a repetitive pattern would mean that only one specific parameter is responsible for the main changes in the solution. On the contrary, a variation in the structure of colours of the similarity matrix suggests that a combination of multiple sampled parameters influences the solution.

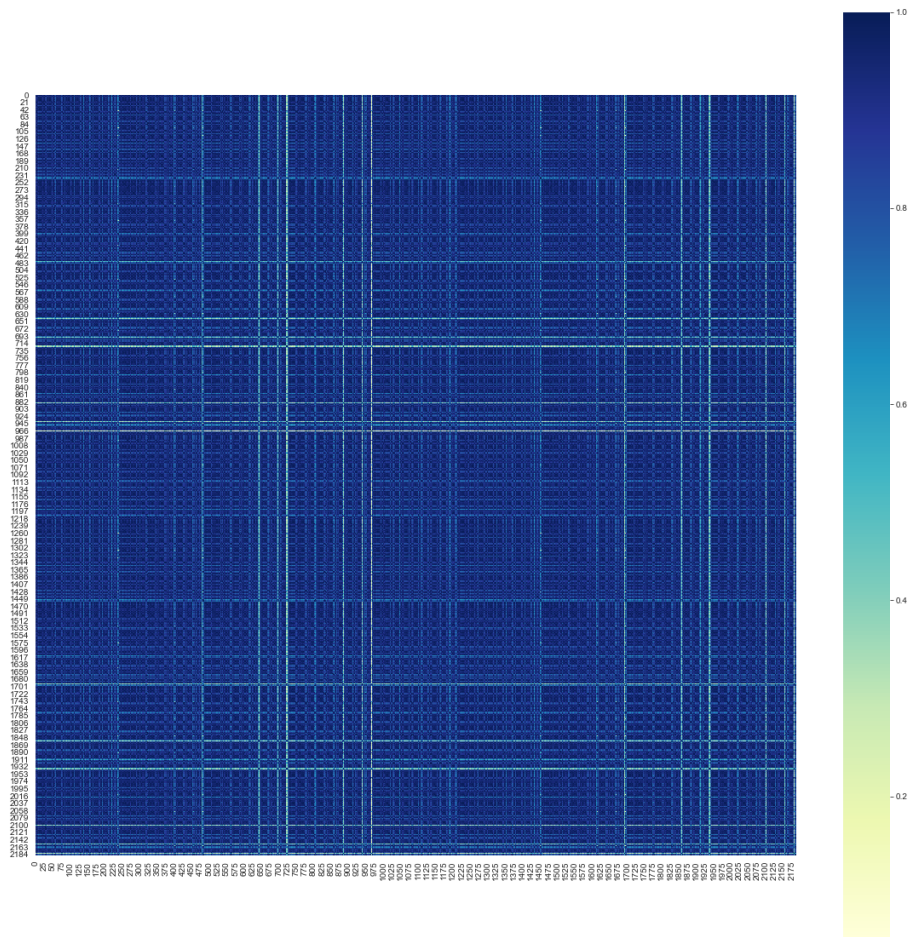


Figure 5.19: Cosine similarity matrix

The method used in this study to group similar outcomes is called hierarchical clustering and it is explained in Section 4.5.3. In Fig 5.20 we report the dendrogram generated from applying agglomerative hierarchical clustering with complete linkage to the computed similarity matrix. The results are equally distanced in the x axis, while the y height at which any two objects are joined together reflects the distance between the elements. An horizontal line can be drawn at some height; the elements that are joined together below that line are part of the cluster represented by the closest horizontal link between elements.

In our case, it is clear that clusters with many elements are already formed at small y values. The great distance between the first joints of elements and the last signifies that the data will probably be well clustered also when considering a small amount of clusters. The silhouette method, presented in Section 4.5.5, can be deployed to choose a correct and representative number of clusters. We tried multiple cluster numbers and computed the silhouette value. The best silhouette value was found in correspondence to 25 and 750 clusters. We choose to group the solutions in 25 clusters, as that would result in a more compact and insightful input for the next phase.

Overall, we run the model for $3^7 = 2187$ times and obtain 2187 solutions, which are clustered into 25 groups of similar results. Within these clusters, green, blue and yellow

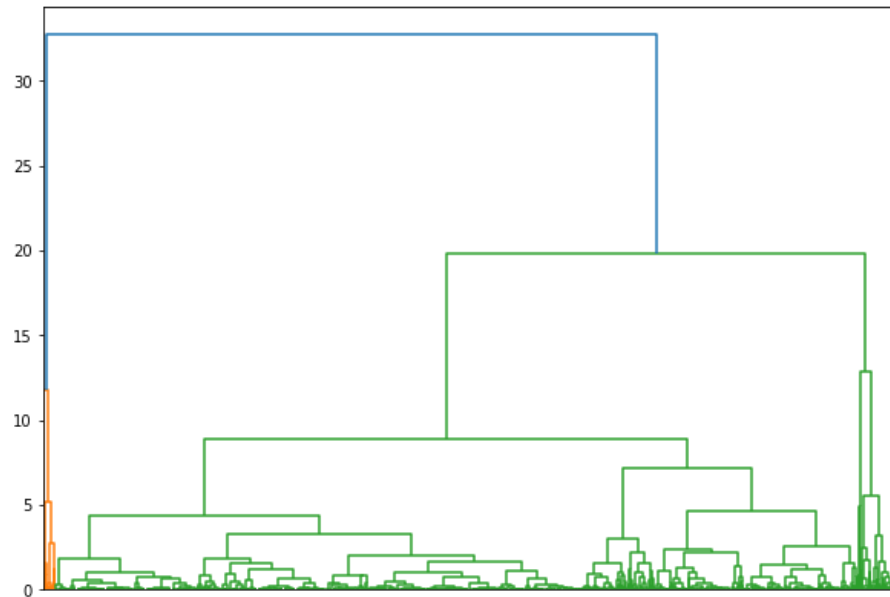


Figure 5.20: Dendrogram for hierarchical clustering applied to the solutions generated from multiple parameters' sampling.

roofs are similarly distributed around the municipality. In the following sections, we will look into the details of each solution vector and the parameters underlying each run to find which parameters determine which group of solutions.

5.5.3. Parametric trade-offs

Through the division in clusters, we can look into the source of variation in the solutions in a more compact way. Ideally, the solutions which are similar to each other should share some similar sampled parameters. Therefore, we use subspace partitioning to find the "rules" behind the distribution in our "experiment-parameters pattern". Classification and regression trees (CART) are part of the subspace partitioning methods. As each experiment has a label assigned by the clustering, we deploy CART for classification [19]. We ask the algorithm to determine the main drivers beneath the given classification.

Running the algorithm, we are able to identify the main parametric drivers of the classification and get a quantification of their importance with command `.feature_importances`. The results are reported in the following table (Tab 5.4).

Parameter	importance
θ	0.501
c_G	0.420
Q	0.068
ad_u	0.011

Table 5.4: Importance of each parameter in the CART classification.

Parameters kb , kg and cy are not reported, as they have an importance score close to 0. Q and ad_u play some minor role. The main parameters that close solutions have in common are θ and c_G . This can be explained by the fact that θ is the parameter that says how much increase in benefits derived by yellow roofs there is when a green roof is placed on the same building, as per the formula below:

$$b_Y(i) = c_Y \cdot Q \cdot d \cdot x_Y(i) \cdot r_Y(i) \cdot (1 + \theta \cdot y_G(i)) \quad \forall i \in R$$

Therefore, θ is determinant for the location choice of each roof type: a bigger θ forces the placement of green roofs in buildings where yellow roofs are there already. Instead, a small θ would leave "freedom" to the green roofs to be assigned to areas with more heat/flooding problems.

Parameter c_G further pushes the model in the same direction. It is a linear term and defines the benefits derived by the green roofs; when c_G is small the heat reduction benefits derived by green roofs are minor. It is important to remember that to place blue roofs, we assume that a green layer has to exist already. Therefore, the smaller number of green roofs, the smaller the probability of placement for a blue roof. In a more detailed analysis reported in Appendix A.2, we see that θ can be determinant for the blue roofs' placement. Parameters k_B and k_G , instead, are less influential. They are linked to the flooding mitigation potential of blue and green roofs, which yields generally low economic benefits. This is due to how the benefits are computed: the shadow cost of a one-time replacement of a sewage system, with the capacity necessary to capture the water quantity during each mid-heavy rainfall event.

We do not underline specifically which locations are picked in spite of others for each cluster, as that would be extremely detailed and not so relevant. However, we can make some general considerations. The cosine distance and the hierarchical clustering assign the same label to experiments with a similar distribution of roofs all around a municipality. The solutions are then similar in any of these two cases:

- if the same types of roofs are placed in close-by locations,
- if there is no big variation in the roofs' types per location or in total.

More specifically, two experiments which differ only because one green roof is placed in a different location are similar and probably clustered together. Two experiments which differ by one yellow roof and one green roof are considered less similar. Indeed, when the parameters change, they change in the same way for each roof; thus, we do not expect a big location change for the same roof type. The parameters influence more the trade-offs between the benefits among different roofing types. Therefore, the parameters will influence more the total composition of roof types, both per location and in total.

Furthermore, the overall goal is to maximize the total gained benefits. Consequently, we are interested in understanding which impact each parameter has on the total benefits gained by the municipality. In Fig. 5.21 a visualization of the share of the total benefits per roof type, for every cluster is given. Later, we will look into the CART tree details to see if the parameters that lead to some specific placement also drive the variation of benefits.

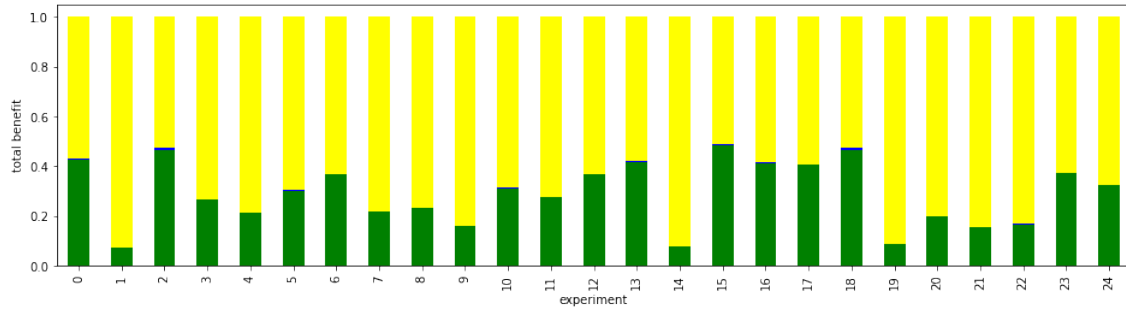


Figure 5.21: Share of benefits for each cluster.

In Fig. 5.21, it is possible to see which clusters contain solutions that have a higher share of total benefits for green, blue or yellow roofs. Through CART, we would like to have quantitative insights about the drivers of some specific type of solution: e.g. when many green roofs are chosen for a cluster, which parameter combination lies beneath the clustered experiments?

We focus on analyzing the tree path towards some meaningful clusters. We thus look into clusters with more than 1% of the total data (22 elements). Among those, we look into some specific clusters with either very high or very low proportion of green roofs: clusters 1, 6, 10, 14, and 19. A simplified scheme of the resulting tree is presented in Fig.5.22. Here, the condition inside one block determines the solutions partition in the next level; the elements for which the condition is satisfied go to the left, the others to the right; the Gini index is reported for each step and refers to the classification of all experiments, not only the ones reported in the leaves.

Clusters 1, 14 and 19 are characterized by a high proportion of yellow roofs' benefits and a small proportion of green roofs' benefits. The reason behind these proportions is easy to understand for cluster 1, when looking at Fig. 5.22: the experiments inside the cluster are defined by the smallest values possible of θ and c_G . The latter parameters are indeed the ones that would favour the presence of green roofs. Going down into the tree, we find out that cluster 1 is also characterized by the highest possible values for Q and lowest for ad_u . Here, a high Q boosts the energy production of yellow roofs, while a low ad_u decreases the potential of both green and blue roofs. As a consequence, this cluster has also one of the smallest proportions of blue roofs benefits.

Furthermore, clusters 14 and 19 do not have the smallest possible value of θ , but they share the smallest possible value of c_G . The latter aspect seems to characterize the experiments with low benefits derived by green roofs, which is completely in line with the shape of the model, and with the results obtained in Table 5.4.

On the contrary, clusters 6 and 10 have the highest presence of green roofs. They are both defined by the highest possible value of c_G . However, Cluster 6 has a smaller proportion of green and blue benefits mainly for two drivers: θ and Q . Indeed, experiments in cluster 10 are characterized by the highest value possible for θ , and the highest value possible for Q . In contrast, cluster 6 exceeds those thresholds for a non-significant number

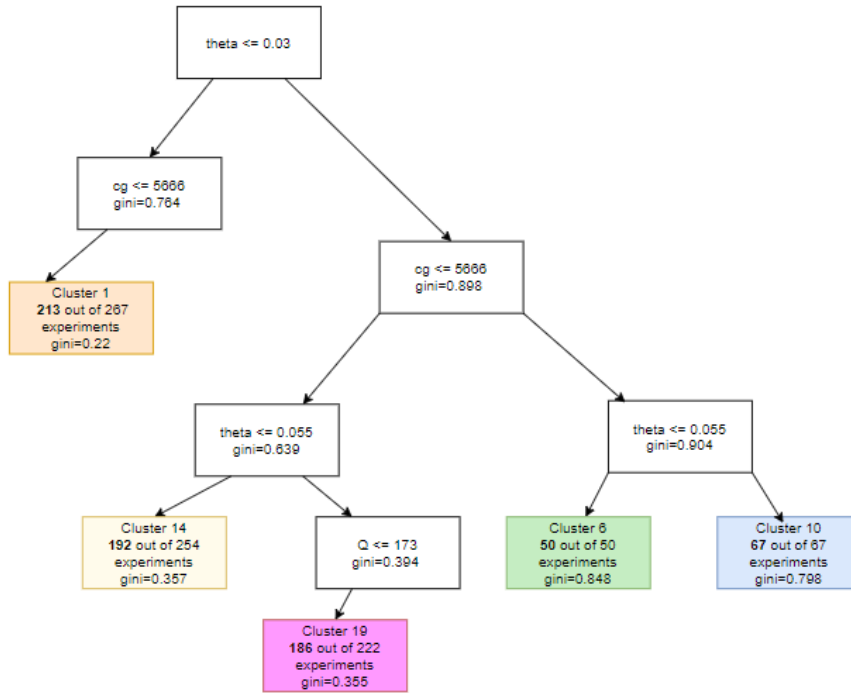


Figure 5.22: Simplified CART tree representation. The tree shows which parametric features lead more strongly to the formation of the clusters.

of experiments. This aspect is in line with the hypothesis made about the fact that highly efficient yellow roofs would "force" green roofs to be placed on the same buildings. As a matter of fact, high Q values lead to high energy production by yellow roofs, and a high θ to an increase in the same production, due to green roofs' presence.

Clus	nr in-clus	Underlying uncertainties	Remarkable characteristics
1	267	$\theta \leq 0.03, c_G \leq 5666$	high yellow roofs' benefits proportion and among lowest of blue roofs' benefits.
6	50	$0.03 < \theta \leq 0.05, c_G > 8333, Q \leq 146$	high proportion of green roofs' benefits but slightly smaller than clus 10
10	67	$\theta > 0.05, c_G > 8333, Q > 146$	high proportion of green roofs' benefits
14	254	$\theta > 0.03, c_G \leq 5666$	high yellow roof benefits
19	222	$\theta > 0.03, c_G \leq 5666$	high yellow roof benefits

Table 5.5: Overview of some clusters' main features and underlying parameters' ranges.

Overall, CART tree classification seems to provide interesting insights into the relevance of the parameters for the different solutions. When the differences among the solutions are evaluated with respect to the roofs types' placement, the most influential parameters are θ and c_G . We further wanted to understand whether the same parameters combinations can explain the variations in benefits among different clusters. Looking at the results in Fig. 5.22 and in Table 5.5 we deduce that examples exist of clusters where there is a clear link between the total sum of benefit per roof type and the parameters. Indeed, the same parameters can lead both to similar distributions of roofs and similar benefits.

5.6. Multi-time step model: results

In this section we introduce a multi-time step model, which is developed starting from the deterministic model presented in Chapter 3. We split the budget over time and look into which roofs will be placed in which moment of time as a response to climate variables.

A new set will be introduced, T , set of years under analysis, spanning from 2021 to 2045. As a consequence of the multi time-step reformulation, the decision variables get one more dimension, time dimension $t \in T$.

$$\begin{aligned} x_Y(t, i) &\in \mathbb{R}^+ && m^2 \text{ of yellow roofs to be placed on roof } i \text{ in year } t \\ y_G(t, i), y_B(t, i) &\in \{0, 1\} && \text{active if Green and Blue roofs are to be placed} \\ &&& \text{on roof } i \text{ in year } t \end{aligned}$$

The problem takes the following shape:

$$\begin{aligned} &\max \sum_{i \in R} \sum_{t \in T} (b_G(t, i) + b_B(t, i) + b_Y(t, i)) \\ \sum_{i \in R} s \cdot (p_G \cdot x_G(t, i) + p_Y \cdot x_Y(t, i) + p_B \cdot x_B(t, i)) &\leq B(t) && \forall t \in T \\ x_Y(t, i) &\leq a(i) && \forall i \in R \quad \forall t \in T \\ y_G(t, i) &\geq y_B(t, i) && \forall i \in R \quad \forall t \in T \\ \sum_{t \in T} y_G(t, i) &\leq 1 && \forall i \in R \\ \sum_{t \in T} y_B(t, i) &\leq 1 && \forall i \in R \\ \sum_{t \in T} x_Y(t, i) &\leq a(i) && \forall i \in R \\ b_G(t, i) &= \sum_{z \in H} \sum_{v \geq t} c_G \cdot m_G(v, i, z) \cdot y_G(t, i) \cdot r_G(i) && \forall i \in R \quad \forall t \in T \\ b_B(t, i) &= \sum_{j \in P} \sum_{v \geq t} c_B(i) \cdot a(i) \cdot (k_B \cdot w(v, j) \cdot y_B(t, i) + k_G \cdot h_G \cdot y_G(t, i)) \cdot r_B(i) && \forall i \in R \quad \forall t \in T \\ b_Y(t, i) &= \sum_{v \geq t} c_Y \cdot Q \cdot d(v) \cdot x_Y(t, i) \cdot r_Y(i) \cdot (1 + \theta \cdot y_G(t, i)) && \forall i \in R \quad \forall t \in T \end{aligned}$$

The objective function will consist of the sum of the benefits for each roof and each year. Note that, since the decision variables are defined to represent which roofing option is placed in one moment, they can be different from 0 only one time. Consequently, the benefits are also expressed in the same way, and benefit in time t for roof i will consist of benefits gathered from time t until the last element of set T for roof i . We run the model with a budget of 5 million € per year and a subsidy rate of 20%. Moreover, some constraints are added, which were not present in the deterministic formulation. They are added to ensure that each roof can be used only once for each roofing option.

To gain further insights into the model's behaviour in response to the climate, we present the solutions derived from applying the presented formulation to two different climate projections: RCP 4.5 CNRM and RCP 8.5 ICHEC.

5.6.1. Results RCP 4.5 CNRM

The first climate projection, RCP 4.5 CNRM, is characterized by the following aspects: 49.3 mm of yearly average of heavy rain (only reporting days with >25 mm/day); 11.4 days of heat on average per year (temperatures between 25 and 31 degrees Celsius); and 372.77 sun peak hours on average per year. We use the same parameters used for the fixed parameters

model runs. The results (Fig. 5.23) show that the first choice will always be for the placement of yellow roofs in the first years, while the other two options are mainly considered in the last years. The last two years do not see any new roof installation since all available buildings with a utility different from 0 will have already been used for all viable options.

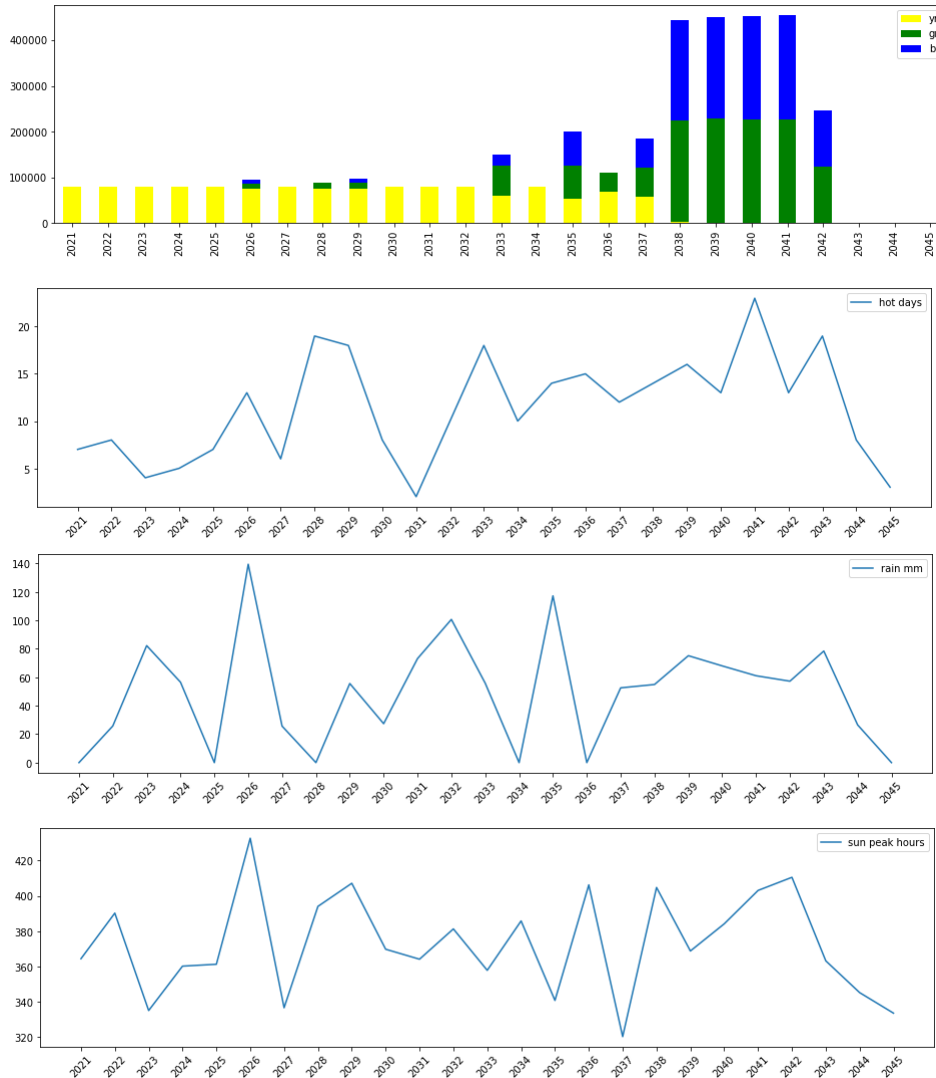


Figure 5.23: RCP 4.5 CNRM outlook.

In Fig. 5.23, we see that some blue and green roof options already appear in 2026. The highest values for total mid-heavy rain is indeed reached in the year 2026. This forces the presence of flooding adaptation strategies like green and blue roofs. Since we force the problem to place blue roofs only as layers beneath the green roof, the high demand for blue roofs may force the same amount of green roofs to be placed this year. Something slightly different happens for the year 2028, where the amount of mid-heavy rain is close to 0, while many hot days would appear, with an average temperature of 27.85 degrees Celsius. Such characteristics would determine high values for the number of people who avoid hospitalization during a heatwave thanks to green roofs. Therefore, some green roofs are placed too. The following year, 2029, some space is also left to green and blue options not only for the relatively high values of hot days and mm of rain but also thanks to the slight

decrease in total sun peak hours for the following years. It should also be noted that in the last years, all the best roofs for PV installations would not be available (high solar irradiation per m^2 , thus high r_Y), as the installation may have happened in the previous years.

The same path of sun peak hours and the sharp peak in mid-heavy rainfall leaves some space for green and blue options again in the year 2033 and lastly in 2035. After this year, since the best roofs for yellow options have already be covered, more green and blue roofs are appearing, covering more m^2 . At this point, the roofs with the highest utility for adaptation will probably have reached levels of benefits that outweigh the performances of the least efficient roof for PV panels installation (low r_Y). In the year 2037, all roofs with a positive utility for yellow roofs placement will be covered, while the same will happen in the year 2042 for green and blue options.

5.6.2. Results RCP 8.5 ICHEC

Fig 5.24 shows RCP 8.5 ICHEC projections for climate and roofing choices. In this case, fewer mid-heavy rainfall events than the previously analyzed projection (21 vs 38) occur, with a slightly lower mean (49.20) per year. Moreover, it presents 8 hot days per year on average and an average amount of sun peak hours comparable to RCP 4.5 CNRM. The results shown below underline the difference in choices for green, blue and yellow roofs, reacting to this different climate projection (Fig 5.24). The main difference between these results and the previous is the absence of green and blue roofs in the first years. The latter phenomenon can be explained by the previously underlined characteristics, specifically looking at the quantity of mid-heavy rainfall in those first years. Very often, they present no mid-heavy precipitation at all. A clear response to the peak in heat and precipitation in 2034 is visible in the amount of green and blue roofs placed.

The most interesting aspect for this climate projection is the complete absence of roofs choices for 2042 and 2043 (2041 has a minimal amount of green roofs installed). This absence confirms that the rainfall amounts are a crucial driver for the decisions made by the model. Indeed, in those years, no mid-heavy precipitation is present. Thus, the benefits derived from flooding protection are 0, leading to no choice for blue roofs. Green roofs absence can be explained through the same reasoning, as in our model, they also work as water collectors, even if for smaller volumes than blue roofs. Furthermore, the benefits derived by heat mitigation are minimal for those years. For 2042 and 2043, less than 5 days per year happen to be hot days, with average temperatures of 25.76 and 26.87, respectively.

In both analyses, a pattern emerges: yellow roofs are also preferred when considering multi-time steps, where benefits are cumulative from year t when the roof option is placed. This result is consistent with the results obtained when time is not considered, and the solution derives from here and now decisions considering the benefits of the next 25 years. Another interesting aspect is the influence of rainfall patterns compared to heat patterns for green, and consequently, blue roofs.

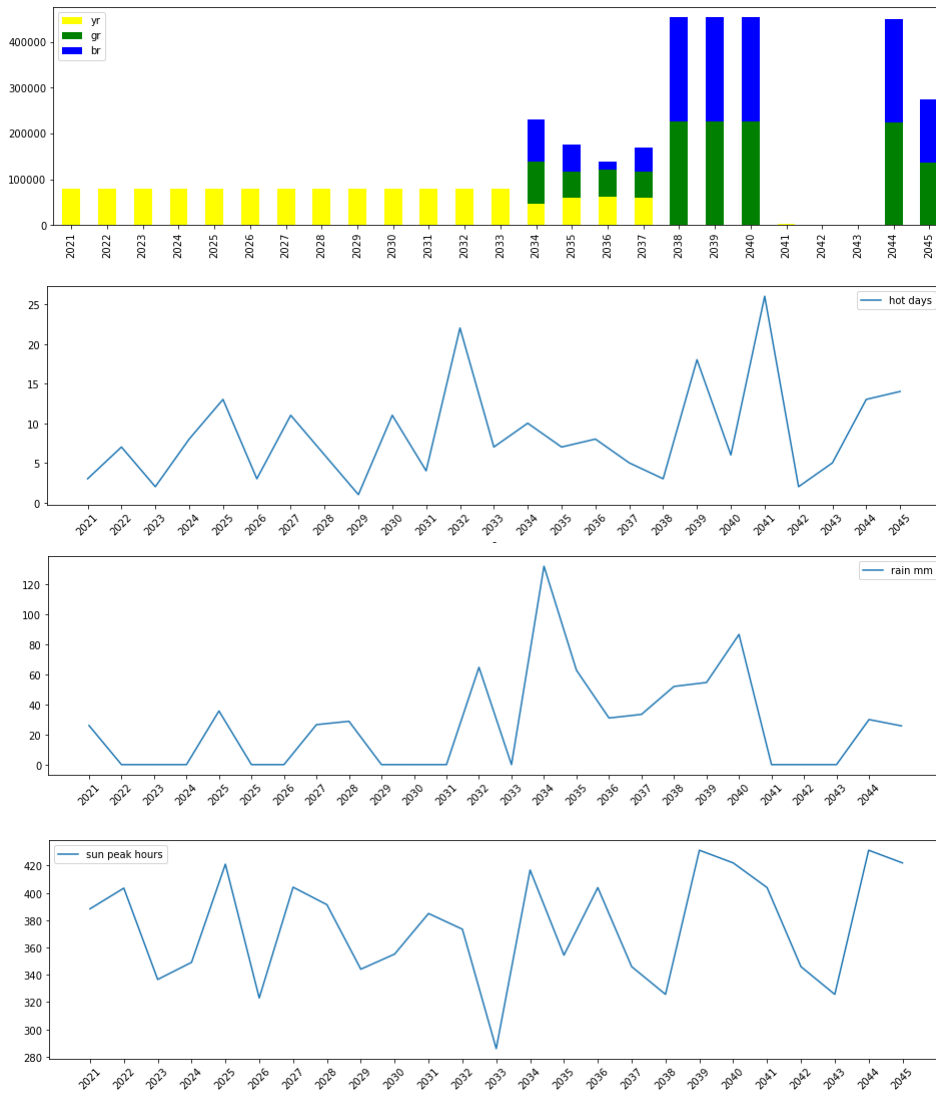


Figure 5.24: RCP 8.5 ICHEC: outlook.

5.7. Multi-time step model and uncertainty

In this section, we analyse the behaviour of the multi-time step model, both when different climate projections and parametric uncertainty are considered. Furthermore, we propose a methodology for the practical use of multiple solutions obtained when uncertainty is integrated into a multi-time step model: the one-branch tree.

5.7.1. Climate scenarios uncertainty

We now examine how the multi-time step model behaves with different climate inputs and compare the derived solutions. The year 2021 presents the same solution for every climate scenario: placing all the m^2 of yellow roofs allowed by the allocated budget. From the following year, the solutions start to diverge from each other as the climate projections do. The likeness between each of these solutions can be investigated through the use of cosine similarity. As explained in section 4.5.3, such measure is able to indicate how close two solution vectors are in terms of locations chosen for each roofing type. The only difference

now is that the solution vector also reports the year when a roof placement is decided. The results of the cosine similarity computations are shown in the table below (Tab 5.6).

	RCP 2.6 C	RCP 4.5 C	RCP 8.5 C	RCP 2.6 I	RCP 4.5 I	RCP 8.5 I
RCP 2.6 C	1.000000	0.214815	0.344474	0.317740	0.274244	0.283933
RCP 4.5 C	0.214815	1.000000	0.399363	0.298959	0.290510	0.311389
RCP 8.5 C	0.344474	0.399363	1.000000	0.236223	0.364884	0.307034
RCP 2.6 I	0.317740	0.298959	0.236223	1.000000	0.329898	0.263473
RCP 4.5 I	0.274244	0.290510	0.364884	0.329898	1.000000	0.310343
RCP 8.5 I	0.283933	0.311389	0.307034	0.263473	0.310343	1.000000

Table 5.6: Similarity matrix for the results of the multi-time step model, run with different climate inputs.

The similarities between the results are relatively low. This mainly happens because of the big dimension of the input and its high sparsity. Indeed, for each projection we report the solution as a vector of length 3(roofing options)x1120(amount of roofs)x 25(the years in which the decision is taken). Moreover, the lower the similarity the more the solution differs in terms of when and where each roofing option is placed. This low average similarity can thus also be a sign that climate variables are influential in the pattern of solutions of the multi time-step model. Extreme weather events logically make adaptation measures such as green and blue roofs more necessary in some moments specifically, while solar radiation heavily depends on the sun's presence and intensity.

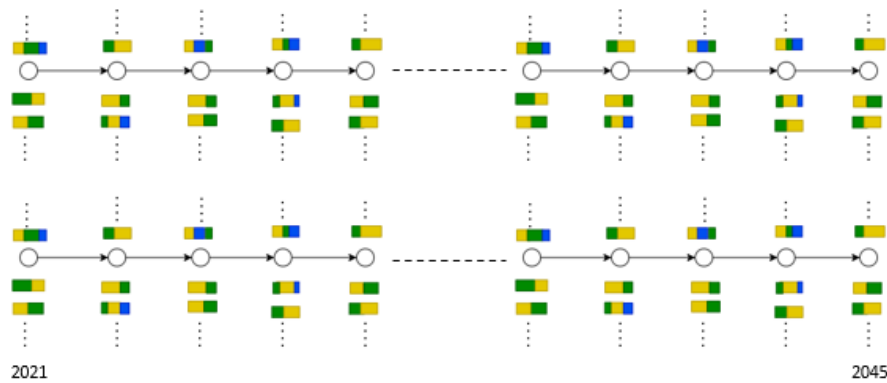


Figure 5.25: Solutions for each time step, climate scenario and combination of parameters.

5.7.2. Climate and parametric uncertainty

In this section we produce multiple results derived from considering both different climate scenarios and multiple options for the uncertain parameters. However, this time, we only look at the more influential parameters: θ and c_G . We sample 4 elements from their uncertainty ranges and store the solutions for each climate projection and each combination of parameters. We are therefore left with $6(\text{climate projections}) \times 4(\text{sampled } \theta) \times 4(\text{sampled } c_G) = 96$ experiments.

The idea behind the multi-time step model is to provide decision-makers with suggestions about when and where to place which roofing option. However, suppose all the uncertainties in the problem are considered. In that case, it turns out to be hard to provide a concise suggestion for all the years to come, as multiple results are determined by multiple climate and parameters' options (Fig 5.25). Therefore, we suggest and implement the use of a one-branch tree. We assume that the solutions derived from the first 5 years can be boiled down to one solution to construct the tree with a proper root. This is indeed feasible, as climate forecasts tend to be closer to each other for the first years. Thus, the branching would happen in correspondence of the year 2026. In Fig. 5.26, we provide an idea about how the tree would look like, with 96 branches.

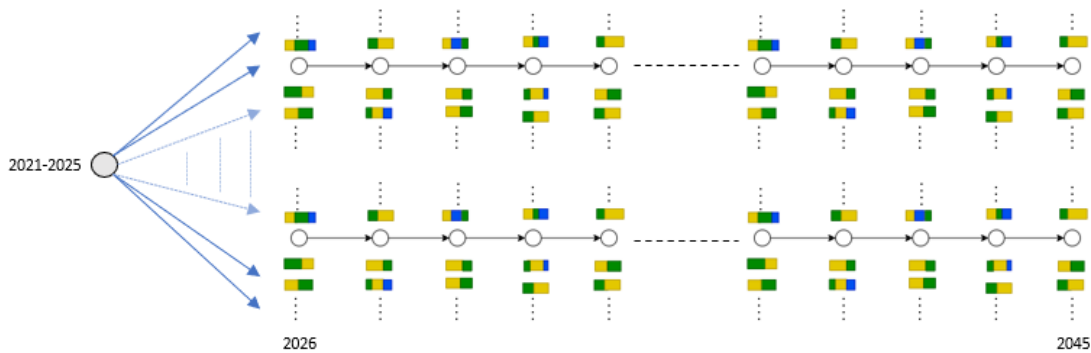


Figure 5.26: One branch tree, where all possible future branches are considered.

To make all these possible solutions more insightful, we decide to cluster all the branches to obtain a one-branch tree with fewer branches. This way, the clusters will have similar results, which can be better explained to a decision-maker. We compute the cosine similarity among all experiments from the year 2026 to the year 2045, which results in Fig. 5.27.

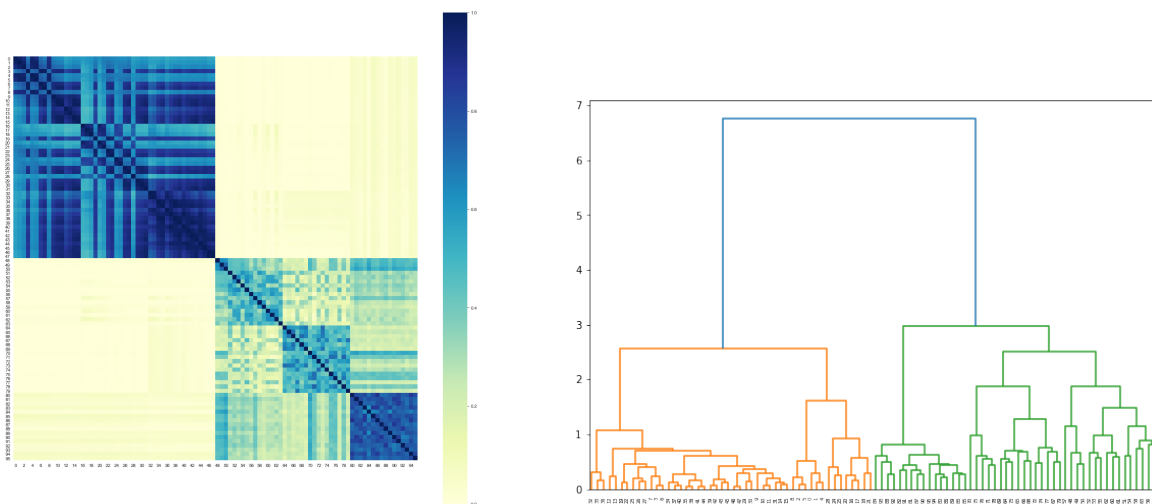


Figure 5.27: Cosine similarity between experiment with varying climate input projection and parameters(right), and dendrogram for hierarchical clustering with complete linkage applied to cosine distance (left).

A dendrogram for the hierarchical clustering with complete linkage is presented in Fig.5.27. We choose the number of clusters with the highest average silhouette value among values between 2 and 6, as we do not wish to visualize more branches. 4 is the number of total clusters with the best silhouette score. This results in the possibility of presenting the tree in a different shape (Fig. 5.28). In practice, we provide a municipality with decisions for the first 5 years, and we explain the future possibilities as 4 different scenarios. After this first consultancy, if required, the model could be run again after the first 5 years to provide a more robust solution as more reliable future climate predictions may become available.

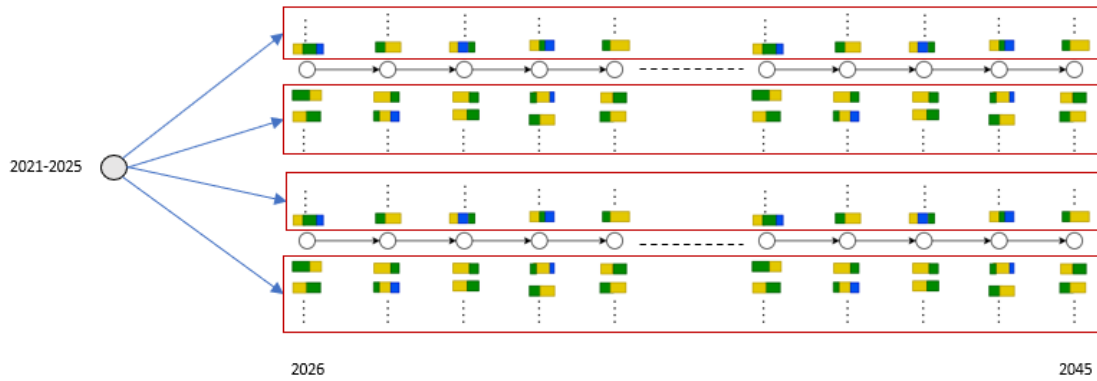


Figure 5.28: One-branch tree with clustered future solutions after year 2026.

6

Conclusion

In this last chapter, we will evaluate which limitations influence the presented work. We will furthermore draw conclusions for the mentioned research questions. Eventually, we will provide some suggestions to further elaborate on this study in the form of recommendations.

6.1. Limitations

Some limitations in our approach will be underlined for the data quality, modeling and analysis choices.

6.1.1. Data limitations

The model constructed in this study can easily be extended and deployed for other municipalities in the Netherlands since all data sources are publicly available. The availability of such data sources comes at a cost: the quality of the data may not be the most reliable, complete, or accurate. Our study focuses on modelling a system that comprises three main parts: climate, buildings, and urban environment (Fig 6.1). Each of these parts has its own data source. For the modeling of each parts, some pre-processing has to be performed on the data retrieved from 3 different data sources.

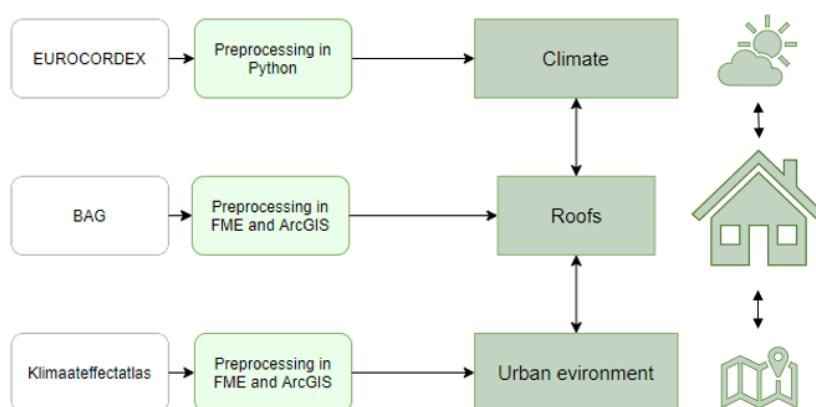


Figure 6.1: The modeled system.

Climate

EUROCORDEX platform is chosen as the source for climate data [26], as it includes numerous projections with the needed time-step and specificity. As it is challenging, if not impossible [26], to assess the reliability of each prediction, we have to accept to use data that is not highly reliable. We have tackled this problem using an ensemble of predictions, as suggested in [26, 34]. Nonetheless, in the multi-step model, the decision variables take a value every year; thus, they are deeply linked to the accuracy of the exact values of the climate data for each year.

Buildings

Buildings' data is needed in this frame for two main aims. Firstly, for retrieving or computing some model parameters. Secondly, for selecting the suitable buildings for roofing application in a given area. Most of the necessary data can be easily retrieved in the open-source BAG and AHN for the first aim. Contrarily, the second case may be presenting some limitations. On the one hand, the data that we use may not be accurate, especially for the slope of the roofs. On the other hand, more information could be needed to investigate the suitability of each roof more properly, e.g. buildings materials or load-bearing capacity of the roofs. Therefore, completeness does not characterize the set of data used for this part of the system under study.

Urban environment

The *Klimaateffectatlas* ([4]) is our primary source when it comes to the urban environment's data. We use it both to retrieve information about greenery and population and assess the impact of extreme weather events on the area of interest. Especially for the latter aspect, some limitations for usability have to be underlined. First, the UHI layer has a thick grid; thus, it is not highly accurate. Secondly, since it is publicly available, we use a layer that indicates the water depth on the streets in the event of heavy rainfall. However, it should be underlined that these predictions are not as accurate as others (e.g. 3Di flood simulation map)[51], which unfortunately are not available for all cities nor freely accessible. Therefore, lack of accuracy should be taken into consideration when working with this type of data.

6.1.2. Modeling limitations

As mentioned in Chapter 3, the formulation proposed in this study is a first attempt to model the complex interactions happening between the system's components (Fig. 6.1). We made some assumptions and simplifications, which we underline in this subsection.

General simplifications

To start, due to the format of the data in our main source ([37]), we chose to simplify the price item. Indeed, we consider a fixed price for m^2 of roof type, while possibilities exist to specify a price based on area and slope of the roof, as is done in [51]. Furthermore, many studies compute future benefits also considering the inflation rate of future years. [31, 49]. Since we do not perform this, the derived benefits must be considered non actualized with the inflation rate.

We also assume that the whole roof area may be covered by green, blue and yellow roofs, while in reality, the area to set up the roofing may be smaller for each option. In the case of green and blue roofs, this may happen mainly because of design choices, while for PV panels, it may be due to the reduced efficiency of the PV panels in some spots, due to shadowing or inclination of the roof [3].

Heat mitigation

Green roofs are very complex systems, which can mitigate two main effects of climate change: extreme heat and extreme rainfall [39, 45]. The phenomena underlying these effects entail complex interactions between the roof and the surrounding environment. It is thus complex to model. Indeed, it is not clear how much decrease in temperature can be achieved in the surrounding micro-climate by each m^2 of green roof. Nor is the amount of rain that can be retained by a layer of green roof easily predictable. Therefore, we simplified these processes and wrote some linear formulas to represent these complex processes.

The utility of heat mitigation is represented by parameter r_G , that takes values between 0 and 1. We shape this parameter following a similar methodology presented in [38] for yellow roofs. The limitation of this approach lies in how r_G influences the computation of benefits $b_G(i)$. More specifically, it acts as a factor that scales the total number of people for which heat-related problems can be avoided. Using this approach means that, in areas where the UHI effect is the most intense, the entire computed population would be benefited. On the contrary, in correspondence to small values of UHI, r_G would reduce the amount of people that benefit from a green roof in each location.

Flooding mitigation

Blue and green roofs' functioning during rainfall is also interesting and challenging to model, as water capture depends on multiple internal and external factors [48]. We chose to simplify this behaviour by introducing a factor that states the average rate of rainfall capture, k_B and k_G . They represent on average, how much water can be captured during a mid-heavy rainfall event.

Moreover, the same limitations mentioned for the green roofs apply to the utility factor of flooding risk mitigation, that is constructed in a similar way (see Appendix A.1). The utility factor, in this case, can be interpreted as follows. The areas where the higher levels of water can be found on the streets in the event of flooding have the highest priority; thus, 100% of the water collected contributes to alleviating the risk. In areas where the water levels are lower, the priority decreases. Therefore, only a part of the total amount of water that could be collected results in a benefit.

6.1.3. Analysis limitations

It is worth mentioning that our approach for the uncertainty analysis may not be the only one possible for our aims. Furthermore, our results are dependent on the amount of clusters considered and on the clustering performance. We report in Appendix A.2, an example of analysis where a different amount of clusters and thresholds are considered.

6.2. Conclusions

The ultimate goal of this thesis is to construct and test the robustness of a model which can identify specific buildings where the placement of green, blue and yellow roofs maximizes the municipalities' climate adaptation and mitigation goals. To the best of our knowledge, we model the functionality of green, blue and yellow roofs, linking it to the climate data and the urban environment information. We use the software *FME* and *ArcGIS* to process the input data and create the parameters for the optimization formulation. Moreover, we use multiple climate projection data in the form of an ensemble to tackle the uncertainty related to future predictions. More precisely, we propose in Sections 4.3 a stochastic and a robust version of the problem that consider multiple projections.

We use *Gurobi* within *Python* to solve the problem for one case study in the city of Schiedam and we compare the outcomes of two different models. The results presented in Section 5.4 show a slight discrepancy between the two models' outcomes, suggesting that both can work properly for practical aims. Moreover, the solutions are in line with common sense. Green and blue roofs are proposed for higher UHI and flooding risk areas, especially in the city centre. Instead, yellow roofs are mainly proposed in industrial areas, which present flatter and bigger roofs with higher solar radiation potential.

Focusing on the stochastic model formulation, we analyze the parametric uncertainty underlying the model. The high average similarity between the solutions suggests that the model is robust: the optimal placement of roofs types is not varying too much. Through the steps described in Section 5.5 we elaborate on which specific variation in the parameters leads to which change in the solutions in terms of total benefits. We conclude that the model is highly sensitive to changes in the values of θ and c_G : the rate of increase in energy production of yellow roofs when green roofs are installed as well, and the cost of heat per person avoiding the hospital every day.

We also implement another model version that can look into time-specific details: the multi-time step model. In this case, we assume that the decision-maker is sure about the roofs' placement in the following 5 years but still wants to look into the possibilities of placement for the following 20 years, considering both climate and parametric uncertainty. We present the solution to this question in the shape of a one-branch tree in Section 5.7.

In conclusion, we have constructed three model versions where we incorporated climate uncertainty through methods derived by the theory of optimization under uncertainty. We analyzed the models' robustness and response to parameters by looking at the results' spatial variability and the variation in total benefits. Moreover, we investigated time variability through the multi-time step model. We gathered all considerations made about the uncertainty of the problem and presented them as practical suggestions to the decision-makers at Sweco. Eventually, the fixed-parameter model version has been merged into a single *FME* flow with the parameters' computation, after having been linearized to be solved by a free solver (see Appendix A.3). This will allow Sweco colleagues to make use of the tool constructed in this study with a single click.

6.3. Recommendations

To the best of our knowledge, this work is the first attempt at constructing a proper optimization formulation for the optimal placement of three types of roofing options interacting with daily climate data and the urban environment. Consequently, there is much to further explore, starting from here. In this section, we provide some suggestions for future research based on the findings of this work.

Two aspects of the methodology can be improved without modifying the model, if more data and computing power is available. Suppose data was available about the current placement of green, blue and yellow roofs. In that case, it could be possible to evaluate the current distribution's efficiency in terms of achieved benefits and compare it to the solution suggested from the model. Secondly, if more computing power was available, more samples could be taken from the distribution of the parameters, and a more in-depth uncertainty analysis could be performed.

However, the same model could be reformulated in order to overcome the limitations drawn in Section 6.1.2. Indeed, the working of green and blue roofs has been investigated in relation to location-specific ([47, 51]) and climate information ([48]). Due to its complexity, the two processes have here been merged simplistically. However, adopting a more detailed perspective would allow computing the resulting benefits in a more precise way. Perhaps, as is done in [48], quantities like humidity and evaporation rates per day could be considered to better specify the amount of water retained by each roof on each day. Moreover, including micro-climate aspects in the parameters' computations may provide more specific insights about the cooling capacities of green roofs, which is here considered fixed.

Furthermore, other beneficial aspects of the roofing options may be considered. For example, the cooling capacity of green roofs for buildings' interior may lead to a decrease in air conditioning usage during heatwaves. In turn, this could lead to societal benefits [24, 45]. Moreover, aspects like biodiversity increase, pollution absorption and water quality increase may be included in such a model. This would perhaps add weight to the potential of green and blue options, which are not always the first choice for the model constructed in this frame.

Bibliography

- [1] Clustering: hierarchical clustering. URL <https://scikit-learn.org/stable/modules/clustering.html>.
- [2] Pairwise metrics, affinities and kernels: cosine similarity. URL <https://scikit-learn.org/stable/modules/metrics.html#cosine-similarity>.
- [3] Estimate solar power potential. URL <https://learn.arcgis.com/en/projects/estimate-solar-power-potential/>.
- [4] Klimaateffect atlas. URL <https://www.klimaateffectatlas.nl/>.
- [5] Latin hypercube sampling, smt documentation. URL https://smt.readthedocs.io/en/latest/_src_docs/sampling_methods/lhs.html.
- [6] Philadelphia stormwater management guidance manual. URL <https://www.pwdplanreview.org/manual/chapter-4/4.6-blue-roofs#>.
- [7] Platte daken in nederland (bag). URL <https://www.atlasleefomgeving.nl/platte-daken-in-nederland-bag>.
- [8] Rotterdam climate change adaptation strategy. URL http://www.urbanisten.nl/wp/wp-content/uploads/UB_RAS_EN_lr.pdf.
- [9] Greendeal groene daken. URL <https://www.greendealgroenedaken.nl/wp-content/uploads/2019/09/GDGD-Facts-and-Values-factsheet-Groenblauwe-daken.pdf>.
- [10] Op weg naar een klimaatbestendig utrecht. URL <https://www.provincie-utrecht.nl/sites/default/files/2020-05/Programma%20Klimaatadaptatie%202020-2023%20provincie%20Utrecht%20mei%202020.pdf>.
- [11] E. Andenæs, T. Kvande, T.M. Muthanna, and J. Lohne. Performance of blue-green roofs in cold climates: A scoping review. *Buildings*, 8:55, 04 2018. doi: 10.3390/buildings8040055.
- [12] M. Barah, A. Khojandi, X. Li, J. Hathaway, and O. Omitaomu. Optimizing green infrastructure placement under precipitation uncertainty. 09 2018. doi: 10.13140/RG.2.2.27940.53123/1.
- [13] L. Bel, D. Allard, J.M. Laurent, R. Cheddadi, and A. Bar-Hen. Cart algorithm for spatial data: Application to environmental and ecological data. *Computational Statistics & Data Analysis*, 53(8):3082–3093, 2009. ISSN 0167-9473. doi: <https://doi.org/10.1016/j.csda.2008.09.012>.

- [14] J. Bender. *Rotterdamse Groene daken, moeten of mogen?Onderzoek of waterbufferende vegetatiedaken wel of niet verplicht gesteld kunnen worden en zo ja, in welke hoedanigheid?* Stadsontwikkeling Gemeente Rotterdam, july 2016. URL <https://cms.4bg.nl/uploads/12/files/Rotterdamse-Groene-daken-moeten-of-mogen-J.-Benders-2016.pdf>.
- [15] U. Berardi. State-of-the-art analysis of the environmental benefits of green roofs. *Applied Energy*, 115:411–428, 03 2014. doi: 10.1016/j.apenergy.2013.10.047.
- [16] F. Bianchini and K. Hewage. Probabilistic social cost-benefit analysis for green roofs: A lifecycle approach. *Building and Environment*, 58:152–162, 12 2012. doi: 10.1016/j.buildenv.2012.07.005.
- [17] A. Ershad. Geographic information system (gis): Definition, development, applications & components. 03 2020. URL https://www.researchgate.net/publication/340182760_Geographic_Information_System_GIS_Definition_Development_Applications_Components.
- [18] H. Feng and K. Hewage. Economic benefits and costs of green roofs. *Nature Based Strategies for Urban and Building Sustainability*, pages 307–318, 02 2018. doi: 10.1016/B978-0-12-812150-4.00028-8.
- [19] J. Fraiture. The robustness of energy systems: A novel method to explore the impact of uncertainties on energy system design optimization models. Master’s thesis, 2020. URL <http://resolver.DelftUniversityofTechnology.nl/uuid:84cd083a-8bf8-4931-a75a-276e2d54c5cc>.
- [20] J. Garcia-Gonzalo, C. Pais, J. Bachmatiuk, and A. Weintraub. Accounting climate change in a stochastic optimization model in forest planning. *Canadian Journal of Forest Research*, 46, 06 2016. doi: 10.1139/cjfr-2015-0468.
- [21] M. Goerigk and A. Schöbel. *Algorithm Engineering in Robust Optimization*, pages 245–279. Springer International Publishing, Cham, 2016. ISBN 978-3-319-49487-6. doi: 10.1007/978-3-319-49487-6_8.
- [22] B. L. Gorissen, İ. Yanıkoğlu, and D. den Hertog. A practical guide to robust optimization. *Omega*, 53:124–137, 2015. ISSN 0305-0483. doi: <https://doi.org/10.1016/j.omega.2014.12.006>.
- [23] M. Groot. Milieuprofiel van stroomaanbod in nederland. 2004. URL <https://ce.nl/publicaties/milieuprofiel-van-stroomaanbod-in-nederland/>.
- [24] J. Habers. *Groene daken Rotterdam maatschappelijke kosten-batenanalyse*. Gemeente Rotterdam, 2014. URL https://cms.4bg.nl/uploads/12/files/2014_MKBA-Begroeide-daken_Habers.pdf.
- [25] S. Hallegatte, A. Shah, C. Brown, R. Lempert, and S. Gill. Investment decision making under deep uncertainty – application to climate change. 09 2012. doi: 10.1596/1813-9450-6193.

- [26] D. Jacob, J. Petersen, B. Eggert, A. Alias, O. B. Christensen, L. M. Bouwer, A. Braun, A. Colette, M. Déqué, G. Georgievski, E. Georgopoulou, A. Gobiet, L. Menut, G. Nikulin, A. Haensler, N. Hempelmann, C. Jones, K. Keuler, S. Kovats, N. Kröner, S. Kotlarski, A. Kriegsmann, E. Martin, E. van Meijgaard, S. Moseley, C. and Pfeifer, S. Preuschmann, C. Radermacher, K. Radtke, D. Rechid, M. Rounsevell, P. Samuelsson, S. Somot, J.-F. Soussana, C. Teichmann, R. Valentini, R. Vautard, and B. Weber. Euro cordex: new high-resolution climate change projections for european impact research regional environmental changes, 2014. URL <https://esgf-data.dkrz.de/projects/esgf-dkrz/>.
- [27] C. Jacobs, M. Budding, J. Spijker, S. Kok, M. de Bel, D. de Jong, J. Kluck, F. Harten, B. Stoop, J. Kluck, W. Noome, E. Slingerland, P. Bosch, J. van Leuken, A. de Bondt, S. Troost, H. Goosen, A. Koekoek, M. van Bijsterveldt, and S. Hofland. Klimaatschadeschatter, rapportage 2019. *Klimaatbestendige Stad, NKWK*, 12 2019. URL <https://library.wur.nl/WebQuery/wurpubs/567016>.
- [28] S. Jerez, I. Tobin, R. Vautard, J. P. Montávez, J. M. López-Romero, F. Thais, B. Bartok, O. Bøssing Christensen, A. Colette, M. Déqué, G. Nikulin, S. Kotlarski, E. van Meijgaard, C. Teichmann, and M. Wild. The impact of climate change on photovoltaic power generation in europe. *Nat Commun*, 6(10014), 2015. doi: <https://doi.org/10.1038/ncomms10014>.
- [29] F. Kreienkamp, H. Huebener, C. Linke, and A. Spekat. Good practice for the usage of climate model simulation results - a discussion paper. *Environmental Systems Research*, 1, 09 2012. doi: [10.1186/2193-2697-1-9](https://doi.org/10.1186/2193-2697-1-9).
- [30] A. Mahdiyar, S. Tabatabaee, A. Sadeghifam, S.R. Mohandes, A. Abdullah, and M. Moharrami. Probabilistic private cost-benefit analysis for green roof installation: A monte carlo simulation approach. *Urban Forestry & Urban Greening*, 20:317–327, 12 2016. doi: [10.1016/j.ufug.2016.10.001](https://doi.org/10.1016/j.ufug.2016.10.001).
- [31] A. Mahdiyar, S. Tabatabaee, K. Yahya, and S.R. Mohandes. A probabilistic financial feasibility study on green roof installation from the private and social perspectives. *Urban Forestry & Urban Greening*, 58, 10 2020. doi: [10.1016/j.ufug.2020.126893](https://doi.org/10.1016/j.ufug.2020.126893).
- [32] K. Manohar. Cost benefit analysis of implementing a solar photovoltaic system. *International Journal of Innovative Research in Science, Engineering and Technology*, 4, 12 2015. doi: [10.15680/IJRSET.2015.0412006](https://doi.org/10.15680/IJRSET.2015.0412006).
- [33] M. Manso, I. Teotónio, C. Matos Silva, and C. Oliveira Cruz. Green roof and green wall benefits and costs: A review of the quantitative evidence. *Renewable and Sustainable Energy Reviews*, 135:110111, 2021. ISSN 1364-0321. doi: <https://doi.org/10.1016/j.rser.2020.110111>.
- [34] D. Mcinerney, R. Lempert, K. Keller, F. Pardee, and D. Building. What are robust strategies in the face of uncertain climate threshold responses?: Robust climate strategies. *Climatic Change*, 112, 11 2009. doi: [10.1007/s10584-011-0377-1](https://doi.org/10.1007/s10584-011-0377-1).

- [35] S. Meijs, Y. Deelstra, A. Grinwis, P. van Hemert, K. van Nieuwaal, T. Solleveld van Helden, H. Westera, and B. van Zeggeren. *Nationale klimaatadaptatiestrategie 2016 (NAS)*. Aanpassen met ambitie, december 2016. URL <https://klimaatadaptatienederland.nl/overheden/nas/>.
- [36] N. Mohammadzadeh. *An Optimization Approach for Integrating Different Roof Functions with Environmental Impacts Constraint: "A Hybrid Framework"*. PhD thesis, 2016. URL <http://www.lib.ncsu.edu/resolver/1840.20/33341>.
- [37] J. Posma. Life urban roofs 2.0 background report key figures. 2021. URL <https://www.rotterdaminnovationcity.com/apps/int-ondernemen010.nl/Themes/energy/Background-Report-LIFE-Urban-Roofs-EN.pdf>.
- [38] M. Ramshani, A. Khojandi, X. Li, and O. Omitaomu. Optimal planning of the joint placement of photovoltaic panels and green roofs under climate change uncertainty. *Omega (United Kingdom)*, 90, 2020. ISSN 03050483. doi: 10.1016/j.omega.2018.10.016.
- [39] M. Razzaghmanesh, S. Beecham, and T. Salemi. The role of green roofs in mitigating urban heat island effects in the metropolitan area of adelaide, south australia. *Urban Forestry & Urban Greening*, 15:89–102, 2016. ISSN 1618-8667. doi: <https://doi.org/10.1016/j.ufug.2015.11.013>.
- [40] A. Goel R.B. Zadeh. Dimension independent similarity computation. *Journal of Machine Learning Research*, 14:1605–1626, 2012. URL <https://www.jmlr.org/papers/volume14/bosagh-zadeh13a/bosagh-zadeh13a.pdf>.
- [41] P. Rosasco and K. Perini. Selection of (green) roof systems: A sustainability-based multi-criteria analysis. *Buildings*, 9:134, 05 2019. doi: 10.3390/buildings9050134.
- [42] P.J. Rousseeuw. Silhouettes: A graphical aid to the interpretation and validation of cluster analysis. *Journal of Computational and Applied Mathematics*, 20:53–65, 1987. ISSN 0377-0427. doi: [https://doi.org/10.1016/0377-0427\(87\)90125-7](https://doi.org/10.1016/0377-0427(87)90125-7).
- [43] M. Shafique and R. Kim. Application of green blue roof to mitigate heat island phenomena and resilient to climate change in urban areas: A case study from seoul, korea. *Journal of Water and Land Development*, 33(1):165–170, 2017. ISSN 20834535. doi: 10.1515/jwld-2017-0032.
- [44] R. Smith, C. Tebaldi, D. Nychka, and L. Mearns. Bayesian modeling of uncertainty in ensembles of climate models. *Journal of the American Statistical Association*, 104: 97–116, 03 2009. doi: 10.1198/jasa.2009.0007.
- [45] A. Solcerova, F. van de Ven, M. Wang, M. Rijdsdijk, and N. van de Giesen. Do green roofs cool the air? *Building and Environment*, 111:249–255, 2017. ISSN 03601323. doi: 10.1016/j.buildenv.2016.10.021.
- [46] I. Teotónio, M. Cabral, C. Cruz, and C. Matos Silva. Decision support system for green roofs investments in residential buildings. *Journal of Cleaner Production*, 249:119365, 11 2019. doi: 10.1016/j.jclepro.2019.119365.

- [47] A. van Gameren. Green roofs and climate resilience in the hague. Master's thesis, 2020. URL <http://resolver.DelftUniversityofTechnology.nl/uuid:55e92e3c-0b43-4064-8cbb-2ea1d1e1e068>.
- [48] A. van Hamel. Towards climate resilient buildings. defining the strengths and weaknesses of green-blue roofs regarding temperature management and water storage. Master's thesis, Delft University of Technology, the Netherlands, 2021. URL <http://resolver.DelftUniversityofTechnology.nl/uuid:80848873-ae55-40c2-8a7c-4158bbdee90b>.
- [49] S. Versluis and J. Weij. Maatschappelijke kosten- en batenanalyse en stimuleringsregelingen. Master's thesis, 2013. URL https://cms.4bg.nl/uploads/12/files/2013_MKBA-en-Stimuleringsregelingen_Versluis-Weij.pdf.
- [50] A. Voltaire and D. Saint-Martin. Climate models. *Encyclopedia of the Environment*, [online ISSN 2555-0950]. URL <https://www.encyclopedie-environnement.org/en/climate/climate-models/>.
- [51] L. Zwaanenburg. Spatial analysis for green roof multifunctionality maximization opportunities in rotterdam. Master's thesis, 2019. URL https://cms.4bg.nl/uploads/12/files/2019_Spatial-Analysis_Applying-Green-Roofs-for-Climate-Resilience_Lars-Zwanenburg-TUD.pdf.

A

Appendix

A.1. GIS parameters

Set of suitable roofs

Not every building is suitable for the placement of all roofing options. Therefore, once the area of interest is selected, it is crucial to identify the buildings whose roofs are suitable for hosting green, blue and/or yellow roofs.

The suitability of each building to a sustainable roofing option is subject to the structural characteristics of the roof. A roof is considered suitable if it can bear the load imposed by the application of the layers and if it allows for a good functioning of the chosen roofing option [47, 51]. Many studies have investigated the link between load-bearing capacity and characteristics of the buildings such as age and dimensions [18, 47, 51]. However, it is difficult to infer any strong relationship between these quantities and the roof's strength, and it is therefore always suggested to perform a real-check on each roof to determine the structural suitability. The functional suitability, thus the characteristics that make green, blue and yellow roofs able to efficiently perform their roles, mainly entail the roof's area and slope. In this study, we extrapolate data about these quantities and infer from that the suitability of the roofs.

Roof's area:

Since applying sustainable roofing options onto small areas would generate few benefits, many studies only consider roofs with a specific minimum area. In this frame, the choice has been made to consider only buildings with an area of at least 30 m^2 . On the one hand, some policies in the Netherlands require a roof to be at least 10 m^2 to be eligible for, e.g., green roofs subsidies [47]. On the other hand, the workflow followed for the estimation of solar power potential [3] suggests that 30 m^2 is the lower limit for a roof to produce enough energy from PV panels installation. Experts at Sweco were also suggesting 30 m^2 as the minimum area needed to install green and blue roofs. The data about each roof's area is extrapolated from the Basisregistratie Adressen en Gebouwen BAG, the database containing all buildings' shapes and information for the Netherlands.

Roof' slope:

Roofs with a maximum slope of 45° are reported to be suitable for green roofs installation [15, 47, 51]. However, the stronger the slope, the higher the costs of installation [51], while the efficiency decreases: water retention capacity of sloped roofs is lower than for flat roofs, and consequently also the potential for heat mitigation is lower. Notwithstanding, the studies taken as the primary sources of parameters' values for this thesis mainly deal with flat roofs [37, 48]. Consequently, for the case study of Schiedam, we consider only flat roofs or roofs which have some portion of flat surface. To be able to select roofs with such characteristics, a dataset has been used, which can be found in [7]. The dataset is constructed based on the current Actueel hoogtebestand Nederland (AHN3), the actual height dataset of the Netherlands, and the BAG. The variation in height for each building is used to estimate which portion of a roof is flat, and a number between 0 and 100 represents it. A 0 indicates a lot of variation in height, e.g. a pitched roof or a roof with chimneys and other objects. 100 indicates that no variation is present in the flatness. After observing the data associated with each building, it was chosen to use 70 as the threshold for selecting suitable buildings in this first phase. Indeed, with this choice, a selection of mainly flat buildings with some elements on top is made.

Other factors:

It is important to stress that all three roofing options considered in this study entail a heavy load on the building' structure. PV panels are light compared to green and blue equivalents per m^2 ($11.4 \text{ kg}/m^2$ for yellow, $40\text{-}80 \text{ kg}/m^2$ for green to which $25\text{-}100 \text{ kg}/m^2$ of weight is added when a blue roof layer is placed beneath the green roof [9]). Indeed, all these options determine a higher load than the one required to be born by construction regulations in the Netherlands (NEN normen en richtlijnen). The link between age and strength of the roofs has been investigated based on existing data about green and yellow roofs. However, the unsatisfying results led to considering all buildings selected (with an area bigger than 30 m^2 and a slope coefficient of at least 70) to be suitable for green, blue and yellow roofs. This assumption was supported through the many interviews with Sweco experts, who could make some considerations regarding roofs' strength. Firstly, it was declared that most of the buildings could be reinforced to increase the roof's load-bearing capacity. Secondly, most flat roofs in the Netherlands are currently covered with white gravel, which could make some space for the other roofing options when removed.

Spatial Parameters

As explained in Section 3.2, the model inputs are required to be building-specific and to encapsulate the usefulness of applying green, blue or yellow roofs solutions on each roof. In the following subsections, it will be explained how each climate-derived risk can be encapsulated into modelling parameters.

Flooding risk:

Heavy precipitation over a short period can cause local flooding. This type of flooding is most common in summer. A large part of the Dutch streets and squares can be flooded during heavy showers [4].

The factor $r_B(i)$ used in the formulation expresses the usefulness of applying water retention roofs (green and blue roofs) on top of buildings, based on their location. The computations behind this factor are formulated into the software FME. The workflow takes as an input the shapes of the buildings (from the BAG dataset) and the dataset from the *Klimaffectatlas* [4], which depicts the water level during a heavy rainfall event. Following the procedures applied by Sweco in a similar project, a buffer of 20m is taken around the building. As can be seen in Fig A.2, the buffer intersects the water depth layer (reported entirely in Fig A.1), and the intersected values are handled to compute an estimation of the volume of water per m^2 which surrounds the building in case of heavy rainfall. This value is computed for each element in the set of suitable inputs and is rescaled between 0 and 1. In this way, buildings surrounded by the highest levels of water would get the highest utility rate. In contrast, the ones positioned in an area that would not be affected by heavy rainfall receive a low utility rate. This way of scoring is derived from the concept behind the formulation of a similar rate for solar radiation in [38].

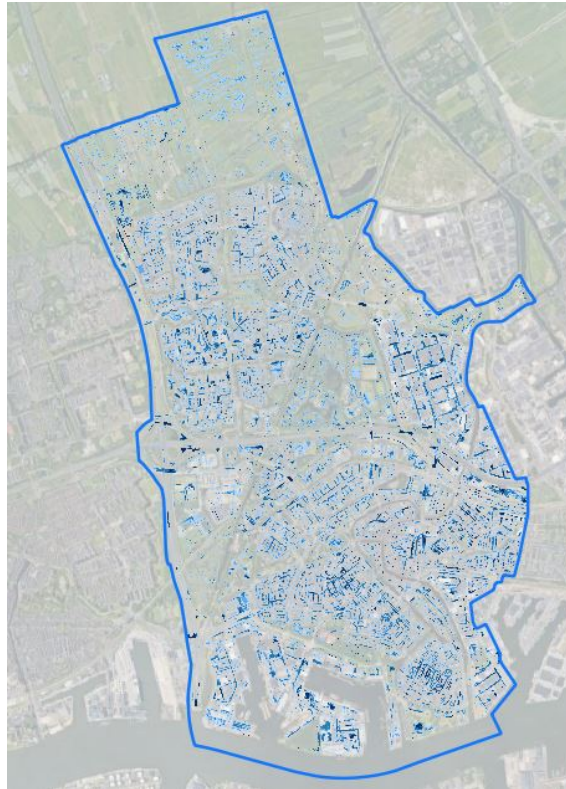


Figure A.1: Water level during heavy rainfall event.

Another important factor that is spatialized starting from the main source [37] is $c_B(i)$: the one-time shadow costs derived from increasing the sewage system capacity. Here, the monetary benefit derived from the roofs' storage is reported as the avoided costs, and spread over the total amount of mid-heavy rainfall events. Such operation is more expensive in an area like the city centre [24]. The scale used in [49] is employed, which considers the value estimated in [24] and derives the following: or dense urban areas like the city centre $500\text{€}/m^3$, other urban areas have a cost of $350\text{€}/m^3$, while rural areas have $200\text{€}/m^3$.



Figure A.2: Flooding risk buffer.

Urban Heat Island:

In any city in the world, the Urban Heat Island (UHI) effect is a phenomenon affecting the health and well-being of its inhabitants. An urban area experiences significantly higher temperatures than its surroundings, composing the "island" of heat. The main sources of this problem can be found in the increased use of materials with high solar absorption and in anthropogenic heat production. The structure of the area also contributes to the phenomenon, mainly affected by the presence of high buildings and the consequent scarcity of air circulation [45]. Since future temperatures are predicted to rise also in the Netherlands [47, 48], it is essential to find smart ways for mitigating this effect.

A map exists for the Netherlands [4], where urban heat island is estimated and presented with an index between 0 and 4 which equally spans a UHI value between $+0.2^\circ$ and $> +2^\circ$ Celsius over the measured temperature. We make use of this layer to compute the utility factor $r_G(i)$ for heat reduction in correspondence to each building. The buffer of $20m$ around each building is taken (Fig A.4), and the utility factor r_G is computed as the average of the UHI index weighted per area of influence. This value is computed for each building and is later rescaled to assume values between 0 and 1.

Urban heat island affects the population living in cities, as high temperatures can cause societal issues like death excess among fragile individuals and labour loss due to heat [37, 45, 51]. The study taken as the main source of parameters values estimates avoided healthcare costs per person and evaluates the reduction in patients per 1000 inhabitants at 1% more green within 200 meters. However, these estimates merge the contribution of multiple factors derived by greening a roof: avoided healthcare costs because of urban heat island mitigation, increase in greenery view, biodiversity increase and improvement of air quality. Therefore, the analysis about heatwaves impact in the Netherlands made in [27] was considered. From this study we derive the amount of patients entering the hospital because of extreme heat, and the consequent costs.

In [27] it is reported that 1.079 people in 100000 go into hospital in the Netherlands every day in which the max temperature reaches or goes above 30° Celsius. We do not assume that the amount of people influenced by each roof is a constant as in [37], but we compute such value based on population density and greenery presence. Population density for each area is taken from the open dataset of Centraal Bureau voor de Statistiek

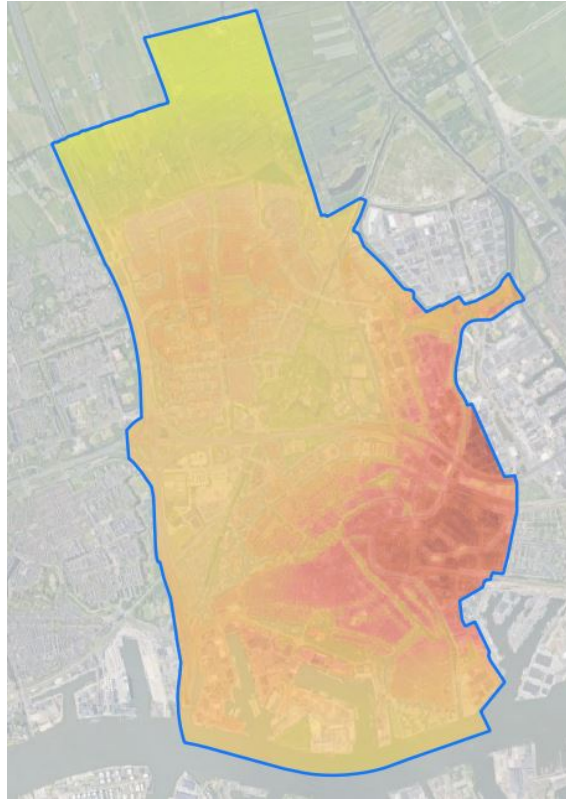


Figure A.3: Heat stress is modeled through the use of a urban heat island layer.



Figure A.4: Heat stress buffer.

(CBS). From the ray of influence considered, it is possible to estimate the number of people for each building, which the decreased temperature could influence in the surrounding micro-climate. This value is multiplied by the rate of hospitalized people due to heat (1.079/100000). Following, since the relative increase of greenery plays a critical role [37], it is assumed that this hospitalization value is valid for a 1% increase in greenery. Thus the value is scaled based on which proportional increase each roof and size is yielding in its surroundings. Note that the latter correspond to the shape of the polygon where the amount of greenery is reported in [4]. The latter computations form the parameter $m_G(i, z)$, which is also depending (thus will be scaled based) on $z \in H$, the temperatures during hot days with more than 25° .

Solar Radiation Potential:

Following the workflow reported in [38] another input, $r_Y(i)$, is needed for the model. This parameter expresses how much solar radiation potential there is on each building, thus provides an indication about how useful and/or efficient it will be to place solar panels on a specific roof.

The procedure described in [3] is followed to compute such values. A digital surface model (DSM) dataset is loaded into the software *ArcGIS*. A DSM shows the elevation of the ground and its features (such as trees, sidewalks and buildings) and it comes in the shape of a raster layer. Such data is processed by a function, *Area Solar Radiation*, which computes the solar radiation based on a sophisticated model. The latter considers the sun's position throughout the year and at different times of day, obstacles that may block sunlight, such as nearby trees or buildings, and the slope and orientation of the surface. The output is provided as a new raster layer where each cell value is the amount of solar radiation in watt-hours per square meter (Wh/m²) at that location. The average of this value is computed for each rooftop and later rescaled between 0 and 1.

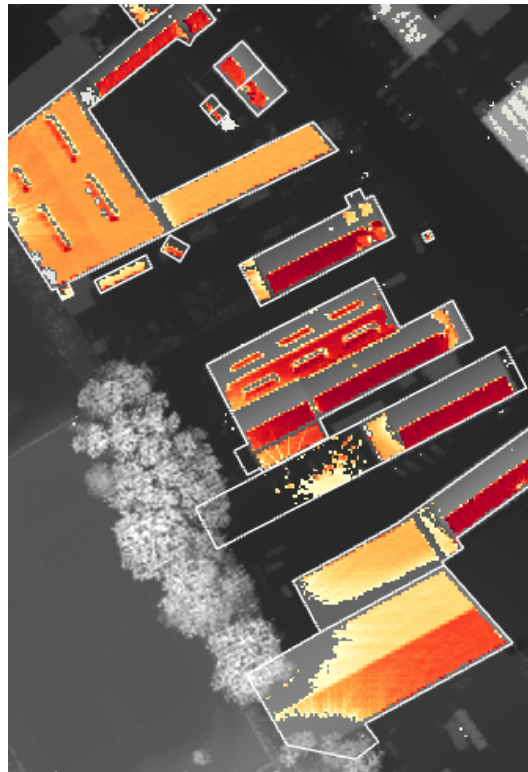


Figure A.5: Solar radiation potential.

Technical parameters

The contribution to the urban climate resilience is not only mapped through the construction of spatially-derived parameters, but it is also linked to the technical functioning of the roofs. Indeed, the roofs' performance against extreme weather events is also a complex theme.

Response to heavy rainfall:

The response to medium/heavy rainfalls is simulated in [48], where an analysis is conducted regarding the water retention potential of a green-blue roof system. For this thesis, the interest lay in discovering an average value of water retention which a base green-blue system could achieve. For rainfall events with more than $25\text{mm}/\text{day}$, it was discovered that such a system would retain the water properly during the summer period but would fail to help in water management during the more wet periods [48]. Therefore, here we will consider a system with an adaptive valve. Such a structure is composed of a water retention layer of 60 mm whose content can be tuned by opening or closing a valve, based on predicted rainfall. A valve would stay close during a heavy rainfall event to allow for a delay of discharge of the water into the sewage system and for water usage for evaporation. In case of predicted heavy rainfall, the valve would be opened to empty the water layer and capture the upcoming rain. A controlled system like the one described is, on average able to retain 80% of the rain over the whole year, considering only rainfall events of more than $25\text{ mm}/\text{day}$ [48].

Performance during heatwaves:

The reduction in hospitalizations mentioned in [27] is referred to every day with a temperature above 30°Celsius . As is done in [47] it is assumed that each roof can reduce the surrounding micro-climate temperature by 1°Celsius . Thus, it can avoid the number of hospitalizations mentioned in [27] for every day with 31° . To make this value more climate-specific, we have scaled the value of hospitalizations per hot day $m(i, z)$ for every possible temperature. We assume that 0 hospitalizations due to heat would occur in correspondence to 25°Celsius ; then, we interpolate the other values linearly up to $1.079/100000$ in correspondence to 31°Celsius .

Relation with solar radiation:

The production of energy from yellow roofs is strictly linked to the amount of solar radiation received by the roof [37, 38]. Among multiple possible methods, we will estimate how much energy is produced by each m^2 of PV panels by looking at the amount of sun peak hours, as is done in [38]. Sun-peak hours are the number of hours per day when the solar radiation is at least $1000\text{ W}/m^2$. Associated with each sun-peak hour, a quantity Q of energy can be produced, based on the PV system's efficiency and the energy grid. The estimation of Q value is taken from [37].

A.2. Computational insights

CART classification complete figure

We report here A.6 the complete version of the simplified CART tree reported in the results. We choose a maximum depth value of 7.

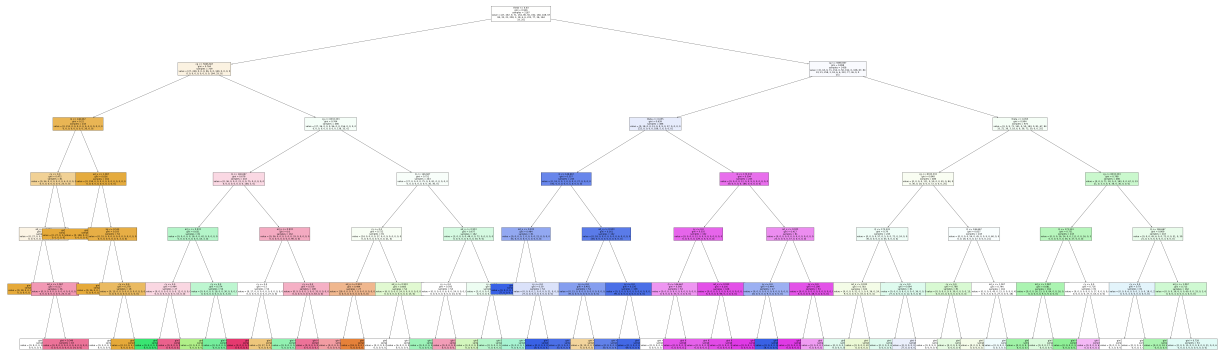


Figure A.6: Caption

CART classification on a smaller sample of experiments

The adopted CART classification algorithm is heavily dependent on the way the classification is made. We here report an analysis made when a different number of clusters is chosen and further analysed. We choose to divide the 2187 solutions into 52 clusters. We then look only into the clusters which explain more than 1% of the data; thus we exclude clusters with less than 21 elements. By doing so, we focus our attention on the clusters which represent more the entire data set. This operation results in 19 clusters to be further analyzed, which we denominate clusters of interest.

For each parameter and each cluster of interest, we compute the inter quartile range (IQR), the difference between the 75th and 25th quantile of the distribution of the data. This procedure would allow to gain some first insights about which parameter may be of higher importance. To make the IQRs from different parameters comparable, we rescale such values using the 50th quantile. We now present both these rescaled IQRs and the 50% quantiles in the tables of Fig A.7. By colouring the internal values with a heatmap, it is possible to have a first impression about which parameters are more characteristic of certain clusters and which are not.

The parameters showing the smallest values in IQRs and highest variation in 50% quantile are the ones which most probably are determinant for each cluster. Indeed, a small IQR shows that for most experiments the parameters were sampled with the same value. Remember that each parameter can take 3 different values. If the IQR is small, this means that most of the experiments were generated using one or two values for the parameter. Instead, different colours, thus values, for the vertical lines in the 50% quantile can also mean that the clusters differ from one another by that parameter. In our case, it looks like k_B will not be extremely significant for the variations in the decision variables, nor will k_G . On the contrary, c_G , ad_u , c_Y , Q and θ may all be more determinant in the choice of location and type

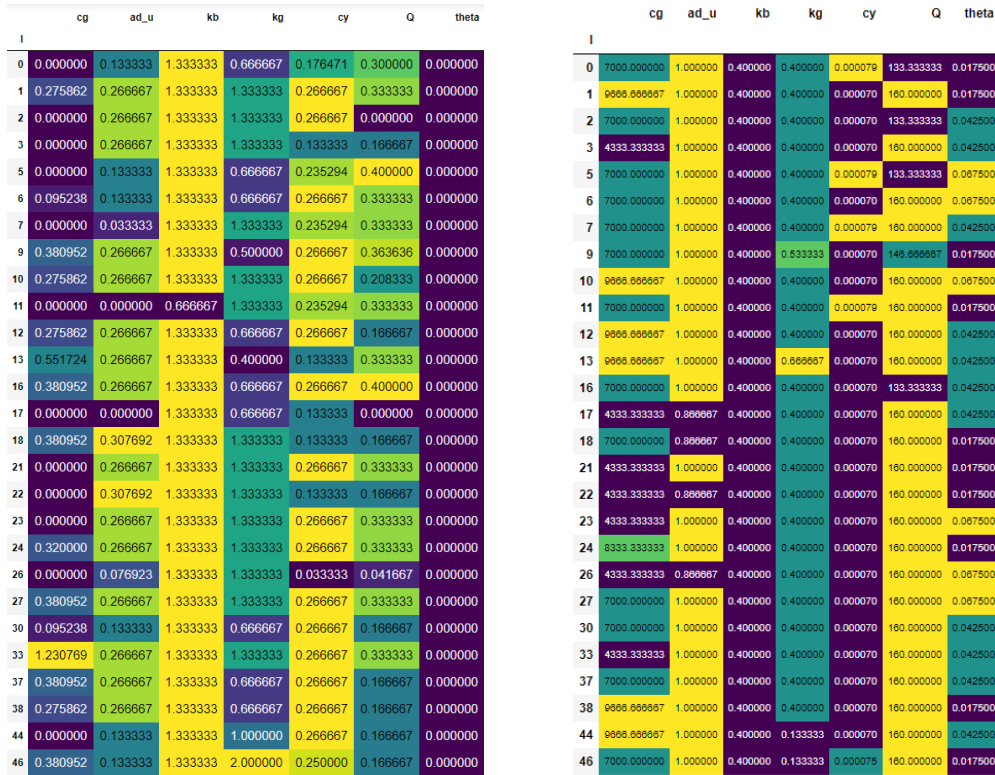


Figure A.7: Inter quantile ranges rescaled and 50% quantile for each parameter sampled and each cluster.

of roof in the solution. We will look into this more in depth in the next step of the analysis: subspace partitioning.

We select only the clusters of interests with a silhouette value of more than 0.7, resulting in a total of 8 clusters to be analysed with the CART algorithm. This way, the results provided by the tree will be more insightful. Using a high silhouette value as a threshold allows to select only clusters which are very well formed: they have a high in-cluster similarity and a low similarity with elements from the other clusters. A simplified scheme of the resulting tree is presented in Fig.A.8.

The fourth cluster is the only one whose elements are all uniquely determined by one specific parameter: θ . All other clusters are created having other main drivers. As an example, cluster 5 has all experiments derived from $\theta > 0.055$ and $c_G \leq 8333$. The other clusters also have some main driver, but they are less influenced by each mentioned parameter. Indeed, the other clusters can be found going down into the tree's branches. For those clustered experiments some division derived by some parameter can be identified. However, such divisions have a higher Gini index, as the parameters characterize a smaller proportion of elements for each cluster.

The most important detail derived by looking at the CART tree is the presence at the first layers of the tree of 2 determinant parameters: θ and c_G . From this analysis, it is shown that the lowest value in the uncertainty range for θ is likely to determine a complete absence of

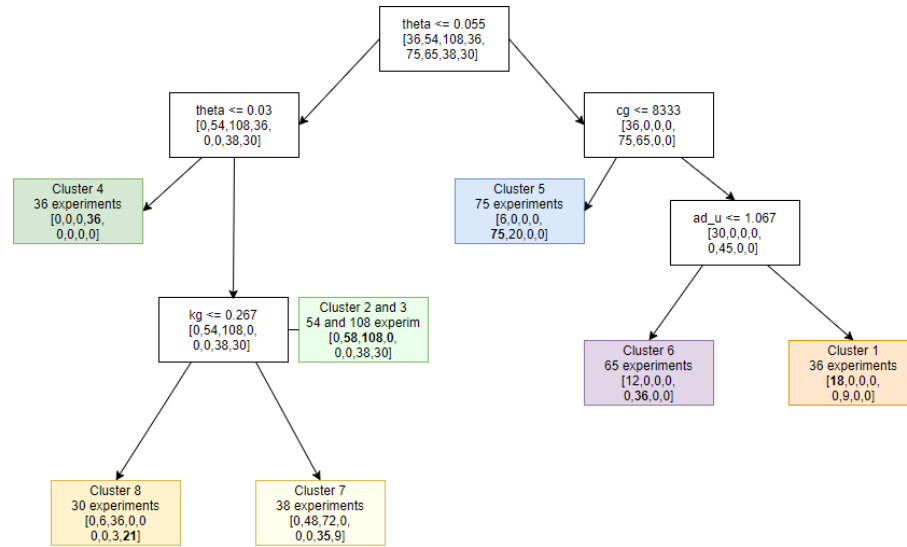
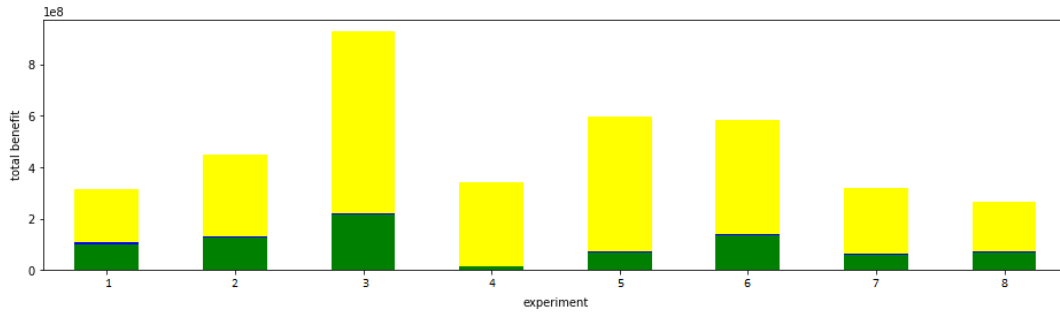


Figure A.8: Simplified CART tree representation. The tree shows which parametric features lead more strongly to the formation of the clusters

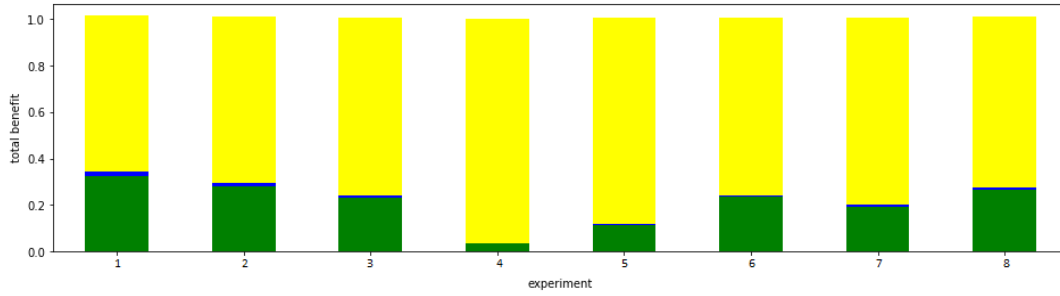
	nr in-cluster	Underlying uncertainties	Remarkable characteristics
1	36	$\theta > 0.055, c_G > 8333, ad_u > 1.067$	highest blue roof benefits proportion
2	54	$0.03 < \theta \leq 0.05, k_G > 0.267$	high proportion of blue roofs but lower benefits
3	108	$0.03 < \theta \leq 0.05, k_G > 0.267$	higher relative amount of yellow roofs compared to cluster 2
4	36	$\theta \leq 0.03$	no blue roofs
5	75	$\theta \leq 0.05, c_G \leq 8333$	highest proportional amount of yellow roofs after cluster 4
6	65	$\theta \leq 0.05, c_G \leq 8333, ad_u \leq 1.067$	relative results comparable to cluster 3
7	38	$0.03 < \theta \leq 0.05, k_G > 0.267$	small amount of roofs
8	30	$0.03 < \theta \leq 0.05, k_G \leq 0.267$	small amount of roofs

blue roofs' presence, and a decrease in green roofs' placement (Fig. A.9). The parameter θ is present in the formula that computes the benefit derived by each roof. It links yellow and green roofs, and it determines an increase in the energy production of yellow roofs when the green roof is present on top of the same building. From previous analysis it has been shown that indeed yellow roofs seem to be always the first and most chosen solution at all given budgets. It is thus significant to see that also the presence of green roofs may be driven by the contribution they could give in the energy production of PV panels. The decrease in green roofs investments has as a consequence the reduction, or even absence in this case, of blue roofs. This happens because the model allows the placement of blue roofs only in correspondence to an already existing green roof. The less green roofs the smaller the possibility of installing blue layers.

It is insightful to both look at the distribution in benefits over the clusters (Fig. A.9), and into the total amount of roofs chosen where to place each option (Fig. A.10). Note that the



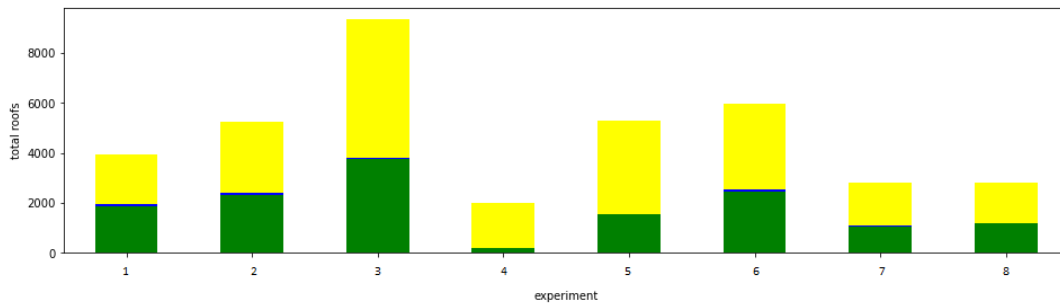
(a) Total benefits derived by green, blue and yellow roofs in the decision variables per cluster. Remind that each cluster has a different amount of elements clustered



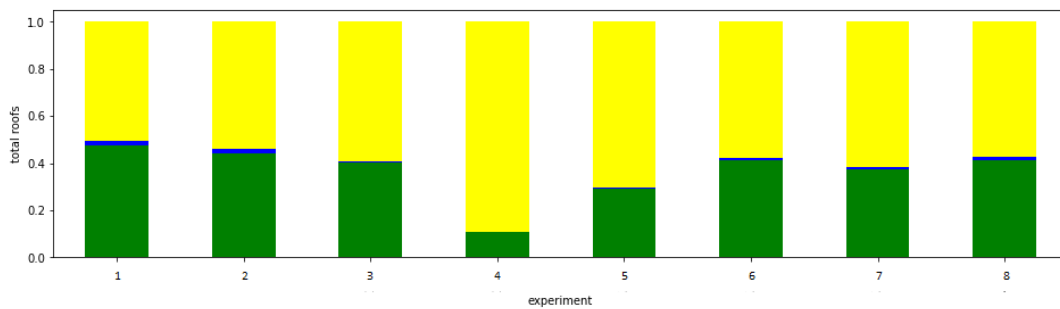
(b) Total benefits derived by green, blue and yellow roofs in the decision variables per cluster, rescaled over total benefit.

Figure A.9: Clusters benefits' distribution

total takes into account all experiments clustered together.



(a) Total roofs covered by green, blue and yellow roofs in the decision variables per cluster. Remind that each cluster has a different amount of elements clustered



(b) Total roofs covered by green, blue and yellow roofs in the decision variables per cluster, rescaled over total roofs.

Figure A.10: Clusters benefits' distribution

The highest green and blue benefits (both total and relative) can be found in cluster 1, which in the CART tree seems to be determined by the highest values possible for θ , c_G and adu . This underlined perfectly how a growth in the linear parameters comprised in the computation of benefits derived by adaptation measures (green and blue) leads to a higher presence of such roofing options in the decision variables. Conversely to what explained in the last paragraph for cluster 4, here the high value of θ is determining a higher presence of green roofs. Moreover, parameter c_G is the monetary equivalent of having one person in hospital due to heat. The highest value possible for this parameter is including both the hospitalization costs and the work loss, as is chosen in our main source, [37]. Parameter adu expresses the variation in the added values derived by adaptation measures, both in terms of heat reduction (green) and flooding mitigation (both blue and green). Therefore, it is clear how these factors can lead the model to propose more locations to have green and blue roofing options installed. Since cluster 5, with a comparable amount of experiments, is presenting the exact complementary values of determinant parameters, it is interesting to notice that it presents much lower values for the total amount of green and blue options (Fig. A.10).

Overall, the results are in line with the ones obtained with fixed values of the parameters, and the difference in the solutions are well explained by the model' shape. In the next sections, we will pick the parameters which determine the highest variations, and combine the uncertainty analysis with a more insightful version of the model: the multi step model.

CART regression

Before feeding the solutions to the CART algorithm, we use clustering as a dimensionality reduction phase. The tree can better detect the discriminant rules behind the assigned (cluster) labels, appearing as a more compact yet labelled input. In our case, we use CART in classification mode.

However, it is possible to deploy CART in regression mode, to directly link the sum of benefits with the parametric drivers. This way, the tree would provide "best guesses" for the continuous values of the benefits, based on some partitioning of the parameters space. We have reported the resulting tree in Figure A.11. We have not followed this as the main methodology since the tree is less insightful due to the many experiments and many values that the benefits can take (see Fig. A.11).

It is interesting to observe that the importance of the parameters is similar in the two cases, except for parameter theta. Theta is very relevant in CART classification, while it loses its importance in CART regression. A change in green roofs' benefits is minor compared to the consistently higher benefits derived by yellow roofs. Moreover, the small added yellow benefit derived for one roof when a green roof is added beneath the PV panels is relatively small compared to the total sum over all buildings of the yellow roofs. Then it makes sense that theta does not play a significant role in the CART regression as that only 'sees' the sum of benefits and not the locations.

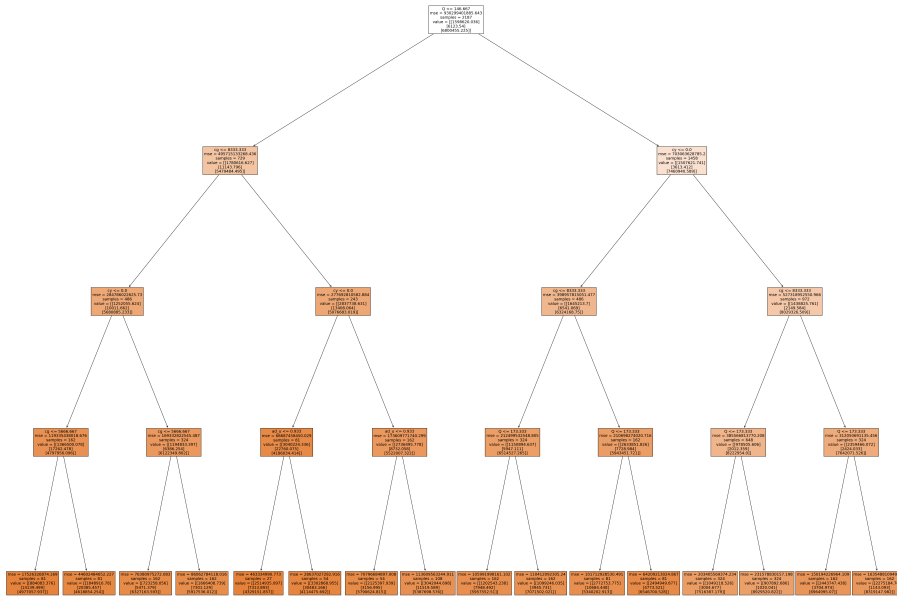


Figure A.11: Results of CART regression, applied to the sum of benefits per roof.

A.3. Linear version of the model

Since *Gurobi* optimizer is not freely available for companies, it was important to find an alternative for Sweco to make use of the constructed model. The most important optimization problem solvers all require the input to be a linear program. Therefore, we had to reformulate our fixed-parameter problem into a linear problem. Then we make use of *pulp* package and solve the model for any input provided.

The main challenge consists in linearizing the expression for the benefits derived by yellow roofs $b_Y(i)$. Indeed the formula contains the multiplication between two decision variables, $x_Y(i)$ and $y_G(i)$.

$$b_Y(i) = c_Y \cdot Q \cdot d \cdot x_Y(i) \cdot r_Y(i) \cdot (1 + \theta \cdot y_G(i)) = c_Y \cdot Q \cdot d \cdot x_Y(i) \cdot r_Y(i) + c_Y \cdot Q \cdot d \cdot x_Y(i) \cdot r_Y(i) \cdot \theta \cdot y_G(i)$$

For the aim, we make use of the big M method, as is done in [38]. To remove the non linearity present in $x_Y(i) \cdot y_G(i)$, we introduce two new continuous variables. We call them $\zeta_1(i)$ and $\zeta_2(i)$. The new variables should satisfy the following constraints $\forall i \in R$:

$$\zeta_1(i) + \zeta_2(i) = x_Y(i) \quad \zeta_1(i) \leq M \cdot y_G(i) \quad \zeta_2(i) \leq M(1 - y_G(i))$$

Here, M has to be a sufficiently large number. Thanks to this, now the expression of benefits for yellow roofs $b_Y(i)$ can be reformulated in a linearized way as follows:

$$b_Y(i) = c_Y \cdot Q \cdot d \cdot x_Y(i) \cdot r_Y(i) + c_Y \cdot Q \cdot d \cdot r_Y(i) \cdot \theta \cdot \zeta_1(i)$$

A.4. Codes

The python codes created in this study are reported in the following Github repository: https://github.com/lisamarietalia/MSc_thesis_repository.git. Here, we report the code needed to extract climate events of interest for this study. Moreover, we report the code for developing the uncertainty analysis using *Gurobi* solver. There are also examples for the use of the robust and stochastic version of the model and of the multi-time step formulation. Lastly, I have stored the code that allows to run the stochastic model without *Gurobi*. Instead we solve the linearized problem using *pulp*.

A.5. Acknowledgement data

We acknowledge the World Climate Research Programme's Working Group on Regional Climate, and the Working Group on Coupled Modelling, former coordinating body of CORDEX and responsible panel for CMIP5. We also thank the climate modelling group of KNMI for producing and making available their model output.